

Dissertation

submitted to the
Combined Faculty of Natural Sciences and Mathematics
of the Ruperto Carola University Heidelberg, Germany
for the degree of
Doctor of Natural Sciences

presented by
Diego Felipe Aponte Santamaría, M.Sc.
born in Bogotá, Colombia
Date of oral examination:

The role of lipids in Wnt secretion and function

Referees:

Prof. Dr. Britta Brügger
Prof. Dr. Michael Boutros

Table of Contents

Summary	1
Zusammenfassung	2
Abbreviations	4
1 Introduction	7
1.1 Wnt protein structure	7
1.2 Wnt signaling pathways	10
1.2.1 β -catenin-dependent/canonical WNT signaling	10
1.2.2 Non-canonical Wnt signaling	11
1.2.3 Wnt-FZD/PCP pathway	11
1.2.4 Wnt/Ca ²⁺ pathway	11
1.3 Lipid modifications of Wnt proteins	12
1.3.1 Do lipids bind to a cysteine or a serine residue?	13
1.3.2 Preference of Wnt fatty acylation by 16:1n-7 over C16:0	15
1.3.3 Porcupine drives Wnt lipidation	15
1.3.4 Is the lipid modification required for secretion and activation of the Wnt signaling pathway? ..	16
1.3.5 Wnt11, an intriguing study case	18
1.4 Lipid composition on HEK cells and HCT116 cells	19
1.5 Aim of the thesis	25
1.6 Organization of the thesis	25
2 Material and Methods	26
Materials	26
Methods	34
2.1 Cell lines, culture media, and cell handling	34
2.2 Treatments with the PORCN inhibitor LGK974	34
2.3 Site-directed mutagenesis	35
2.4 Bacterial transformation	36
2.5 Plasmid DNA amplification	36
2.6 DNA sequencing	36
2.7 Plasmid transfection	36
2.8 Silencing of the acyltransferases ZDHHC5, ZDHHC6 and CPT1A by siRNA	37
2.9 Confirmation of silencing of acyltransferases candidates by RT-qPCR	38
2.9.1 RNA extraction.....	38
2.9.2 Synthesis of complementary DNA (cDNA).....	38
2.9.3 RT-qPCR	39
2.10 Short-guide (sg) RNA design, cloning and generation of knockout cells	40
2.11 Cell lysate and determination of protein concentration	40
2.12 Immunoprecipitation	41
2.12.1 Wnt-Evi interaction by co-immunopercipitation	41
2.13 SDS-PAGE and Western Blot	41

2.13.1	Electrophoresis	41
2.13.2	Incubation with antibodies and membrane developing	42
2.14	Detection of covalent lipid modification of Wnt11 or Wnt11 mutants by immunoprecipitation and alkyne-azide-cycloaddition click reaction	42
2.14.1	Seeding and incubation of cells with cC16:0 or cC16:1n-7 alkyne fatty acids	43
2.14.2	Transient transfection of Wnt3a, Wnt11 or the mutants	43
2.14.3	Click labeling	43
2.15	Deglycosylation assay	45
2.15.1	Procedure to assess glycosylation in proteins from cell lysates	45
2.15.2	Procedure to assess glycosylation in proteins from extracellular medium	46
2.16	Wnt secretion assay with Blue Sepharose beads.....	46
2.17	Analysis of lipidation sites on Wnt3a and Wnt11 by mass spectrometry	47
2.18	Incorporation of cC16:0 and cC16:1n-7 into lipid species.....	48
2.18.1	Thin Layer Chromatography assays (TLC)	48
2.18.2	Lipidomic analysis of incorporated cC16:0 and cC16:1n-7	48
2.19	Lipidomics analysis of HEK293T and HCT116 cells	49
2.19.1	Lipid extraction	50
2.19.2	Mass spectrometry measurements	50
2.20	Canonical and non-canonical TCF4/Wnt-reporter activity assay.....	51
2.21	Gelatin degradation assay	52
3	Results	54
A.	Alternative acylation sites and types of fatty acid modification of Wnt11.....	54
3.1	Role of serine 215, cysteine 80 and Porcupine in Wnt11 palmitoylation	54
3.2	Click metabolic labeling with cC16:1n-7 fatty acid: Wnt11 lipidation occurs at the serine 215 residue and is critically mediated by porcupine	56
3.2.1	Lipidation of serine 215 of Wnt11 with cC16:1n-7	56
3.2.2	cC16:1n-7 lipidation mediated by Porcupine	56
3.2.3	Only mutation of serine 215 impairs cC16:1n-7 dependent lipidation of Wnt11	57
3.3	Additional lipid modifications of Wnt11 beyond the canonical acylation site.....	58
3.3.1	Towards mass spectrometric identification of additional acylation sites in Wnt11.....	58
3.4	Differences between cC16:0 and cC16:1n-7 with respect to acylation and metabolic labeling.....	59
3.4.1	cC16:0 versus cC16:1n-7 acylation	59
3.4.2	cC16:0 and cC16:1n-7 are metabolically incorporated into distinct lipid classes.....	62
3.5	Summary of the part A: alternative acylation sites and and types of fatty acid modification of Wnt11	66
B.	Molecular factors that contribute to Wnt11 secretion and function	67
3.6	Secretion of Wnt variants	67
3.7	Amino acids involved in the activation (Wnt3a) or inhibition (Wnt11) of Wnt/ β -catenin canonical pathway.....	68
3.8	Dissecting the region in Wnt that regulates Evi-independent Wnt secretion	71
3.9	Evaluation of other candidate acyltransferases possibly involved in Wnt11 secretion...74	

3.10	Summary of part B: Molecular factors that contribute to Wnt11 secretion and function	77
C. Lipidomic analysis of HEK293T and HCT116 cells 77		
3.11	Lipid profile in HEK293T cells overexpressing Wnts.....	78
3.12	Lipid profile of HEK293T cells after inhibition of PORCN, knockout of PORCN and knockout of Evi	82
3.13	Lipid profile of HCT116 cells after LGK974 inhibition of PORCN and knockout of Evi.....	87
3.14	Summary of the part C: Lipidomic analysis in HEK293T and HCT116 cells	91
4	Discussion	92
4.1	Alternative acylation site and the role of saturation on Wnt11 lipidation	92
4.2	Molecular factors that contribute to Wnt11 secretion and function.....	94
4.3	Lipidomics analysis in HEK293T and HCT116 cells.....	96
5	Appendix.....	99
5.1.1	Non detectable conversion of free cC16:0 into cC16:1n-7 in Hek293T cells	100
5.1.2	Gelatin degradation assay	105

Summary

Wnt signaling pathways are a set of signal transduction cascades which are activated through the interaction of Wnt proteins with so-called Frizzled receptors [1-3]. These pathways are critically involved in many biological processes such as embryonic development, regeneration, organogenesis, cell division, cellular and tissue homeostasis, among many others [3, 4]. In addition, alterations of these signaling pathways have been linked to various types of diseases such as cancer [5-7], familial tooth agenesis [8], bipolar disease [9], Alzheimer's disease [10], and cardiac valve formation [11]. Wnt signaling components are accordingly promising drug targets to treat these diseases. Wnt pathways are probably among the best characterized receptor-ligand signaling pathways. Wnt proteins are therefore key players in biological signaling and promising drug targets to treat a plethora of diseases.

Although several proteins involved in Wnt trafficking and secretion have been identified over the past years, little is known about the contribution of different lipid species into these processes. The trafficking and secretion of Wnts could be modulated by the type and number of acyl species covalently linked to Wnt proteins. Currently, the best-described acyl modification is the palmitoylation of a serine residue located around amino acids 205-215 mediated by the ER-resident O-acyltransferase Porcupine is responsible for this process. This lipid modification has been described for Wnt3a, Wnt5, xWnt8, and Wnt1, and it has been assumed to also take place in other members of the family of Wnt proteins. Despite the extensive data available, the debate around the lipid-modified amino acids in Wnt proteins has not yet reached a consensus. Recent results from O. Voloshanenko (M. Boutros group, DKFZ, Heidelberg, Germany) suggested that there may be other amino acid residues in Wnts that are lipidated, apart from this canonical serine residue. Furthermore, the specific saturation of the acylated chain that binds to Wnt remains inconclusive.

In this thesis, I aimed to define other putative acylation types and lipid-modified sites in Wnt proteins and to determine the role of these alternative lipidations in Wnt secretion and signaling. Furthermore, I evaluated the impact of Wnt signaling and Wnt secretion on the lipidome of HEK293T and HCT116 cells. To achieve this, I employed a combination of chemical biology tools, mutagenesis experiments, and mass spectrometric measurements. In particular, I focused on Wnt11 as a working model. I studied its acylation using clickable lipids such as palmitic acid alkyne (cC16:0) and palmitoleic acid alkyne (cC16:1n-7). One of the early observations was that palmitoylation and secretion of Wnt11 were not wholly abolished in Porcupine knockout cells or some mutant variants of Wnt11. However, these observations seem to depend on the type of clickable fatty acid used. Our results suggest a lipid modification of Wnt11 at serine 215 via the monounsaturated fatty acid cC16:1n-7, consistent with the previously predicted models. However, lipid modification with the saturated fatty acid cC16:0 showed variations in the experimental replicates, which did not fully resolve whether Wnt11 contains another modification site. Importantly, our experiments stress that unsaturation is a key feature for Wnt acylation. The relevance of covalent lipid binding for the secretion and signaling activity of Wnts has also been assessed. It was demonstrated that lipidation is essential for the signaling activity of Wnt11 but is not strictly necessary for its secretion. In addition, an impact of Wnt protein expression on the overall cellular lipidome of HEK293T and

HCT116 cells has been tested, yielding preliminary observations on the crosstalk between the Wnt signaling and the overall cellular lipid homeostasis. This study is expected to contribute to our understanding of how post-translational lipid modifications influence Wnt cellular secretion, signaling and, conversely, how proteins of the Wnt signaling pathway affect the lipid composition of cells.

Zusammenfassung

Wnt-Signalwege sind eine Reihe von Signaltransduktionskaskaden, die durch die Interaktion von Wnt-Proteinen mit sogenannten Frizzled-Rezeptoren aktiviert werden [1-3]. Diese Signalwege sind an vielen biologischen Prozessen wie Embryonalentwicklung, Regeneration, Organogenese, Zellteilung, Zell- und Gewebekomöostase und vielen anderen von entscheidender Bedeutung [3, 4]. Darüber hinaus wurden Veränderungen dieser Signalwege mit verschiedenen Krankheiten in Verbindung gebracht, wie z. B. Krebs [5-7], familiärer Zahnausfall [8], bipolare Erkrankung [9], Alzheimer-Krankheit [10] und Fehler bei der Ausbildung der Herzklappen [11]. Wnt-Signalkomponenten sind daher vielversprechende Ansatzpunkte für die Behandlung dieser Krankheiten. Wnt-Signalwege gehören wahrscheinlich zu den am besten charakterisierten Rezeptor-Liganden-Signalwegen. Wnt-Liganden die Hauptakteure der Wnt-Signalübertragung sind daher Schlüsselproteine der biologischen Signalübertragung und vielversprechende Zielproteine für die Behandlung einer Vielzahl von Krankheiten.

Obwohl in den letzten Jahren mehrere Proteine identifiziert wurden, die am Wnt-Trafficking und an der Wnt-Sekretion beteiligt sind, ist nur wenig über den Beitrag verschiedener Lipidspezies zu diesen Prozessen bekannt. Der Transport und die Sekretion von Wnt-Proteinen könnte durch die Art und Anzahl der kovalent an Wnt-Proteine gebundenen Acylspezies moduliert werden. Die derzeit am besten beschriebene Acylmodifikation ist die Palmiteoylierung eines Serinrests, der sich um die Aminosäuren 205-215 befindet. Die im ER ansässige O-Acyltransferase Porcupine ist für diesen Prozess verantwortlich. Diese Lipidmodifikation wurde für Wnt3a, Wnt5, xWnt8 und Wnt1 beschrieben, und es wurde angenommen, dass sie auch bei anderen Mitgliedern der Wnt-Proteinfamilie stattfindet. Trotz der umfangreichen Datenlage ist die Debatte um die lipidmodifizierten Aminosäuren in Wnt-Proteinen noch nicht abgeschlossen. Jüngste Ergebnisse von O. Voloshanenko (Arbeitsgruppe von M. Boutros, DKFZ, Heidelberg, Deutschland) deuten darauf hin, dass es neben diesem kanonischen Serinrest auch andere Reste geben könnte, die lipidiert sind. Darüber hinaus ist die spezifische Sättigung der acylierten Kette, die an Wnt bindet, nach wie vor nicht eindeutig geklärt.

In dieser Arbeit habe ich versucht, andere mutmaßliche Acylierungsarten und lipidmodifizierte Stellen in Wnt-Proteinen zu definieren und die Rolle dieser alternativen Lipidierungen bei der Wnt-Sekretion und -Signalgebung zu bestimmen. Darüber hinaus habe ich die Auswirkungen der Wnt-Signalisierung und Wnt-Sekretion auf das Lipidom von HEK293T- und HCT116-Zellen untersucht. Zu diesem Zweck habe ich eine Kombination aus chemisch-biologischen Werkzeugen, Mutagenese-Experimenten und massenspektrometrischen Messungen eingesetzt. Insbesondere habe ich mich auf Wnt11 als Arbeitsmodell konzentriert. Ich untersuchte seine Acylierung mit klickbaren Lipiden wie Palmitinsäurealkin (cC16:0) und

Palmitoleinsäurealkin (cC16:1n-7). Eine der ersten Beobachtungen war, dass die Palmitoylierung und die Sekretion von Wnt11 in Porcupine-Knockout-Zellen oder einigen mutierten Varianten von Wnt11 nicht vollständig aufgehoben waren. Diese Beobachtungen scheinen jedoch von der Art der verwendeten klickbaren Fettsäure abzuhängen. Meine Ergebnisse deuten auf eine Lipidmodifikation von Wnt11 an Serin 215 über die einfach ungesättigte Fettsäure cC16:1n-7 hin, was mit den zuvor vorhergesagten Modellen übereinstimmt. Die Lipidmodifikation mit der gesättigten Fettsäure cC16:0 zeigte jedoch Schwankungen in den experimentellen Wiederholungen, so dass nicht vollständig geklärt werden konnte, ob Wnt11 eine weitere Modifikationsstelle enthält. Wichtig ist, dass unsere Experimente zeigen, dass eine einfach ungesättigte Fettsäure eine Schlüsselfunktion für die Wnt-Acylierung darstellt. Die Bedeutung der kovalenten Lipidbindung für die Sekretions- und Signalaktivität von Wnts wurde ebenfalls untersucht. Es wurde gezeigt, dass die Lipidierung für die Funktion von Wnt11 wesentlich ist, aber nicht unbedingt für seine Sekretion. Darüber hinaus wurde der Einfluss einer Wnt-Protein-Überexpression auf das gesamte zelluläre Lipidom von HEK293T- und HCT116-Zellen untersucht, was zu ersten Erkenntnissen über die Wechselwirkungen zwischen der Wnt-Signalgebung und der zellulären Lipidhomöostase führte. Diese Studie soll zu unserem Verständnis darüber beitragen, wie posttranslationale Lipidmodifikationen die zelluläre Wnt-Sekretion und -Signalgebung beeinflussen und wie umgekehrt einige Proteine des Wnt-Signalwegs die Lipidzusammensetzung von Zellen beeinflussen.

Abbreviations

AAG	Alkyl/alkenyl-acylglycerol
ACN	Acetonitrile
ACS	Acetyl-coenzyme A synthetase
Acyl-DHAP	Acyl-dihydroxyacetone phosphate
ADAG	Alkyl/alkenyl-diacylglycerol
AGP	1- <i>O</i> -alkyl-G3P
AGPS	alkylglycerone phosphate synthase
Alkyl-DHAP	Alkyl-dihydroxyacetone phosphate
AMFR or GP78	E3 ubiquitin-protein ligase AMFR
APC	Adenomatous polyposis coli protein
Axin	<i>Axis inhibition protein</i>
B.S.	Blue Sepharose
BCA	Bicinchoninic acid
CaMKII	Calmodulin-dependent protein kinase II
CDase	Neutral ceramidase
CDP-AAG	Cytidine diphosphate Alkyl/alkenyl-acylglycerol
CDP-Cho	Cytidine diphosphate Choline
CDP-DAG	Cytidine diphosphate diacylglycerol
CDP-Etn	Cytidine diphosphate Ethanolamine
CDS1	Phosphatidate cytidyltransferase 1
CE	Cholesterol Ester
Cer	Ceramide
CerS	Ceramide synthase
CGRRF1	Cell growth regulator with RING finger domain protein 1
Cho	Choline
Chol	Cholesterol
CK1	Casein kinase 1
CL	Cardiolipins
CLS1	Cardiolipin synthase
CMP	Cytidine monophosphate
COP-I	coat protein complex - I

COP-II	coat protein complex - II
CPT1	Carnitine <i>O</i> -palmitoyltransferase 1
Cryo-EM	cryogenic electron microscopy
CTD	C-terminal cysteine-rich region
DAAM	Disheveled-associated activator of morphogenesis
DAG	Diacylglycerol
DDase	Dihydroceramide desaturase
DGAT1	Diacylglycerol <i>O</i> -acyltransferase 1
DHAP	Dihydroxyacetone phosphate
DMEM	Dulbecco's Modified Eagle's Medium
DTT	Dithiothreitol
Dvl	Dishevelled
E3	E3-ubiquitin ligase β -TrCP
EDTA	Ethylenediaminetetraacetic acid
EPT1	Choline/ethanolaminephosphotransferase 1
ER	Endoplasmic reticulum
Etn	Ethanolamine
Evi	Protein evenness interrupted homolog
FA	Formic acid
FAR1 or FAR2	Fatty acyl-CoA reductase
FAS	Fatty acid synthase
Fz8	Frizzled 8
FZD	Frizzled
G3P	Glycerol 3-phosphate
G3PDH	Glycerol 3-phosphate dehydrogenase
GCCase	Glc-ceramide synthase
GNPAT	Glyceronephosphate <i>O</i> -acyltransferase
GSK-3	Ser/Thr kinases glycogen synthase kinase 3
Hex2Cer	Hexosyl2ceramide
HexCer	Hexosylceramide
HRP	Horseradish peroxidase

HSC70	Heat shock cognate 70 kDa protein
IAA	Iodoacetamide
JNK	c-Jun N-terminal kinase
LEF	Lymphoid enhancer factor
LPA	Diacyl phospholipid precursor lysophosphatidic acid
LPAAT	Lysophosphatidic acid acyltransferase
LPC	Lysophosphatidylcholine
LRP5/6	Low-density lipoprotein receptor-related protein (LRP)5 and 6
NFAT	Nuclear factor of activated T-cells
NFκB	Nuclear factor kappa-light-chain-enhancer of activated B cells
NLK	Nemo Like Kinase
NTD	N-terminal α-helical domain
P-Cho	Phosphocholine
P-Etn	Phosphoethanolamine
p24	Endomembrane protein precursor of 24 kD
PA	Phosphatidic acid
PA O-	Ether linked Phosphatidic acid
PAP	PA phosphatase
PBS	Phosphate buffer-red saline
PC	Phosphatidylcholine
PC O-	Ether lipid Phosphatidylcholine
PCP	Planar polarity pathway
PDAT	Phospholipid:diacylglycerol acyltransferase 1
PE	Phosphatidylethanolamine
PE O-	Ether linked Phosphatidylethanolamine
PE-P	Phosphatidylethanolamine Plasmalogen
PexRAP	Acyl/alkyl DHAP reductase
PG	Phosphatidylglycerol
PG O-	Ether linked Phosphatidylglycerol
pgpA	Phosphatidylglycerophosphatase A
PGS1	CDP-diacylglycerol--glycerol-3-phosphate 3-phosphatidyltransferase
PI	Phosphatidylinositol
PI O-	Ether linked Phosphatidylinositol
PI4K	Phosphatidylinositol 4-kinase

PI4P	Phosphatidylinositol-4-phosphate
PI4P5K	Phosphatidylinositol 4 phosphate - kinase
PIP2	Phosphatidylinositol 4,5-bisphosphate
PIS1	CDP-diacylglycerol--inositol 3-phosphatidyltransferase
PLC	Phospholipase C
PORCN	Porcupine
PS	Phosphatidylserine
PS O-	Ether linked Phosphatidylserine
PSD1	Phosphatidylserine decarboxylase proenzyme 1
Rab8	Ras-related protein Rab-8
Rac	Subfamily of the family Rho family of GTPases
Rac1	Ras-related C3 botulinum toxin substrate 1
Ras GTPase	Rat sarcoma virus GTPase
Rho	Ras homolog family member
RhoA	Ras homolog family member A
ROCK.	Rho-associated protein kinase
ROR	Receptor tyrosine kinase-like orphan receptor
ROR1	Tyrosine-protein kinase transmembrane receptor ROR1
ROR2	Tyrosine-protein kinase transmembrane receptor ROR2
RPMI	Roswell Park Memorial Institute
RYK	Receptor Like Tyrosine Kinase or Tyrosine-protein kinase RYK
S.O.C.	Super Optimal broth with Cata-bolite repression
Sar1	Small COP-II coat GTPase SAR1
Sec12	Regulator of COP-II vesicle coat Sec12
Sec22	Protein transport protein SEC22
SM	Sphingomyelin
SMS	Sphingomyelin synthase
SMS	sphingomyelin synthase
SPT	Serine palmitoyltransferase
TAG	Triacylglycerol
TCEP	Tris-(2-carboxyethyl)-phosphin
TCF	T-cell factor
TCF4	T-cell factor 4

TLC	Thin Layer Chromatography
TSC10	3-ketosphinganine reductase
UBC	Ubiquitin C gene
Wnt/Ca²⁺	Non-canonical WNT calcium pathway

Wnt/PCP	Non-canonical WNT/PCP pathway
ZDHHC5	Palmitoyltransferase ZDHHC5
ZDHHC6	Palmitoyltransferase ZDHHC6
β-TrCP	Beta-transducin repeats-containing proteins

1 Introduction

Cells detect external stimuli and transfer that information to the cell interior through complex signaling pathways. In such pathways, a machinery of biomolecules orchestrates to efficiently and selectively transduce external signals into chemical and physical events. One of the most common mechanisms of signal transduction is the activation of receptors by the binding of specific ligands. The activation of receptors triggers chemical and conformational changes of primary effectors (usually proteins). In turn, in a cascade of events, the primary effectors transduce the signal downstream, activating or inhibiting either proteins or second messengers. The final target in such signal transduction pathways are proteins that regulate the transcription of genes (transcription factors) or a specific metabolic process.

Among the most known receptor-ligand signaling pathways are the Wnt pathways. The Wnt signaling pathways are a set of signal transduction cascades activated through the interaction of Wnt proteins with so-called Frizzled receptors [1-3]. Such cascades are involved in many biological processes such as embryonic development, regeneration, organogenesis, cell division, cellular and tissue homeostasis, among others [3, 4]. Malfunction of these signal pathways has been linked to various types of cancer [5-7] such as colorectal cancer, familial adenomatous polyposis (FAP), hepatocellular carcinoma, medulloblastoma, ovarian endometrial adenocarcinomas, esophageal squamous cell carcinoma, pancreatic tumors, prostate cancer and breast cancer. Also, they have been linked to other diseases such as familial tooth agenesis [8], bipolar disease [9], Alzheimer disease [10], and cardiac valve formation [11]. Wnt signaling components are accordingly promising drug targets to treat these diseases. In consequence, understanding the mechanism of functions of Wnt proteins and Wnt signaling is a central question in biology, and carries a plethora of applications in medicine.

1.1 Wnt protein structure

For 40 years, the family of Wnt proteins has been intensively studied. These are probably one of the most ever investigated signaling proteins. Wnts have been found in all phyla of the animal kingdom, from placozoans, poriferans, and cnidarians to chordates [12]. In mammals, including humans, 19 highly-conserved Wnt proteins have been identified. Wnts are proteins of approximately 40 kDa in mass and 350-400 amino acids in length. They are highly hydrophobic, and rich in cysteine residues [3, 4, 13] (Figure 1.1). The structure of four different Wnts was elucidated by either X-ray crystallography or cryogenic electron microscopy (Cryo-EM) [14-17]. Janda and co-workers resolved the structure for *Xenopus* Wnt8 [14], Mihara et al. determined the structure for human Wnt3 [18], Chu et al. obtained the structure for a truncated version of WntD [15], and Nygaard et al. revealed the structure for human Wnt8 [17]. Based on this structural information, Wnt proteins have been described to adopt a semi-close hand that extends the “thumb” and “index” fingers from a central “palm” domain [14-17] (Figure 1.1A-C). The structure of human Wnt3, human Wnt8, and the *Xenopus* Wnt8 (Figure 1.1A-C) comprise an N-terminal α -helical domain (NTD), from residue 1 until approximately residue 250, containing seven α -helices (α 1- α 7) and a C-terminal cysteine-rich region (CTD) ranging from residue 260 until approximately residue 350 (Figure 1.1D). The NTD

contains two large inter-helical loops. One of these loops precisely corresponds to the “thumb”, in which a serine was identified to be lipid-modified (as it is described in more detail in **section 1.3**). The CTD features a long 40 amino acid β -strand hairpin that is also stabilized by an extensive network of disulfide bonds.

conserved disulfide bond between the cysteine residue highlighted as green spheres. **D.** Multiple sequence alignment of the 19 humans Wnts was obtained from Uniprot. Helices are drawn as cylinders and labeled $\alpha 1$ to $\alpha 7$. Green lines indicate the disulfide bonds. Three hairpins (1-3) are indicated as red lines. Conserved residues are colored in gray scale. The predicted serine residue bound to palmitoleic acid is highlighted with a red star.

1.2 Wnt signaling pathways

The Wnt signaling pathways are a set of signal transduction cascades activated through the interaction of Wnt ligands with cell surface-localized Frizzled receptors[1-3]. These cascades are grouped in canonical or non-canonical pathways, depending on whether the protein β -catenin is involved as an effector of the pathway or not [3, 4].

Wnt proteins grouped into the canonical pathway are Wnt1, Wnt2, Wnt 2b, Wnt3, Wnt3a, Wnt8a, Wnt8b, Wnt10a and Wnt10b, and Wnt proteins of the non-canonical pathways are Wnt4, Wnt5a, Wnt5b, Wnt7a, Wnt7b and Wnt11 [19].

1.2.1 β -catenin-dependent/canonical WNT signaling

The canonical pathway remains inactive when there is no extracellular stimulus triggered by Wnt (**Figure 1.2**). Under this condition, cytoplasmic β -catenin is targeted for proteolysis by the destruction complex. The destruction complex is a multiprotein assembly composed of the scaffolding protein Axin, the adenomatous polyposis coli protein (APC), the Ser/Thr kinases glycogen synthase kinase 3 (GSK-3), casein kinase 1 (CK1), and the E3-ubiquitin ligase β -TrCP. In the absence of Wnt stimulus, β -catenin binds to Axin, APC, CK1, and GSK-3 [4, 20]. This induces the phosphorylation of β -catenin and its binding to β -TrCP. Subsequently, ubiquitination and degradation of β -catenin occurs via the proteasome [4, 20]. In the presence of Wnt, signal transduction is activated when Wnt binds to Frizzled and the co-receptor LRP5/6 on the extracellular side of the plasma membrane, thereby forming a heteromeric complex that induces a conformational change in both membrane proteins. On the cytosolic side, the tail of LRP5/6 is phosphorylated by several kinases, including Gsk3 and CK1. This leads to the binding of Dishevelled (Dvl) and Axin to the intracellular domains of FZD and LRP5/6 [3, 4, 6, 21]. The translocation of Dvl and Axin to the signaling complex inhibits the phosphorylation and subsequent proteasomal degradation of β -catenin. The rise of β -catenin levels promotes its translocation to the nucleus, where it binds the T-cell factor/lymphoid enhancer factor (TCF/LEF) transcription factors and induces the expression of the Wnt-responsive genes [3, 4, 6, 21].

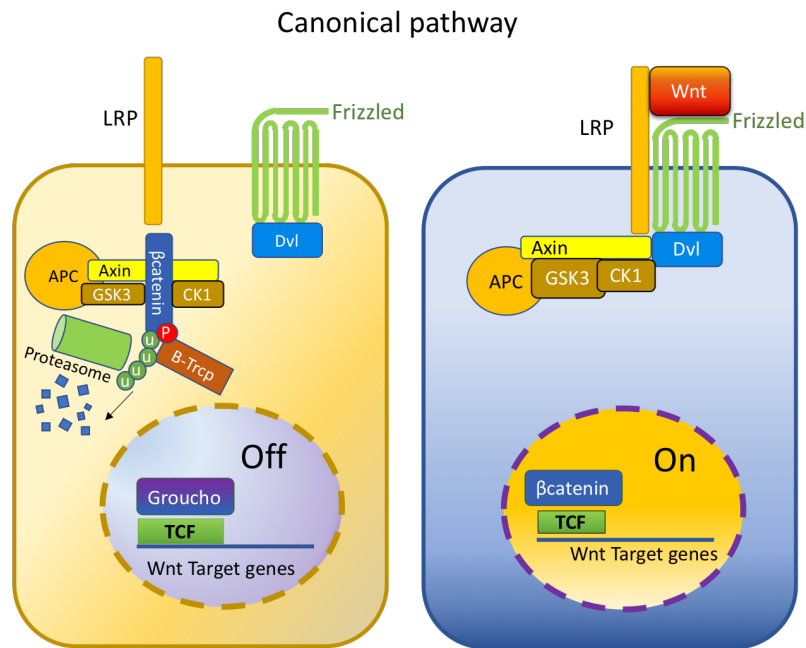


Figure 1.2: Canonical Wnt/β catenin pathway.

In the inactive state of the Wnt/β catenin pathway (left side of the figure), the cytosolic transcription factor β-catenin is phosphorylated by GSK3 and CK1 with the help of the scaffold protein Axin and APC. The phosphorylated residues in β-catenin are recognized by the β-TrCP E3 ubiquitin–ligase complex. β-TrCP polyubiquitinates β-catenin and targets it such that it is degraded in the proteasome. In an active state (right side of the figure), Wnt proteins bind to the Frizzled and LRP5/6 receptors on the cellular surface, triggering the signal transduction. On the cytosolic side, the tail of LRP5/6 is phosphorylated by several kinases, including Gsk3 and CK1, and leads to the binding of Dishevelled (Dvl) and Axin to the intracellular domains of FZD and LRP5/6 [3, 4, 6, 21]. The translocation of Dvl and Axin to the FZD/LRP receptor complex inhibits the phosphorylation of β-catenin, stabilizing it in the cytosol. The rise of β-catenin levels promotes its translocation to the nucleus, where it binds TCF/LEF transcription factors and serves as a coactivator for the expression of the Wnt-responsive genes.

1.2.2 Non-canonical Wnt signaling

In the non-canonical pathway, there have been primarily two cascades studied, namely, WNT-FZD/PCP and Wnt/Ca²⁺ (Figure 1.3).

1.2.3 Wnt-FZD/PCP pathway

In the Wnt-FZD/PCP signal pathway, the protein Ras homolog family member A (RhoA) and c-Jun N-terminal kinase (JNK) act as downstream effectors [6, 22, 23]. The pathway is active when Wnt ligands bind to the ROR-Frizzled receptor complex, which subsequently binds and activates Dvl and DAAM. At the same time, Dvl associates with the small GTPase RhoA and Rac1 and they together activate the Rho-associated protein kinase ROCK. ROCK mediates cytoskeleton rearrangement by actin polymerization [6, 22–24]. Besides, Rac can also activate the JNK signaling cascade to regulate gene expression [6, 22–24].

1.2.4 Wnt/Ca²⁺ pathway

The Wnt/Ca²⁺ signaling pathway is activated when Wnt binds to the Frizzled receptor and either ROR1, ROR2 or RYK receptors [6, 25, 26]. This induces the activation of phospholipase C (PLC), a lipase which cleaves phosphatidylinositol 4,5-bisphosphate (PIP₂) into inositol 1,4,5-triphosphate (IP₃) and 1,2-diacylglycerols (DAG) [6, 25, 26]. DAG remains in the plasma membrane, while IP₃ is released into the cytosol and binds to calcium channels at the ER

membrane, thereby triggering the release of Ca^{2+} into the cytosol [6, 25, 26]. Calcium ions together with calmodulin activate the Ca^{2+} /calmodulin-dependent protein kinase II (CaMKII). Meanwhile, DAG together with calcium ions activate protein kinase C (PKC), and thereby induces CDC42-mediated actin rearrangements [6, 25-28]. Several transcription factors are activated by this signaling pathway, such as NF κ B, NFAT and NLK [6, 25-28].

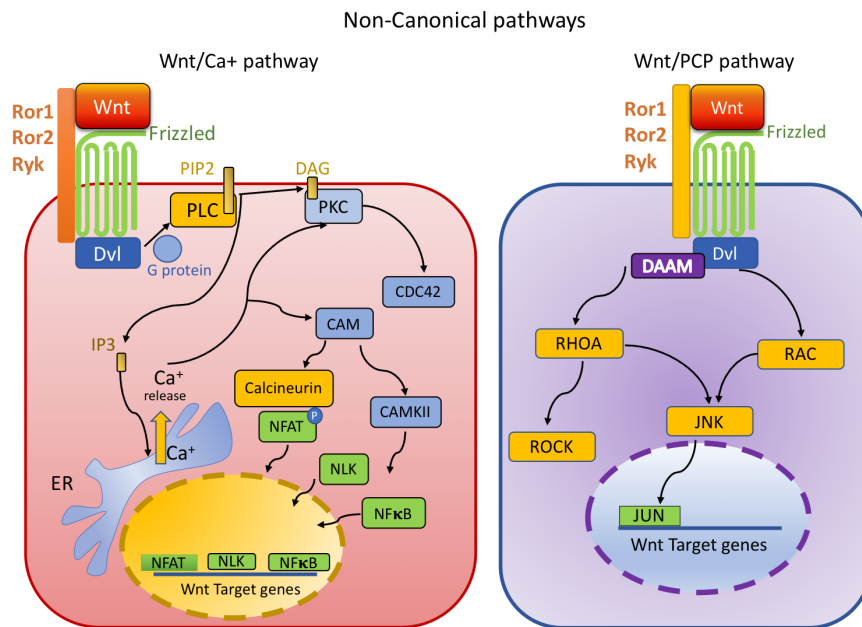


Figure 1.3: Non-canonical WNT signaling. The signal pathway is activated when non-canonical Wnts, such as Wnt11 or Wnt5A, binds to Frizzled receptor and the co-receptors ROR1, ROR2 or RYK receptors [6, 25, 26]. It can then take two pathways, the **Wnt/Ca²⁺ signaling pathway** (Left) which is induced by the activation of phospholipase C (PLC) [6, 25, 26], or the **Wnt/PCP pathway** (Right), which is induced by the activation of Dvl and DAAM in the cytosol [6, 22-24]. This graph was adapted from [25].

1.3 Lipid modifications of Wnt proteins

Lipid-protein interactions and protein lipidations are emerging concepts in understanding membrane-associated protein functions at a molecular level [29, 30]. For many years the cellular functions have been attributed mainly to proteins but nowadays it is becoming clearer that lipids also play a key role modulating biological processes. These processes include cell signaling, regulation of protein-membrane interactions, membrane trafficking, protein stability, enzymatic activities and even protein-protein interactions [29, 30]. Post-translational lipid modification of proteins can occur by adding e.g. fatty acyl or polyisoprenyl groups to side chains of cysteine, serine, threonine, and lysine residues, or to the N-termini of proteins [29, 30].

Wnt trafficking, secretion and signaling is tightly regulated by post-translational modifications [31-36]. In particular, lipidation has emerged as a key regulatory mechanism to control the signaling ability of Wnts [32, 34, 36-41]. Nevertheless, there still exists a debate on where within the amino acid sequence Wnt proteins are lipidated and, ultimately, on the functional implications of such specific lipidation.

Many attempts to characterize Wnt proteins in the active state have been hampered by their high degree of insolubility. The first work in which a lipidated Wnt protein was successfully isolated was published by Willert and Nusse in 2003 [42]. In the process of biochemical purification of murine Wnt3a, the authors observed that Wnt3a was highly hydrophobic. The high degree of hydrophobicity was contradictory to the fact that the Wnt3a protein sequence itself does not show particularly high hydrophobic regions. This led to the suggestion that post-translational lipid modifications, increasing the overall hydrophobicity of Wnt3a, must be in place. This hypothesis was confirmed with the binding of radiolabeled palmitic acid (C16:0) to Wnt3a [42].

1.3.1 Do lipids bind to a cysteine or a serine residue?

As Wnt proteins are lipidated, the question arises as to which amino acid side chains of the protein the lipid moieties are bound. The same study of Willert and Nusse identified by mass spectrometry cysteine 77 in murine Wnt3a and cysteine 51 in *Drosophila* Wnt8 as the lipid attachment sites. Mutation of cysteine 77 in murine Wnt3a, and highly conserved across all members of the Wnt family [13], made the protein water-soluble [42] (Figure 1.1).

Years later, Takada and co-workers identified another putative acylation site in murine Wnt3a [43]. Through metabolic radiolabeling in the presence of disulfide reducing agents which targets S-palmitoylation on cysteines, they still observed lipidation of Wnt3a. [43]. These results suggested an oxyester linkage bond instead of a thioester bond between palmitic acid and a cysteine residue of Wnt3a. The oxyester linkage bond could be associated with lipid modification on a serine, threonine or tyrosine instead of a cysteine. The same results were observed for Wnt5a expressed from L-cells (cells located in the intestine, which function is to secrete glucagon-like peptide-1 or 2, incretin, or oxyntomodulin) [43]. Metabolic radiolabeling of truncated and point mutated versions of Wnt3a, together with liquid chromatography and mass spectrometry, revealed that serine 209 was the residue responsible for the lipidation of Wnt3a [43]. Furthermore, mass spectrometry showed that the protein is modified with the monounsaturated palmitoleic acid (C16:1) instead of its saturated counterpart palmitic acid (C16:0) [43].

The results from Willert [42] and Takada [43] opened a debate about which amino acid residues are lipidated in Wnts and which implications such specific lipidation sites have for Wnt functions. A wealth of experimental evidence supported lipidation of both the cysteine and the serine residues of Wnts. In line with the studies from Willert, mouse Wnt5a was found to be palmitoylated at cysteine 104 with palmitic acid (a residue that is equivalent to cysteine77 in Wnt3a) [31]. Other studies with Wnt1 showed that mutations in serine 224 (equivalent to serine 209 in Wnt3a) resulted in the expression of a non-acylated form of Wnt1 [32]. This result was interpreted as whether serine 224 was lipidated but also required for another lipid modification at the cysteine 93 [32]. Mutations of serine 224 and cysteine 93 also affected the functional activity of Wnt1 on the Wnt/ β -catenin pathway [40, 44].

The structure of *Xenopus* Wnt8 (xWnt8) in complex with the cysteine-rich domain (CRD) of mouse Frizzled 8 (mFZD8) was determined by X-ray crystallography [14] (Figure 1.1B). This structure revealed that the serine 187 in xWnt8, which is positioned at the interface of xWnt8 with mFZD8 CRD and equivalent to serine209 on Wnt3a, is lipidated [14]. Moreover, it was observed that the cysteine 55 in xWnt8 was not palmitoylated due to its engagement in a

disulfide bond [14]. The structure of xWnt8 thus supported the hypothesis that a serine, rather than a cysteine, is the main fatty acyl acceptor in Wnts, as originally proposed by Takada et al. [17]. Analogously, MacDonald et al. reported that cysteine 77 is disulfide bonded, stressing the relevance of such cysteine-mediated disulfide bonds for Wnt folding, activity, and secretion [13]. Subsequent work on Wnt3a and Wnt1 mutant variants, using radiolabelling [45, 46] or nonradioactive fatty acid labeling with palmitic acid alkyne (cC16:0), in combination with click chemistry, also supported the idea that serine 209 (in Wnt3a) or their homolog residue in other Wnts is the unique lipidation site in Wnts[47-51].

Recent work by Divya Dhasmana et al. investigated for Wnt3 distinct functional role of cysteine and serine residues implicated in disulfide formation and lipid modification, respectively, using different microscopy and fluorescence correlation spectroscopy (FCS) techniques [52]. Removal of either the key cysteine 80 or the serine 212, by mutagenesis, did not affect secretion and membrane localization of Wnt3, but instead affected the Wnt signaling [52]. Furthermore, removal of the two residues at the same time impaired Wnt localization and secretion [52]. Also, only serine 212 seemed to be indispensable for the interaction with the Frizzled receptor [52]. Altogether, these results suggested that lipidation of cysteine 80 and serine 212 residues in Wnt3 play different functional roles in Zebrafish [52]. Azbazar et al. also observed that mutations on serine 212 neither affect the interaction with Fz8 nor the secretion of Wnt3 in Zebrafish [53]. However, serine 212 was relevant for the binding to specific plasma membrane domains and for activation of the Wnt canonical pathway [53].

Until 2017, when this project started, five Wnt proteins were described to be modified by lipidation, namely, Wnt1, Wnt3a, Wnt5a, xWnt8, and Wnt11 [14, 32, 35, 36, 39, 40, 42-45, 51, 54]. During the course of this work, other studies brought to light the lipidation in other Wnt proteins [16, 17, 21, 55]. In 2019, the crystal structure of human Wnt3 in complex with the murine Frizzled 8 (Fz8) Cys-rich domain (CRD) showed to be almost identical conformation to the one observed for xWnt8 [14, 16]. This study [16] displayed the lipid moiety bound to serine 212 of Wnt3 (equivalent to the serine 209 in Wnt3a), extending through a hydrophobic groove to facilitate the interaction with the Fz8 CRD domain. Even more, the electron density was compatible with a bend of the fatty acid at the C9-C10 position, corresponding to a cis- Δ^9 unsaturation of palmitoleic acid (C16:1n-7) [16]. Moreover, Nygaard et al. revealed for the first time the cryogenic electron microscopy (Cryo-EM) structure of the carrier protein Evi (Evenness interrupted) in complex with human Wnt8a [17]. Evi is a conserved multipass transmembrane protein required for the transport of Wnt proteins from the ER to the extracellular media, this has been observed for Wg, Wnt1, Wnt3a and Wnt5a [56, 57]. In this structure, the palmitoleic acid bound to Wnt8a extends deep into a conserved hydrophobic cavity in the transmembrane domain of Evi [17].

Besides these structural studies, Wnt lipid modification has been investigated through nonradioactive fatty acid labeling with palmitic acid alkyne (cC16:0) and palmitoleic acid alkyne (cC16:1n-7), in combination with click chemistry [55]. In this study, a highly efficient Wnt lipid modification using cC16:1n-7 was observed, which was not the case for cC16:0 [55]. These data unveiled the lipid modification on Fc-tag-tagged Wnt proteins: Wnt1-Fc, Wnt3a-Fc, Wnt5b-Fc, Wnt7b-Fc, Wnt9b-Fc, Wnt10a-Fc, and Wnt10b-Fc. Altogether, eleven Wnt proteins have thus been confirmed to be lipidated. For the remaining eight Wnt proteins, namely, Wnt2, Wnt2b, Wnt4, Wnt7a, Wnt8b, Wnt9a, and Wnt16, an investigation of their lipidation is still missing.

1.3.2 Preference of Wnt fatty acylation by 16:1n-7 over C16:0

Not only the site in which Wnts are lipidated has been the subject of intense research, but also the type of fatty acid that binds to them. Identification of the lipid binding of palmitate to cysteine 77 of Wnt3a, cysteine 51 of *Drosophila* Wnt8, and cysteine 105 of Wnt5a suggested that the most likely fatty acid bound to Wnts is the saturated palmitic acid [42, 58]. Computational approaches supported this idea in suggesting that the saturated palmitic acid, and not the unsaturated one, fits better the conformation of the lipid seen in the crystal structure of xWnt8 in complex with Fz8-CRD [53]. However, results from Takada et al. [43] Rios-Esteves et al. [45] and Tuladhar et al. [55] showed that the Wnt proteins studied have a high preference for being lipidated with the monounsaturated palmitoleic acid (C16:1n-7).

Other studies reported Wnt lipidation signals using saturated radioactive palmitic acid [31, 43, 45] and saturated non-radioactive palmitic acid [49-51, 55, 59], but are in line with studies suggesting that. These results proposed that the cells first converted the saturated fatty acid (C16:0) is converted to monounsaturated fatty acid (C16:1n-7), by action of the Stearoyl-CoA desaturase 1 [36, 45, 60, 61], which is then attached to the Wnt proteins by the O-acyltransferase Porcupine (PORCN).

1.3.3 Porcupine drives Wnt lipidation

The question arises as to which enzyme performs the Wnt lipidation process. Based on the work supporting a lipid modification of a cysteine residue [31, 42], lipidation should be carried out by an acyltransferase that generates a thioester bond between an acyl moiety and a cysteine residue. This process is known as S-palmitoylation and is catalyzed by enzymes of the family of DHHC acyl transferases [62, 63]. However, there is no evidence linking this family of proteins to the lipidation of Wnts. Instead, this function was attributed to the protein Porcupine (PORCN). PORCN was first described as a crucial component in the embryonic pattern formation and secretion of Wnt ligands [44, 64, 65]. PORCN is a membrane protein that localizes to the endoplasmic reticulum (ER). PORCN belongs to the Membrane-bound O-acyltransferase (MBOATs) family [66]. The main function of this family is the transfer of fatty acids onto hydroxyl groups of serine or threonine residues, a process also known as O-acylation [66]. The reaction requires acyl-CoA substrates, which are produced during fatty acid metabolism [36]. There are about 11 members of the MBOATs family, but only five of them have been studied [66]. PORCN has been associated with the lipidation of *Drosophila* Wg, *Drosophila* Wnt1, chicken Wnt1, mouse Wnt1, chicken Wnt3a, mouse Wnt3a, human Wnt3a, and mouse Wnt5a [43, 44, 46, 48, 50, 67, 68]. It is of note that the O-acyl-transferase activity of PORCN, which is localized to the ER lumen, supports the idea that lipid modification is carried out on a serine instead of a cysteine residue.

The structure of PORCN has not been resolved yet, however, the topology of PORCN has ten predicted transmembrane domains, with both the N and C termini oriented towards the cytosolic side [67, 69]. The polar residues H341, N306, Y334, and S337 have been identified to be critical regulators of the catalytic activity of PORCN [44-46, 55, 67, 68]. Concerning the saturation of the acyl chain, cis- Δ 9 monounsaturated palmitoleoyl-CoA fits better into the bent cavity of PORCN, and this lipid was strongly preferred as the substrate for Wnt lipidation in an in vitro assay using substrate peptides based on human Wnt1, human Wnt3a and human Wnt11 [67]. Once the fatty acid transfer is complete, the kinked shape of the monounsaturated

fatty acid facilitates the release of Wnt from PORCN [55]. Recently, Jia Yu and coworkers [69] built a structural homology model of PORCN in complex with hWnt8a, based on previous results of Wnt [45, 46, 55, 67, 68] and the structure of the O-acyltransferases DGAT1 (PDB 6VP0, [70]). In this model, palmitoleic acid is transferred to Wnt via two tunnels inside PORCN. The first tunnel faces towards the luminal face of the ER, with the hairpin loop containing the serine 186 of hWnt8a [71]. The second tunnel points towards the cytosol and contains a kink in the middle which can only be occupied by palmitoleoyl-CoA [71]. Both tunnels are predicted to be located in such a way that serine 186 from hWnt8a is positioned near the thioester bond of the palmitoleoyl-CoA and thus in an optimal distance to allow the acyl transfer from CoA to this serine residue [71]. Accordingly, this model strongly supports the preferential transfer of C16:1 onto serine 186 of Wnt8a [55, 67].

1.3.4 Is the lipid modification required for secretion and activation of the Wnt signaling pathway?

Trafficking of Wnt proteins through the secretory pathway and secretion from cells is a crucial process which involves several interaction partners (**Figure 1.4**). The initial step in this transport route starts with Wnt ligands being co-translationally imported into the lumen of the ER. There, PORCN carries out the lipid modification [36, 43, 50, 64, 65]. The lipidation allows the binding of Wnt to the cargo protein Evi, which acts as a chaperone to assist in Wnt secretion [17, 33, 56, 57, 72]. The Wnt-Evi complex is incorporated into Sec22/COP-II vesicles with the help of Sar1, Sec12, and p24 proteins [73-75], to subsequently transport the complexes from the ER to Golgi. From the Golgi to the plasma membrane, the Wnt-Evi complex is transported in a Rab8 dependent mechanism or are released via a multivesicular body pathway on exosomes to the extracellular space [76, 77]. Once at the plasma membrane, Wnt proteins can be delivered to other target cells in different ways: either by filopodia; forming multimer complexes, or interacting with glypicans, lipoproteins, or lipid-binding proteins such as Swim or Afamin [78, 79].

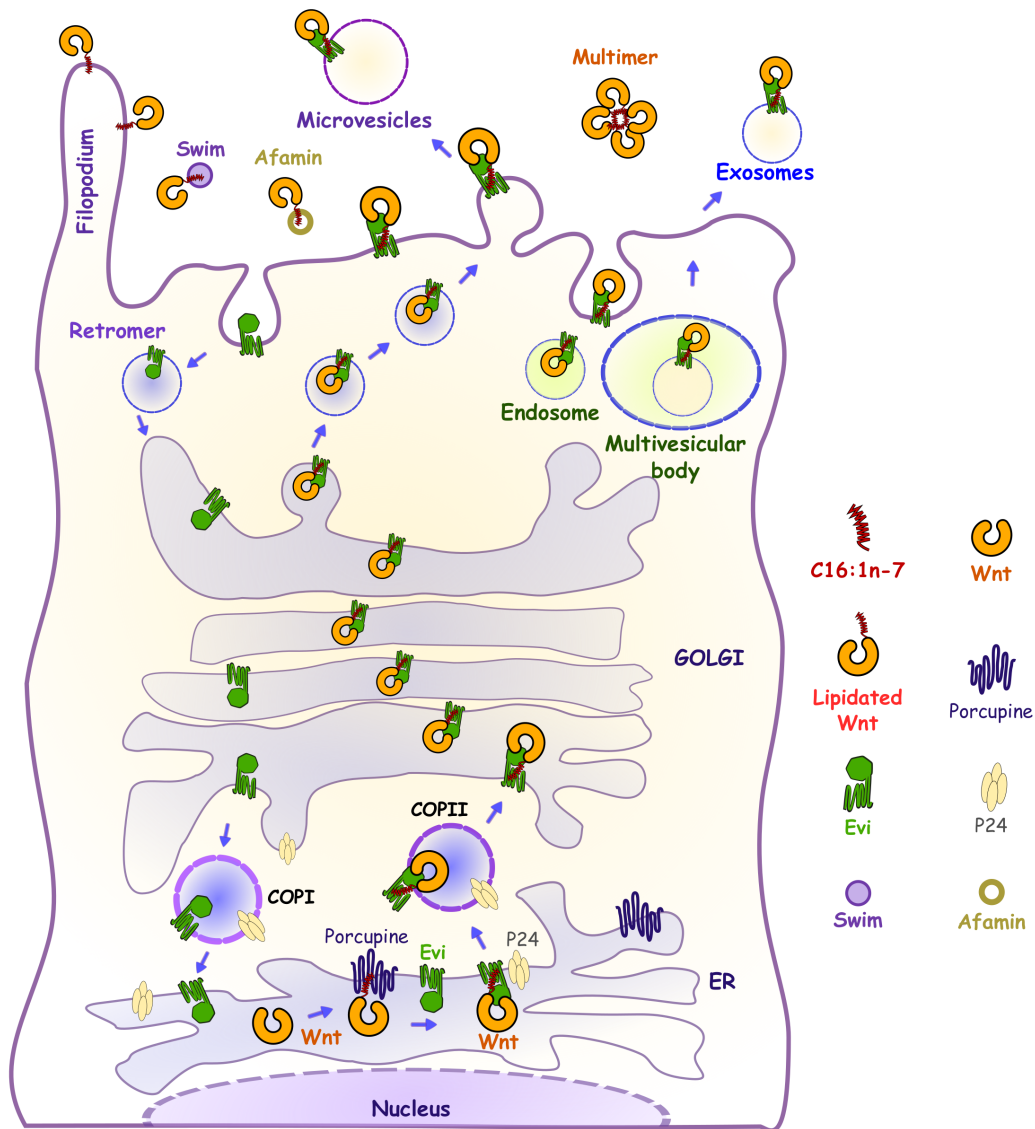


Figure 1.4: Wnt secretion. Wnts proteins can be secreted in different ways: either by exosomes, filopodia, by forming Wnt multimer complexes, or by interacting with glypicans, lipoproteins, or lipid-binding proteins such as Swim or Afamin [69, 70]. Wnts are lipid-modified by the O-acyl-transferase Porcupine in the endoplasmic reticulum (ER). Lipidated Wnts bind to the cargo protein Evi and are transported to the plasma membrane through the Golgi apparatus. After secretion, Evi is re-internalized from the plasma membrane and transported back to the Golgi assisted by the retromer complex. From the Golgi, Evi is recycled back to the ER by COP-I vesicles. Adapted from [25].

Over the years, it has been widely accepted that lipid modification of Wnts is a key requirement for their transport to the extracellular media and the subsequent activation of the signal pathway. However, recent reports suggest that Wnts could be secreted independently of their lipid-modification [52, 53, 80-83]. However, these observations have been linked to specific cellular and tissue contexts. Wnts that have been reported to be secreted independently of the lipid-modification include Wnt1, Wnt2b, Wnt3, Wnt5b and Wnt10b, from human astrocytes and Wnt1, Wnt3, Wnt6, Wnt7a, Wnt10a and Wnt16a from human CD8+ T cells [80]; Wnt3 from zebrafish [52, 53]; Wnt4 from human invasive lobular carcinoma cells (ILC) [82]; Wnt8 from *Xenopus* [81]; WntD from *Drosophila* [83], and in a few reports Wnt3a from human invasive lobular carcinoma cells (ILC) and in HEK293 cells [50, 81, 82]. Both the molecular

mechanisms and the players involved in Wnt secretion independent of lipidation still remain unknown.

While most reports suggest that lipidation of serine 209 is indispensable for the exit of Wnt3a from the ER and its subsequent secretion to extracellular media [17, 32, 43, 57, 72, 84], other studies have shown that mutation at serine 209 either impaired the secretion but not the localization of Wnt3a at the cell surface [32], or that secretion of human Wnt3a was reduced but not fully abolished [50, 81, 82].

Wnt lipidation has also been linked to the activation of the Wnt signaling pathway. Structural studies have shown that the fatty acid attached to Wnt binds to the hydrophobic groove in the CRD of Frizzled receptors [14, 16]. Furthermore, the fatty acid mediates Frizzled dimerization and thereby contributes to initiate the signaling cascade [16, 61, 85]. These results support the hypothesis that Wnts need to be lipidated in order to activate the signaling cascade. Nevertheless, Speer and co-workers, working in *Xenopus* and zebrafish embryos, have shown that non-acylated mutant variants of xWnt8 and hWnt3a are able to bind to the CRD of xFZD8 and thereby retain some residual ability to activate Wnt signaling [81].

Altogether these results suggest that a population of Wnt can be transported to the plasma membrane, secreted into the extracellular media, and there activate signaling pathways by an alternative mechanism that does not involve the lipidation on the conserved, canonical serine residue of Wnt.

1.3.5 Wnt11, an intriguing study case

Wnt11 is a 354 amino acid protein with a molecular mass of around 45 kDa. It is classified into the non-canonical pathway and accordingly, it shares similar features with the non-canonical Wnt5a. One of the shared features is an inhibitory impact on the canonical Wnt/ β -catenin pathway [66-70]. Wnt11 is involved in the development of the mammalian heart, liver and kidney [86-93]. In zebrafish, Wnt11 is part of the PCP (planar cell polarity) pathway and controls convergent extension of the embryonic axis during gastrulation and cardiac differentiation [94-96]. Wnt11 has also been reported to be involved in intestinal host defense mechanisms [97]. In mammalian adults, Wnt11 is expressed in heart, liver, skeletal muscle and pancreas [98].

In 2013 Yamamoto et al. [30] used liquid chromatography and mass spectrometry to assess the lipidation of Wnt11. Purified from conditioned media of polarized L and Madin-Darby Canine Kidney cells (MDCK cells) Wnt11 was found to be lipidated with palmitoleic acid (C16:1) at the canonical serine 215 site [30]. Apart from lipidation, the amino acids N40, N90 and N300 were identified to be glycosylated [30]. Specifically, complex/hybrid glycans for N40, high-mannose sugars for N90 and high-mannose/hybrid glycans for N300 were confirmed by mass spectrometry [30]. Interestingly, mutagenesis experiments demonstrated that N40, which is not conserved among Wnts but instead unique to Wnt11, was crucial to the apical secretion of the protein in MDCK polarized cells [30]. These results indicate that glycosylation of the amino acid N40, in addition to lipidation of S215, is essential for Wnt11 secretion in polarized cells.

Recent unpublished data showed that Wnt11 was secreted in HEK293T Δ PORCN and HEK293T Δ Evi knockout cells, indicating that Wnt11 trafficking occurred independently both of the lipidation

of serine 215 and of the presence of the carrier protein Evi (Dr. Oksana Voloshanenko in the group of Prof. Michael Boutros, German Cancer Research Center (DKFZ), Division Signaling and functional Genomics and Heidelberg University, Heidelberg, Germany). Furthermore, mutation of serine 215 did not abolish the secretion of Wnt11 in HEK293T cells. In TX114 phase separation experiments, the mutant Wnt11 S215A was still detected partially in the detergent phases, suggesting that the proteins retained some hydrophobicity. Together, these results suggested that in HEK293T cells, Wnt11 is acylated at a site different from serine 215 and that besides PORCN another acyltransferase is involved in the lipidation of Wnt11. In addition, these data suggest an alternative secretion mechanism that may not depend on the lipidation of serine 215 and/or on the presence of the carrier protein Evi. Although lipidation in serine 215 is thought to be essential for the inhibitory function of Wnt11 on the canonical Wnt/ β -catenin pathway [66-70], there is currently no direct evidence to confirm this.

1.4 Lipid composition on HEK cells and HCT116 cells

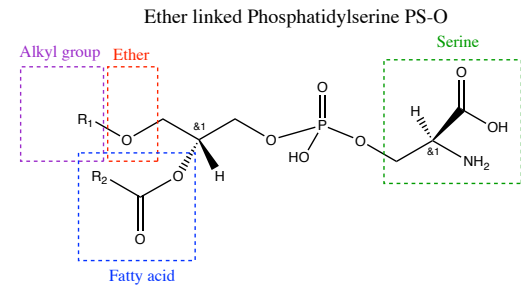
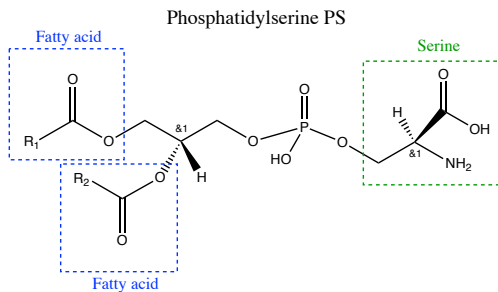
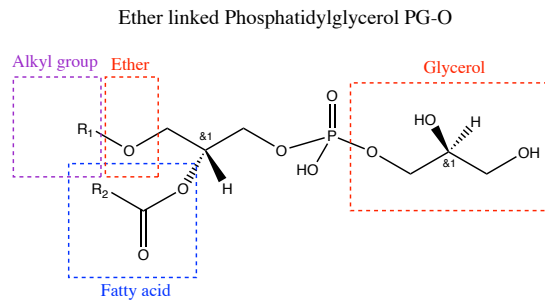
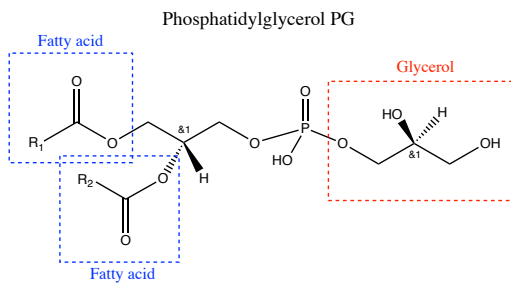
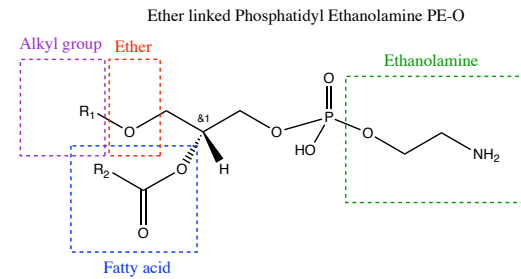
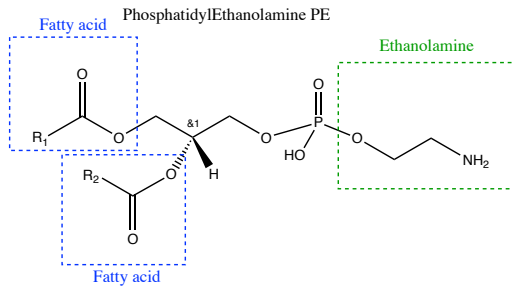
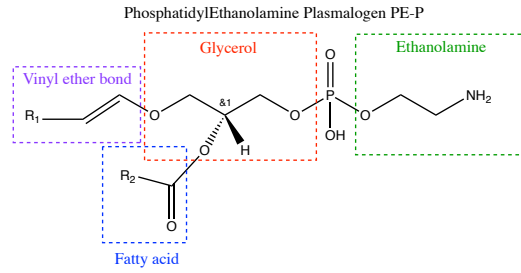
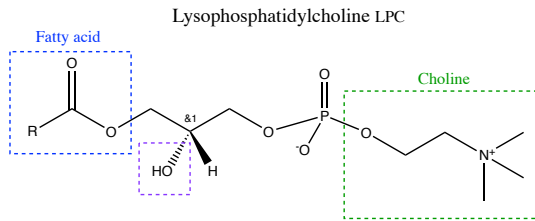
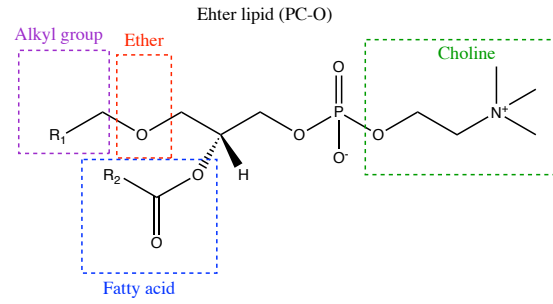
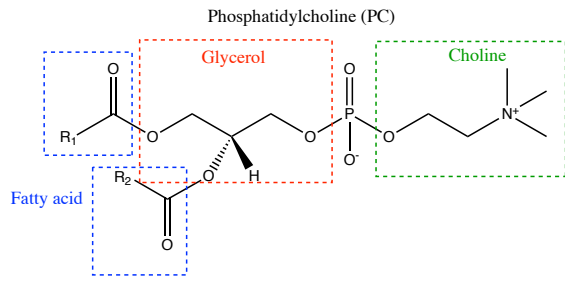
Wnt trafficking and signaling is intricately linked to membranes, and thus alterations of cellular lipid homeostasis, a hallmark of a number of metabolic diseases, is likely to impact Wnt function. Vice versa, signaling pathways activated by Wnt proteins can target lipid metabolism and thus membrane lipid compositions. So far, only a few studies have investigated the influence of the Wnt pathways on the lipid composition of cells, tissues or whole organisms. These studies are framed in specific contexts, such as lipid metabolism of hepatocytes [99], positioning of the mitotic spindle of dividing epiblast cells [100] or fat metabolism in *Drosophila* [101]. In the following, a few examples are briefly described.

The effect of canonical Wnt signaling on the lipid metabolism in hepatocytes after Ras oncogenic activation has been previously studied [99]. In this study, it was found that a high level of Wnt activity reduces the accumulation of lipid droplets in human hepatocellular cancer cells. Also, a Kras-induced lipid accumulation in the liver was significantly compromised in transgenic Zebrafish characterized by activation of the canonical Wnt pathway in hepatocytes [99]. Furthermore, lipidomic and transcriptional analyses revealed that Wnt signaling activation upon Ras oncogenic activity promoted a metabolic shift from triacylglycerol (TAG) to glycerophospholipids. Moreover, Wnt signaling activation upon Ras oncogenic activity caused alterations in saturation levels and lengths of fatty acyl moieties of glycerophospholipids [99]. Another study carried out by Zhang, Ji et al., revealed that hyperactive Wg (the homologue Wnt in *Drosophila*) signaling disrupts fat metabolism and results in fat accumulation in *Drosophila* mutant larvae [101]. Specifically, they observed an increase of free fatty acids and a reduction in triacylglycerols. Also, most of the adipocytes within mutant abdominal fat bodies failed to accumulate fat at the cellular level and remained small [101]. Overall, these studies [99, 101] show a correlation between the activation of Wnt signaling pathways and changes in the lipid metabolism under specific cellular and tissue contexts.

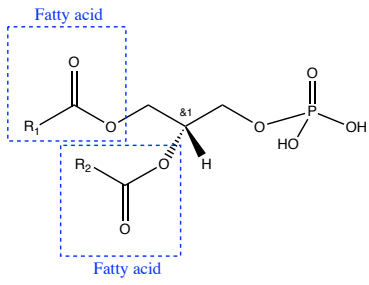
There are other fields in which lipid changes and Wnt signaling have been related to each other, namely during cell division. The palmitoylation of the Anthrax receptor coordinates the positioning of the mitotic spindle of dividing epiblast cells [100]. Wnt signaling affected this process by modulating the activity of serine palmitoyltransferase (SPT) and with this sphingolipid *de novo* synthesis, which in turn had an impact on Anthrax receptor palmitoylation [100].

Another example that links lipid alterations and Wnt secretion involves the p24 protein, a machinery component of COP-I and COP-II dependent vesicular transport, which had also been shown to be important for Wnt trafficking [73]. Changes in the cellular sphingolipids or ether lipid concentrations could affect the vesicular transport in the early secretory pathway through the binding of these lipids to P24 [102, 103] and thus could have a direct impact on Wnt secretion [73, 74].

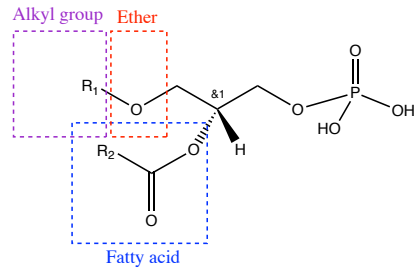
Mammalian membranes are composed of different lipid classes, including glycerophospholipids, sphingolipids, and cholesterol, but also a low amount of glycerolipids. **Figure 1.5** shows the chemical representation of the major mammalian lipid classes, and **Figure 1.6** shows the biosynthesis pathways from which etherlipids, sphingolipids and glycerolipids are they are formed.



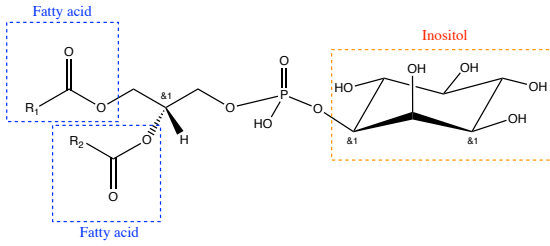
Phosphatidic acid PA



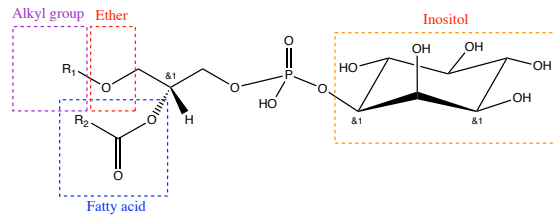
Ether linked Phosphatidic acid PA-O



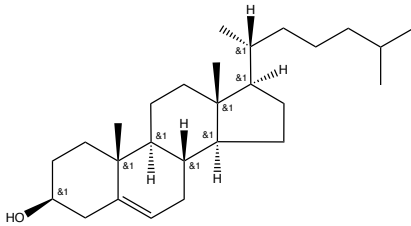
Phosphatidylinositol PI



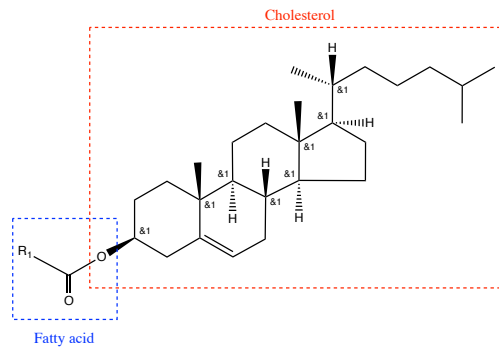
Ether linked Phosphatidylinositol PI-O



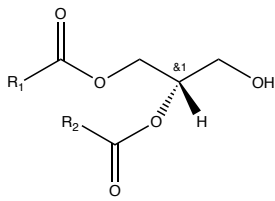
Cholesterol



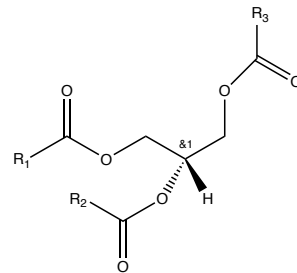
Cholesterol Ester



Diacylglycerol (DAG)



Triacylglycerol (TAG)



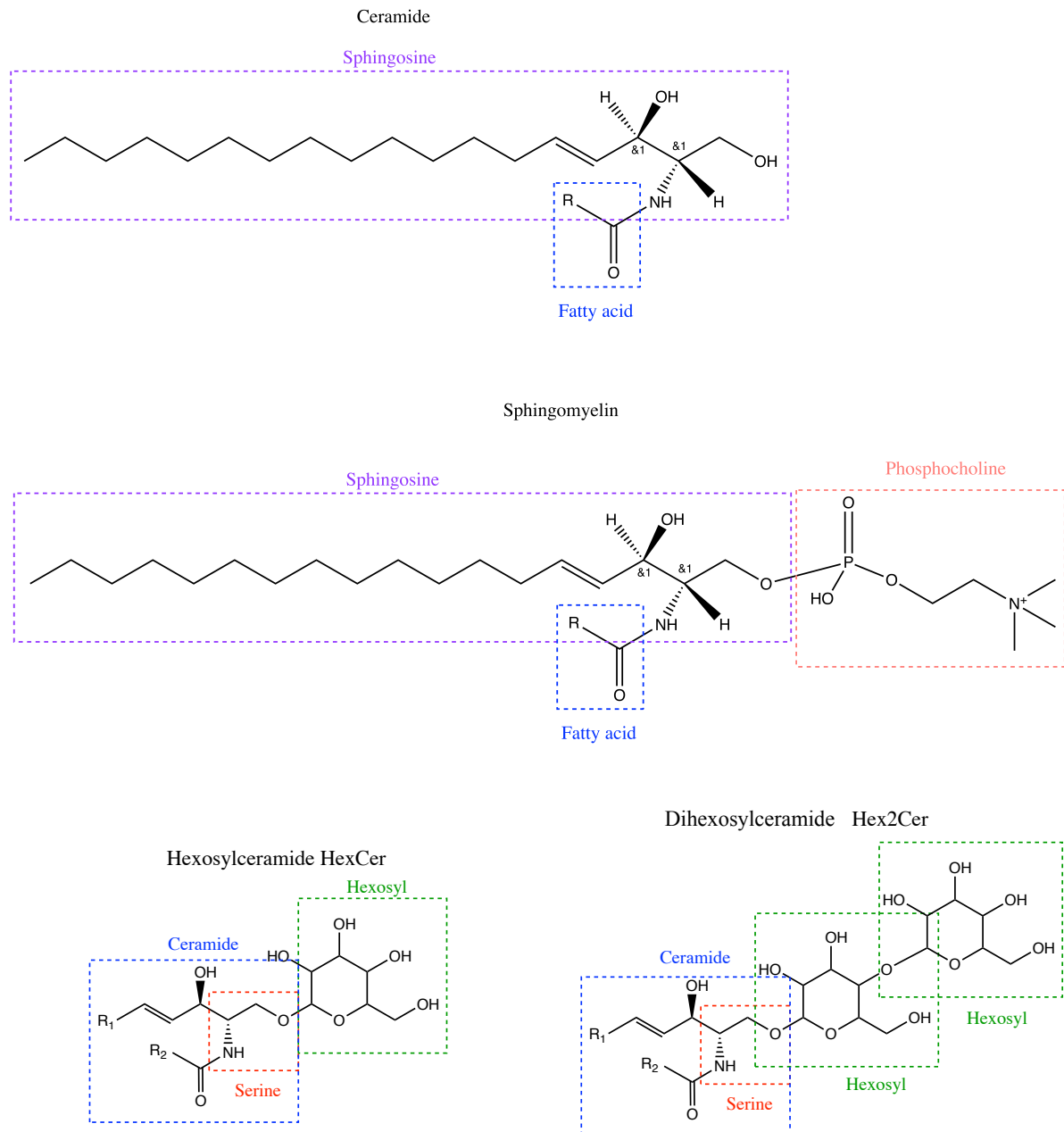


Figure 1.5: Chemical representation of the lipid classes: Phosphatidylcholine (PC), alkyl-Phosphatidylcholine (PC-O), Lysophosphatidylcholine (LPC), Phosphatidylethanolamine Plasmalogen (PE P-), Phosphatidylethanolamine (PE), Ether linked Phosphatidylethanolamine (PE O-), Phosphatidylglycerol (PG), Ether linked Phosphatidylglycerol (PG O-), Phosphatidylserine (PS), Ether linked Phosphatidylserine (PS O-), Phosphatidic acid (PA), Ether linked Phosphatidic acid (PA O-), Phosphatidylinositol (PI), Ether linked Phosphatidylinositol (PI O-), Cholesterol (Chol), Cholesterol Ester (CE), Diacylglycerol (DAG), Triacylglycerol (TAG), Ceramide (Cer), Sphingomyelin (SM), Hexosylceramide (HexCer) and Dihexosylceramide (Hex2Cer).

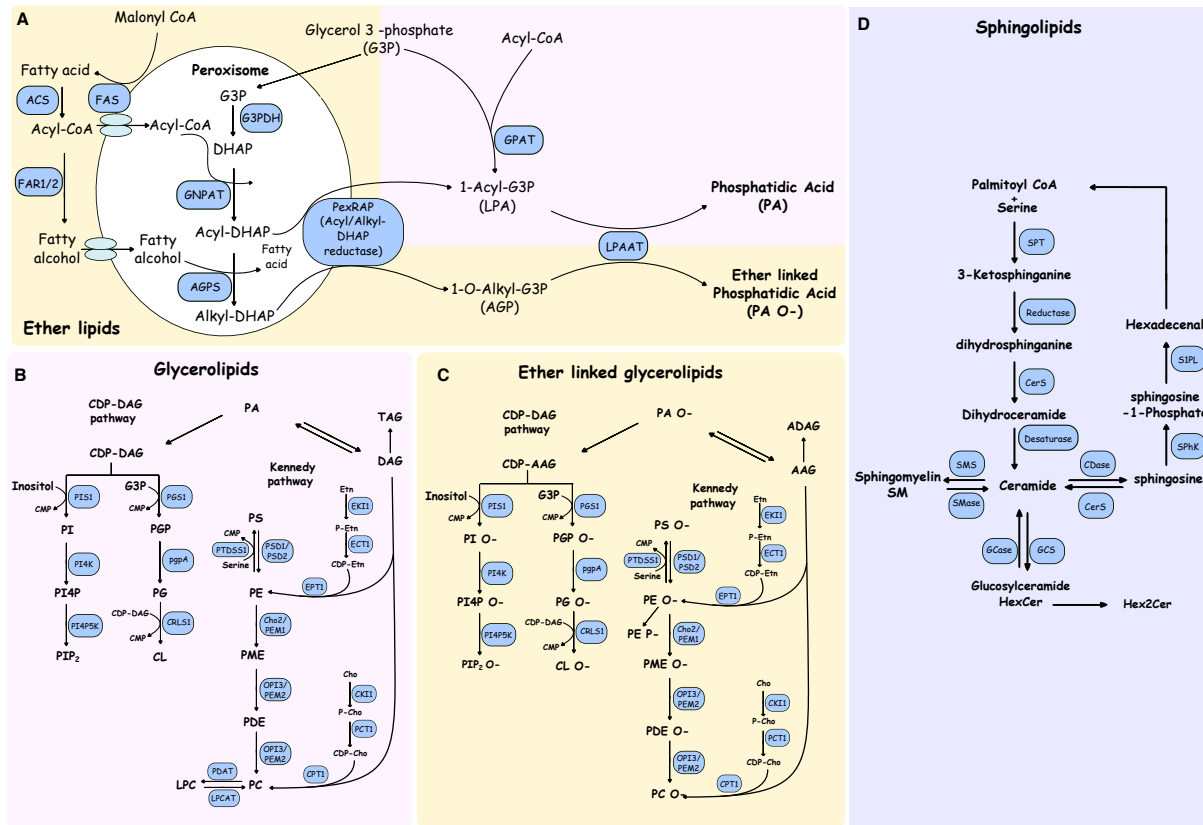


Figure 1.6: Biosynthesis of glycerolipids, ether-linked glycerolipids, and sphingolipids. In pink is the pathway that follows the biosynthesis of glycerolipids, in yellow is the biosynthesis of ether-linked lipids, and in purple is the biosynthesis of sphingolipids. **A. Acyl-DHAP pathway of ether lipid synthesis.** The ether lipid synthesis starts in the peroxisomes and is subsequently completed in the ER. De novo lipogenesis produces fatty acids from **malonyl CoA** by the fatty acid synthase (**FAS**). The generated fatty acids are transformed to fatty **acyl-CoA** by the acetyl-coenzyme A synthetase (**ACS**). The **acyl-CoA** can be incorporated into the peroxisomes or can be converted to **fatty alcohol** by the fatty acyl-CoA reductases **FAR1** or **FAR2**. **Fatty alcohol** is also included in the peroxisomes. Glycerol 3-phosphate (**G3P**) is internalized in the peroxisomes and transformed to dihydroxyacetone phosphate (**DHAP**) by the glycerol 3-phosphate dehydrogenase (**G3PDH**). Using as substrate **Acyl-CoA** and the **DHAP**, the glycerophosphate O-acyltransferase (**GNPAT**) produces **Acyl-DHAP**. The alkylglycerone phosphate synthase (**AGPS**) takes the **Acyl-DHAP** and, together with **fatty alcohol**, exchanges the acyl chain for an alkyl group into **Alkyl-DHAP**, forming the ether bond that gives the name to the ether lipids. An acyl/alkyl DHAP reductase (**PexRAP**) generates the ether lipid precursors, 1-O-alkyl-G3P (**AGP**), or the diacyl phospholipid precursor lysophosphatidic acid (**LPA**). **B. The glycerolipids synthesis occurs in the ER.** Phosphatidic acid (**PA**) can be generated via **LPA** by the lysophosphatidic acid acyltransferase (**LPAAT**). Then **PA** can form **DAG** by the PA phosphatase (**PAP**), or the **PA** can form **CDP-DAG** by phosphatidate cytidyltransferase 1 (**CDS1**). Starting from **DAG** via the Kennedy pathway the enzyme carnitine O-palmitoyltransferase 1 (**CPT1**) can form **PC**, which subsequently can form **LPC** catalyzed by the phospholipid:diacylglycerol acyltransferase 1 (**PDAT**), the enzyme choline/ethanolaminephosphotransferase 1 (**EPT1**) can form **PE**, from **PE** can be form **PS** by phosphatidylserine decarboxylase proenzyme 1 (**PSD1**) [104]. Via the **CDP-DAG** pathway, the enzyme CDP-diacylglycerol--glycerol-3-phosphate 3-phosphatidyltransferase (**PGS1**) catalyzed the production of **PGP**, which subsequently form **PG** through phosphatidylglycerophosphatase A (**pgpA**) [105]. The Cardiolipin synthase (**CLS1**) can form cardiolipins **CL** from **PG** [105]. Also, by the **CDP-DAG** pathway is form **PI** through CDP-diacylglycerol--inositol 3-phosphatidyltransferase (**PIS1**)[105]. The **PI** can be converted to **PIP₂** by the kinases Phosphatidylinositol 4-kinase (**PI4K**) and phosphatidylinositol 4 phosphate -kinase (**PI4P5K**) [105]. **C. The formation of ether linked glycerolipids** is similar to the glycerolipids synthesis just that it begins with the **PA O-** which can form **CDP-AGG** or **AGG**. Through the **CDP-AGG** pathway is formed **PI O-**, **PGP O-**, and **PG O-**. Through the Kennedy pathway is formed **PC O-**, **PE O-**, **PE P-** and **PS O-**. **D. The sphingolipids biosynthesis** starts with the formation of **3-ketosphinganine** from **palmitoyl-CoA** and **serine**, the enzyme serine palmitoyltransferase (**SPT**) catalyzes this reaction. Then **3-ketosphinganine** is transformed to **dihydrosphinganine** by the 3-ketosphinganine reductase (**TSC10**). The **dihydrosphinganine** is transformed to **dihydroceramide** by the

ceramide synthase (**CerS**). Then **dihydroceramide** is transformed to **ceramide** by the dihydroceramide desaturase (**DDase**). The **ceramide** can be transformed into **sphingosine** by neutral ceramidase (**CDase**), or into **sphingomyelin** by the sphingomyelin synthase (**SMS**), or into **hexosylceramides** by the Glc-ceramide synthase (**GCase**).

1.5 Aim of the thesis

1. Despite the extensive data available, the debate around the lipid-modified amino acids in Wnt proteins has not yet reached a consensus. The recent results from O. Voloshanenko (M. Boutros group, DKFZ, Heidelberg) suggests that apart from the canonical serine residue there may be other Wnt residues that are lipidated, apart from the canonical serine residue. Furthermore, the specific acylation type, either saturated or unsaturated, that binds to Wnts remains inconclusive. The first goal of my doctoral thesis addresses these two issues. I aim to define other putative acylation types and lipid-modified sites in Wnt proteins. To achieve this, I employed a combination of chemical biology tools and mutagenesis experiments, and mass spectrometry measurements. This combined approach represented a first step towards a detailed characterization of the types and sites of acyl modifications of Wnt proteins.

2. Unpublished data by O. Voloshanenko (M. Boutros group, DKFZ, Heidelberg) suggest that Wnt11 is secreted independently of Evi, PORCN, and lipidation of the canonical serine. The second goal of the thesis aims at testing whether other amino acids or acyltransferases, besides PORCN, are involved in this process. To this end, a combination of biochemical approaches and cell biology assays were used.

3. Finally, the third goal of my Ph.D. thesis focuses on exploring a functional link of Wnt expression and trafficking and cellular lipid homeostasis in HEK293T and HCT116 cells. To this end, the lipid composition of cells overexpressing Wnt proteins and cells depleted of PORCN and Evi was determined by mass spectrometry-based lipidomics.

1.6 Organization of the thesis

The thesis is organized as follows. Chapter 2 describes the material and methods. In chapter 3, the results of this investigation are presented in three sections; the first section focuses on the lipidation site of Wnt11 and the role of fatty acid saturation on Wnt11 lipidation. This is a link with the first goal of the thesis. The following section presents other molecular factors that contribute to the secretion and function of Wnt11. This is a link to the second goal of the thesis. The last section is focused on the relation of Wnt proteins and the role of PORCN and Evi with the lipidome composition of cells. This section is linked to the third goal of my thesis. In chapter 4, is presented the discussion and main concluding remarks of this thesis.

2 Material and Methods

Materials

The following tables contains the list of chemicals, antibodies, buffer solutions, cell lines and consumables used in this thesis.

Table 2.1: Chemical reagents

Name	CAS Registry Number or order number	Manufacturer	Storage
1,4-Dithio-D,L-threitol	3483-12-3	Gerbu, Heidelberg, Germany	4 °C
2-Amino-2-(hydroxymethyl)propane-1,3-diol	77-86-1	Roth, Karlsruhe, Germany	RT
2-Mercaptoethanol	60-24-2	MerckMillipore, Darmstadt, Germany	4 °C
3-Morpholinopropanesulfonic acid (MOPS)	A1076	AppliChem GmbH	RT
5x siRNA Buffer	B-002000-UB-100	Horizon Discovery	4 °C
ABC99 inhibitor Notum	SML2410	Sigma-Aldrich	-20 °C
Acetic acid	64-19-7	MerckMillipore, Darmstadt, Germany	RT
Acetonitrile	75-05-8	Sigma-Aldrich	RT
Acrylamide-bisacrylamide	79-06-1	Sigma-Aldrich	4 °C
Agar	A0949,0500	AppliChem GmbH	RT
Agarose	9012-36-6	Roth, Karlsruhe, Germany	RT
Albumin fraction V	9048-46-8	Roth, Karlsruhe, Germany	4 °C
Alkaline Phosphatase, Calf Intestinal (CIP)	M0290L	NEB, Ipswich, USA	-20 °C
Ammonium bicarbonate	1066-33-7	Honeywell Fluka™	4 °C
Ammoniumperoxodisulfat (APS)	7727-54-0	Roth, Karlsruhe, Germany	4 °C
Ampicillin sodium salt	69-52-3	SigmaAldrich, Munich, Germany	4 °C
AsiSI	R0630S	NEB, Ipswich, USA	-20 °C
Bacto Agar	214010	BD Biosciences, Franklin Lakes, USA	RT
Bacto Tryptone	211705	BD Biosciences, Franklin Lakes, USA	RT
Bacto Yeast Extract	212750	BD Biosciences, Franklin Lakes, USA	RT
BamHI-HF	R3136L	NEB, Ipswich, USA	-20 °C
Benzonase® Endonuclease, 250 U/μL	70764	Sigma-Aldrich	-20 °C
Benzonase® Nuclease, 250 U/μL	E1014	Sigma-Aldrich	-20 °C
BglII	R0144L	NEB, Ipswich, USA	-20 °C
Bicine	sc-216087A	Santa Cruz Biotechnology	RT
BIS-Tris	sc-216088A	Santa Cruz Biotechnology	RT
Bond-Breaker TCEP Solution	77720	Thermo Fisher Scientific	4 °C
Bromophenol blue	115-39-9	Waldeck, Muenster, Germany	RT

Buffer EB	19086	Qiagen, Hilden, Germany	RT
Calcium chloride dihydrate	10035-04-8	SigmaAldrich, Munich, Germany	RT
Carbenicillin; dinatriumsalz	A1491,0010	AppliChem GmbH	4 °C
Cell Dissociation Buffer, Enzyme-free, PBS-based	13151-014	Gibco, Waltham, USA	RT
Chloroform (CHCl ₃) VWR	31717-44-9	MERK	RT
cOComplete™, EDTA-free Protease Inhibitor Cocktail	11873580001	Roche, Rotkreuz, Switzerland	4 °C
cOComplete™, Mini Protease Inhibitor Cocktail	11836153001	Sigma-Aldrich	4 °C
Coomassie brilliant blue G-250	6104-59-2	ThermoFisher Scientific	RT
Copper(II) sulfate pentahydrate (CuSO ₄)	7758-98-7	Sigma-Aldrich	RT
Crystal violet	H412	Sigma-Aldrich	RT
CutSmart	B7204S	NEB, Ipswich, USA	-20 °C
DAPI	28718-90-3	ThermoFisher Scientific	4 °C
Dichloro(1,10-phenanthroline)copper(II)	14783-09-6	Sigma Aldrich, Munich, Germany	RT
Dimethyl sulfoxide (DMSO)	67-68-5	SigmaAldrich, Munich, Germany	RT
DNA Polymerase I, Large (Klenow) Fragment	M0210S	NEB, Ipswich, USA	-20 °C
Dodecylsulfate-Na-salt (in pellets)	151-21-3	Serva, Heidelberg, Germany	RT
Dpnl	R0176L	NEB, Ipswich, USA	-20 °C
DTT BioChemica	A2948,0005	AppliChem GmbH	4 °C
Dulbecco's Modified Eagle's Medium (low glucose)	D6046	SigmaAldrich, Munich, Germany	4 °C
Dulbecco's Phosphate Buffered Saline	D8537	SigmaAldrich, Munich, Germany	
EcoRI-HF	R3101S	NEB, Ipswich, USA	-20 °C
EcoRV-HF	R3195L	NEB, Ipswich, USA	-20 °C
EDTA, Tetrasodium Tetrahydrate Salt	sc-204735	Santa Cruz Biotechnology	4 °C
Ethanol absolute	20.821.330	VWR™	RT
Fetal bovine serum (FBS), Lot: CBX9154	F7524-500 mL	Merck Millipore/Sigma	-20 °C
Fetal Bovine Serum, charcoal stripped	12676029	Gibco, Waltham, USA	-20 °C
Fixation reagent for histology (PFA 4 %)	12004	Morphisto	RT
FuGENE® HD Transfection Reagent	E2312	Promega, Mannheim, Germany	4 °C
GelPilot® Loading Dye, 5x	1037650	QIAGEN	-20 °C
GeneRuler 100 bp DNA ladder	SM0243	Thermo Fisher Scientific	-20 °C
Gibco™ DMEM, high glucose	41965062	Thermo Fisher Scientific	4 °C
Gibco™ PBS, pH 7.4	10010056	Thermo Fisher Scientific	RT
Gibco™ RPMI-1640, without l-glutamine	31870074	Thermo Fisher Scientific	4 °C
Gibco™ Trypsin-EDTA (0.25 %), Phenolred	25200056	Thermo Fisher Scientific	-20 °C
Glycerol	56-81-5	SigmaAldrich, Munich, Germany	RT
Glycine	56-40-6	Labochem international	RT
HEPES	7365-45-9	Roth, Karsruhe, Germany	RT

Hydrochloric acid	7647-01-0	Honeywell, Morristown, USA	RT
Hydrochloric acid (HCl)	H/1200/PC15	Fisher Chemical	RT
Immobilon Western Chemiluminescent HRP Substrate	WBKLS0100	Merck Millipore	4 °C
Kanamycin sulfate	60615	SigmaAldrich, Munich, Germany	RT
PORCN inhibitor LGK974	Custom	Wuxi AppTec (Tianjin)	4 °C
Lipofectamine RNAiMAX	13778075	Thermo Fisher Scientific	4 °C
Magnesium chloride hexahydrate	7791-18-6	MerckMillipore, Darmstadt, Germany	RT
Manganese(II)chloride tetrahydrate	13446-34-9	SigmaAldrich, Munich, Germany	RT
Methanol	67-56-1	VWR Chemicals	RT
MluI-HF	R3198S	NEB, Ipswich, USA	-20 °C
N-Ethylmaleimide	128-53-0	SigmaAldrich, Munich, Germany	4 °C
NEB, Ipswich, USAuffer™ 3.1	B7203S	NEB, Ipswich, USA	-20 °C
Nitric acid, min 65 %	30709-1L	Sigma-Aldrich	RT
Nonidet P-40 Substitute	11754599001	Roche, Rotkreuz, Switzerland	4 °C
NotI-HF	R3189L	NEB, Ipswich, USA	-20 °C
NuPAGE™ Antioxidant	NP0005	Invitrogen, Waltham, USA	4 °C
NuPAGE™ LDS Sample Buffer (4X)	NP0008	Invitrogen, Waltham, USA	4 °C
NuPAGE™ Tris-Acetate SDS Running Buffer (20X)	LA0041	Invitrogen, Waltham, USA	4 °C
One Shot TOP10 Chemically Competent Escherichia coli	C404006	Thermo Fisher Scientific	-20 °C
Opti-MEM™ Reduced Serum Medium	31985070	Gibco, Waltham, USA	4 °C
PageRuler plus prestained protein ladder, 10 to 250 kDa	26619	Thermo Fisher Scientific	-20 °C
Palmitic Acid Alkyne	13266	Cayman chemicals	-20 °C
Palmitic Acid, [9,10-3H(N)]-	NET043	PerkinElmer, Waltham, USA	-20 °C
Palmostatin B, APT1 Inhibitor.	178501	SigmaAldrich	-20 °C
Paraformaldehyde (PFA) BioChemica	A3813,1000	AppliChem GmbH	RT
Penicillin-Streptomycin	P4333	SigmaAldrich, Munich, Germany	-20 °C
PfuPlus! DNA Polymerase	E1118-02	EurX, Gdansk, Poland	-20 °C
Phosphingosine, D-erythro [3-3H]	ART2048	American Radiolabeled Chemicals, St.Louis, USA	-20 °C
Pierce™ High Capacity NeutrAvidin™ Agarose	29202	ThermoScientific, Waltham, USA	4 °C
Pierce™ Western Blot Signal Enhancer	21050	Thermo Fisher Scientific	RT
PmeI	R0560S	NEB, Ipswich, USA	-20 °C
Poly D-lysine	A-003-E	Millipore	4 °C
Polyethylenimine, Linear, MW 25000	9002-98-6	Polysciences, Warrington, USA	RT
Ponceau S solution	P7170-1L	Sigma-Aldrich	RT
Potassium acetate	127-08-2	SigmaAldrich, Munich, Germany	RT

Potassium chloride (KCl)	P-9541	Sigma-Aldrich	RT
Powdered milk	T145.2	Roth, Karlsruhe, Germany	RT
Precision Plus Protein™ All Blue Prestained Protein Standards	1610373	Bio-Rad, Hercules, USA	-20 °C
Propan-2-ol	33539	Honeywell Research Chemicals	RT
Q5® High-Fidelity DNA Polymerase	M0491A	NEB, Ipswich, USA	-20 °C
Q5® Reaction Buffer	B9027S	NEB, Ipswich, USA	-20 °C
Restore™ Plus Western Blot Stripping-Buffer	46430	Thermo Fisher Scientific	RT
Roche, Rotkreuz, Switzerland X-treme Gene HP	6366244001	Roche, Rotkreuz, Switzerland	4 °C
Rubidium chloride	7791-11-9	AlfaAesar, Karlsruhe, Germany	RT
Seebblue plus2 standard	LC5925	Thermofisher	-20 °C
S.O.C. Medium	15544034	Thermo Fisher Scientific	4 °C
Sodium chloride	7647-14-5	Fisher Chemicals, Loughborough, UK	RT
Sodium Deoxycholate	302-95-4	SigmaAldrich, Munich, Germany	RT
Sodium dodecyl sulfate (SDS)	75746-250G	Sigma-Aldrich	RT
Sodium hydroxide	1310-73-2	SigmaAldrich, Munich, Germany	RT
Sodium phosphate dibasic dihydrate	10028-24-7	Honeywell, Morristown, USA	RT
Spectinomycin Dihydrochloride	22189-32-8	Fisher Bioreagents, Schwerte, Germany	4 °C
Standardized Fetal Bovine Serum	S0615	Biochrom, Berlin, Germany	-20 °C
SuperSignal West Femto Maximum Sensitivity Substrate	34095	Thermo Fisher Scientific	4 °C
T4 DNA ligase	M0202S	NEB, Ipswich, USA	-20 °C
T4 DNA Ligase Reaction Buffer	B0202S	NEB, Ipswich, USA	-20 °C
Taq DNA Polymerase	22466	Axon, Kaiserslautern, Germany	-20 °C
TRANSIT-LT1 transfection reagent, 10 mL	731-0029	VWR™	4 °C
Triton X100	9036-19-5	MerckMillipore, Darmstadt, Germany	RT
Trizma® base (Tris)	T1503-1KG	Sigma-Aldrich	RT
Trypsin-EDTA solution	T3924	Sigma Aldrich, Munich, Germany	4 °C
Tryptone	8952	Carl Roth GmbH + Co. KG	RT
Tween-20	127.1	Roth, Karlsruhe, Germany	RT
Ultima Gold™ Universal LSC-Cocktail	USA 6013329	PerkinElmer, Waltham	RT
Urea	57-13-6	SigmaAldrich, Munich, Germany	RT

Table 2.2: Antibodies

Antibody	Reference	Working dilution	Company	Source	Target protein or epitope
Western blot					
Wnt11	GTX105971	1:1000	Genetex, (Alton Pkwy Irvine, USA)	Rabbit	Human Wnt11
HSC70 (B-6)	sc-7298	1:1000	SantaCruz, (Heidelberg, Germany)	Mouse	Human HSC70
Wnt3a/ Wnt3	ab28472	1:1000	Abcam (Cambridge, UK)	Rabbit	Mouse and human Wnt3a
Wnt3a	GTX128101	1:1000	Genetex (Alton Pkwy Irvine, USA)	Rabbit	Human Wnt3a
β -actin-HRP	sc-47778	1:10000	SantaCruz (Heidelberg, Germany)	Mouse	Gizzard Actin of chicken origin
Wnt5a/b (C27E8)	(C27E8) #2530	1:1000	Cell Signaling (Beverly, Massachusetts, United States)	Rabbit	Human Wnt5a/b
Evi	65590	1:1000	BioLegend (San Diego, CA, USA)	Mouse	Human Wntless protein
Peroxidase AffiniPure Goat Anti-Mouse IgG (H+L)	115-035-003	1:10000	Jackson/Dianova, (Cambridgeshire, United Kingdom)	Goat	Mouse IgG
Peroxidase AffiniPure Goat Anti-Rabbit IgG (H+L)	111-035-003	1:10000	Jackson/Dianova, (Cambridgeshire, United Kingdom)	Goat	Rabbit IgG
Anti-Rabbit DyLight 680 conjugated	680-18-4416-32	1:10000	Rockland (Pennsylvania, USA)	Mouse	Rabbit IgG

Anti_rabbit IgG IRDye 800CW	611-131-002	1:10000	Rockland (Pennsylvania, USA)	Goat	Rabbit IgG
Streptavidin-HRP	S000-03	1:10000	Rockland (Pennsylvania, USA)	Streptomyces avidinii	Anti-Biotin
IRDye 800CW Streptavidin	925-32230	1:5000	LI-COR (Nebraska, USA)	_____	Anti-Biotin
Immunoprecipitation					
Wnt11	GTX105971	1:700	Genetex	Rabbit	Human Wnt11
Wnt3	GTX128100	1:700	Genetex	Rabbit	Human Wnt3

Table 2.3: Beads for protein purification

Name	Specificity	Type of beads	Reference	Supplier
Dynabeads Protein G	Immunoglobulin Fc-region	Magnetic beads	10004D	Thermo Fisher Scientific
BLUE SE-PHAROSE 6 Fast Flow	General protein purification from supernatant	Sepharose	17-0948-01	GE Healthcare

Table 2.4: Buffer solutions

Name	Composition
Blocking solution (IF staining)	1 % goat serum, 3 % FCS, 0.1 % Triton X100, all volume fraction in PBS
Blocking solution (Western blot)	5 % skim milk/TBST (mass fraction)
Wash buffer	50 mM Tris-HCl, pH 7.5; 150 mM KCl; volume fraction of 1 % Triton X100 in ddH ₂ O
Lysis buffer with EDTA	20 mM Tris-HCl, pH 7.4; 130 mM NaCl; 2 mM EDTA; supplemented before use with a volume fraction of 1 % of Triton X100, 1 complete™, mini-Protease Inhibitor Cocktail tablet per 10 mL buffer.
Lysis buffer without EDTA (For Wnt Immunoprecipitation and click reaction)	20 mM Tris-HCl, pH 7.4; supplemented before use with a volume fraction of 1 % of Triton X100, 1 complete™, mini Protease Inhibitor Cocktail tablet per 10 mL buffer, 50 μM APT1 Inhibitor- Palmostatin B (MW: 376.53 g/mol), 10μM ABC99 inhibitor Notum (MW: 456.88 g/mol)
Fixation solution	4 % PFA/PBS (mass fraction)
HRP inactivation so-lution	5 % acetic acid/H ₂ O (volume fraction)
Laemmli buffer (5x)	312.5 mM Tris-HCl, pH 6.8; 0.5 M DTT; mass fraction of 10 % SDS, and 0.1 % bromphenol blue; volume fraction of 10 % TCEP, and 50 % glycerol
Laemmli buffer (5x) without DTT	312.5 mM Tris-HCl, pH 6.8; mass fraction of 10 % SDS, and 0.1 % bromphenol blue; volume fraction of 10 % TCEP, and 50 % glycerol
LB medium liquid	1 % Tryptone, 1 % NaCl, 0.5 % yeast ex-tract in ddH ₂ O (all mass fraction), pH 7.0
LB medium solid (for agar plates)	1 l LB medium liquid, 15 g Agar, antibiotics as needed
MOPS SDS running buffer (20x)	1 M MOPS, 1 M Tris-Base, 20 mM EDTA, 69.3 mM SDS in ddH ₂ O

NuPAGE transfer buffer (20×)	500 mM Bicine, 500 mM Bis-Tris, 20 mM EDTA (supplement with 10 % volume fraction methanol before use)
PBS (1×)	1.0588236 mM KH ₂ PO ₄ , 155.17241 mM NaCl, 2.966418 mM Na ₂ HPO ₄ -7H ₂ O (Thermo Fisher Scientific, 10010056)
Stock solution TRIS-HCL pH=7,4 buffer, 500 mL.	10 mL of TRIS-HCL pH=7,4 (20 mM) 4,97 g, NaCl (130 mM) Water until 500 mL
TBS	50 mM Tris-HCL, pH 7.4 and 150 mM NaCl in ddH ₂ O
TBST (10×)	1,37 M NaCl, 200 mM Tris-HCL, pH 7.6, and 1 % Tween-20 (volume fraction)

Table 2.5: Cell lines

Cell line	Specification	Source	Culture medium
HEK293T	Embryonic kidney	ATCC® CRL 11268™	DMEM, 10 % FBS
HEK293T ^{ΔPORCN_2}	PORCN KO_clone_2	Boutros group, DKFZ	DMEM, 10 % FBS
HEK293T ^{ΔEvi}	Evi KO	Boutros group, DKFZ	DMEM, 10 % FBS
HEK293T ^{Wnt11}	Constitutive expression of Wnt11	Boutros group, DKFZ	DMEM, 10 % FBS
HEK293T ^{ΔPORCN_1_Wnt11}	PORCN KO_clone_2 with constitutive expression of Wnt11	Boutros group, DKFZ	DMEM, 10 % FBS
HCT116	Colon cancer cells	ATCC® CCL-247™	McCoy's, 10% FBS
HCT116 ^{ΔEvi_2.1}	Evi KO clone 2.1	Boutros group, DKFZ	McCoy's, 10% FBS
HCT116 ^{ΔEvi_2.2}	Evi KO clone 2.2	Boutros group, DKFZ	McCoy's, 10% FBS
HCT116 ^{ΔEvi_2.3}	Evi KO clone 2.3	Boutros group, DKFZ	McCoy's, 10% FBS
RPMI7951	Malignant melanoma	ATCC® HTB-66™	DMEM, 10 % FBS
Pool of cells treated with sgRNA without clonal selection			
HEK293T ^{ΔPORCN_sgRNA_192}	Human embryonic kidney cells treated with sgRNA 192 targeting PORCN	Boutros group, DKFZ	DMEM, 10 % FBS
HEK293T ^{ΔPORCN_sgRNA_11}	Human embryonic kidney cells treated with sgRNA 11 targeting PORCN	Boutros group, DKFZ	DMEM, 10 % FBS
HEK293T ^{ΔPORCN_sgRNA_35}	Human embryonic kidney cells treated with sgRNA 35 targeting PORCN	Boutros group, DKFZ	DMEM, 10 % FBS

Table 2.6: Consumables

Consumables Name	Reference	Supplier
Amersham Hyperfilm ECL	28906836	Cytiva/GE Healthcare
Amersham Protran 0.45 nitrocellulose membranes	10600002	Cytiva/GE Healthcare
Autoklavierband Rolle	27005	neoLab Migge GmbH
Bad Stabil®	16095	neoLab Migge GmbH
Beschriftungsklebeband Rainbow-Pack	817-0027	VWR™
Bolt 4-12 % Bis-Tris plus gels, 10-well	NW04120BOX	Thermo Fisher Scientific
Bolt 4-12 % Bis-Tris plus gels, 12-well	NW04122BOX	Thermo Fisher Scientific
Bolt 4-12 % Bis-Tris plus gels, 15-well	NW04125BOX	Thermo Fisher Scientific
Cell Culture Multiwell Plate, 12 Well, CELLSTAR®	665180	Greiner Bio-One International GmbH
Cell Culture Multiwell Plate, 24 Well, CELLSTAR®	662160	Greiner Bio-One International GmbH

Cell Culture Multiwell Plate, 6 Well, CELLSTAR®	657160	Greiner Bio-One International GmbH
Cell scraper	99002	TPP®
Cover slip, round, 12 mm	9161064	Gerhard Menzel
Disposable scalpel	200140021	Feather®
Falcon® 100 mm TC-treated Cell Culture Dish	353003	Corning, Inc.
Falcon® 14 mL Round-Bottom Tube	352059	Corning, Inc.
Falcon® 25cm ² Rectangular Canted Neck Cell Culture Flask with Vented Cap	353108	Corning, Inc.
Falcon® 75cm ² Rectangular Canted Neck Cell Culture Flask with Vented Cap	353136	Corning, Inc.
Falcon® 96-well Clear Flat Bottom TC-treated Culture Microplate, with Lid	353072	Corning, Inc.
Falcon® Serological Pipet 1 mL	357521	Corning, Inc.
Falcon® Serological Pipet 10 mL	357551	Corning, Inc.
Falcon® Serological Pipet 2 mL	357507	Corning, Inc.
Falcon® Serological Pipet 25 mL	357525	Corning, Inc.
Falcon® Serological Pipet 5 mL	357543	Corning, Inc.
Falcon® Serological Pipet 50 mL	357550	Corning, Inc.
Filter tip PP, premium surface, 0.1-10 µl	07-612-8300	nerbe plus GmbH & Co. KG
Filter tip PP, premium surface, 0-20 µl	07-622-8300	nerbe plus GmbH & Co. KG
Filter tip PP, premium surface, 0-200 µl	07-662-8300	nerbe plus GmbH & Co. KG
Filter tip PP, premium surface, 100-1000 µl	07-693-8300	nerbe plus GmbH & Co. KG
Finn tip™ pipette tips	613-2597	VWR™
Folded Filters	4.303.090	MUNKTELL & FILTRAK GmbH
Gel Saver II Tip 1-200µl, protein gel loading tip)	11022-0600	STARLAB International GmbH
Grade 3 mm Chr Cellulose, Chromatography Papers	3030-917	Cytiva/GE Healthcare
Hand towel zigzag fold	66424	Essity Hygiene and Health
Injekt-F Tuberculin (1 mL)	9166017V	BRAUN Melsungen AG
LEITZ 4020, flush fold, Sichthüllen	1079554	Lyreco
Lid for microplate, low profile	656191	Greiner Bio-One International GmbH
LightCycler® 480 Sealing Foil	4729757001	Roche
Medoject 25Gx1"	CH25100	Chirana T. Injecta, a.s.
Microplate, 96 well, clear, F-bottom	655101	Greiner Bio-One International GmbH
Millex-GP Syringe Filter Unit, 0.22 µm	SLGP033RS	Merck Millipore
Müllbeutel Blau 100 L	400.350	DKFZ Lager
Nalgene™ General Long-Term Storage Cryogenic Tubes, 1.2 mL	11740573	Thermo Fisher Scientific
PARAFILM® M	PM996	Merck Millipore
PCR 384-Well TW-MT-Plate, white, for RT-qPCR	712456X	Biozym Scientific GmbH
PCR tubes 12er SoftStrips	711068	Biozym Scientific GmbH
Petri dish, 94 x 16 mm, without vent	632180	Greiner Bio-One International GmbH
Safe-Lock microcentrifuge tubes 1.5 mL	0030 120.086	Eppendorf AG
Safe-Lock microcentrifuge tubes 2 mL	0030 120.094	Eppendorf AG
Spezial Vernichtungsbeutel/ disposal bags	646201	Greiner Bio-One International GmbH
Super Frost Plus™, Adhesion slides	J1800AMNZ	Thermo Fisher Scientific
Syringe, 20 mL, with BD Luer-Lok™ Tip	BDAM302830	V_W_R_™
TipOne® Tip, 10 µl Graduated, Refill (non-sterile)	S1111-3700	STARLAB International GmbH
TipOne® Tips, 1000 µl Blue Graduated, Refill (non-sterile)	S1111-6701	STARLAB International GmbH
TipOne® Tips, 200 µl Yellow, Refill (non-sterile)	S1111-0706	STARLAB International GmbH
TUBE, 15 mL, Centrifuge Tube, CELLSTAR®	188271	Greiner Bio-One International GmbH

TUBE, 50 mL, Centrifuge Tube, CELLSTAR®	227261	Greiner Bio-One International GmbH
Vernichtungsbeutel, 200X300; autoclavable bags	09-302-0020	nerbe plus GmbH & Co. KG
XCEED® Nitrile Gloves, L	XC-INT-L	STARLAB International GmbH

Methods

2.1 Cell lines, culture media, and cell handling

Human embryonic kidney (HEK293) cells, human colon cancer cells (HCT116 cell line), and RPMI-7951 melanoma cells were used throughout this thesis. These cells were considered either in their wild-type form or with the proteins PORCN and Evi knocked out (see a summary of all cell lines in **Table 2.5**). Cells were kindly provided by Dr. Oksana Voloshanenko and Dr. Lucie Wolf (M. Boutros group, DKFZ, Heidelberg).

All HEK293T cell lines and RPMI-7951 were cultured in Dulbecco's MEM high glucose, while colon cancer HCT116 cells in McCoy's medium (GIBCO, Life Technologies GmbH, Darmstadt) supplemented with 10% fetal bovine serum (Biochrom GmbH, Berlin, Germany), with 100 U/mL penicillin and 0.1 mg/mL streptomycin (P/S) antibiotics.

For cell maintenance and experiments, cells were cultured as monolayers in 75 cm² flask or 10 cm plates with the respective medium at 37 °C and 5% CO₂, in incubators (Forma SteriCycle CO₂ incubator, ThermoFisher, Waltham, USA) with humidified atmosphere. Cells were subculture when reached 80 % to 90% confluency. For this, cells were washed with phosphate buffered saline (PBS) and were then trypsinized with 3 mL Trypsin-EDTA solution, until the cell layer was dispersed at 37 °C (usually for 5 min). Then, 7 mL of complete growth medium was added and cells were aspirated by gentle pipetting. 1/10 or 1/20 of resuspended cells were reseeded into a new 75 cm² flask or 10 cm plate with 10 mL of complete medium.

To cryopreserve cells, 1 × 10⁶ cells in 1 mL of the respective medium with 20% FBS and 10% dimethyl sulfoxide (DMSO, volume fraction) was frozen at -80 °C using cryotubes with the help of Freezing Containers for slow freezing. For long term storage, cells were kept immersed in a liquid nitrogen tank. To defrost the samples, the cryotubes were thawed in a water bath at 37 °C for 2 min, followed by resuspension of the cells in culture medium. Next, the cell suspension was centrifuged at 200 × g for 5 min to remove the medium containing DMSO. The pellet was resuspended with 10 mL of new culture medium and added into a new 75 cm² flask or a 10 cm plate.

2.2 Treatments with the PORCN inhibitor LGK974

HEK293T and HCT116 cells were seeded in 10 cm plates at a density of 1 × 10⁶ cells/plate. Twenty-four hours after seeding, cells were treated with 5 μM or 20 μM of the chemical LGK974 to inhibit PORCN activity. For this purpose, LGK974 (stock solution: 10 mM in DMSO) was diluted in the respective culture medium (see **Table 2.5**) to reach the specific working concentration. Twenty-four hours later, the medium was carefully removed and exchanged for a new medium with LGK974 and incubated for another 24 hours to reach 48 hours of incubation with LGK974.

2.3 Site-directed mutagenesis

To generate different mutants of Wnt3a and Wnt11 a QuikChange® II Site-Directed Mutagenesis Kit from Agilent (catalog #200523) was used. The procedure was performed according to the manufacturer's instructions. The primers were designed using the primer design program of Agilent (**Table 2.7**). The polymerase chain reaction (PCR) method was employed. To carry out PCR, a master mix was prepared using 5 µl of 10x reaction buffer, 50 ng of dsDNA template (pcDNA Wnt3a and pcDNA Wnt11 plasmids), 2 µl (120 ng) of forward and reverse oligonucleotide primers, 1 µl of DNTPs mix, ddH₂O to a final volume of 50 µl and 1 µl of PfuUltra High-Fidelity DNA Polymerase (2.5 U/µl).

Table 2.7: Primer sequences for site point mutation of Wnt3a and Wnt11

Wnt3a					
Mutation type	Nucleotides change	to	Primer Sequence (5' to 3')		T _m
			Forward	Reverse	
C155A	t463g g464c		5'-ggaagtgggtggcctagcaggacatcg-3'	5'-cgatgtcctcctagcggcccccacttcc-3'	78.30 °C
S300A	a898g g899c		5'-cgatgccgtgaggcagcttgcaggtgc-3'	5'-gcacctgcaactgcctcgcacggcatcg-3'	79.67 °C
S301A	t901g		5'-tcgatccgtgctgacgttgcag-3'	5'-ctgcaactgcagcgcacggcatcga-3'	78.61 °C
S338A	a1012g g1013c		5'-tgcactcctggcaggcagctagcagcacc-3'	5'-ggctgtgctacgtcctgccaggagtga-3'	78.30 °C
T343A	a1027g		5'-cgtagacgcgcgactcctggca-3'	5'-tgccaggagtgcgcgctctacg-3'	78.38 °C
Wnt11					
Mutation type	Nucleotides change	to	Primer Sequence (5' to 3')		T _m
			Forward	Reverse	
C157A	t469g g470c		5'-gtgtccgagctcctcccagcggttccc-3'	5'-gggaaccgctggggaggagctcggacaac-3'	79.67 °C
S217A	t649g		5'-ggatggagcaggcgcagacacccc-3'	5'-ggggtgtctggcctgctccatcc-3'	78.38 °C
S219A	t655g		5'-caggtgctgagcgcagcagcagcagc-3'	5'-gtctggctcctgcgcatccgacatcg-3'	80.13 °C
K332A	a994g a995c		5'-gagcgggtgccactgtgctaccactggtgctg-3'	5'-cagcaccagtggtagcagcagtgccaccgctc-3'	78.50 °C
T340A	a1018g		5'-cacctgcggcaggcagctagcagcac-3'	5'-gtgctgctacgtcgcctgccaggtg-3'	80.13 °C
E345A	a1034c		5'-tcacggtagcgcacacctgcggc-3'	5'-gccaggtgtgcgctacctgga-3'	78.38 °C

The PCR was performed with the following the cycles indicated in **Table 2.7**.

Table 2.7: Setting PCR site-directed mutagenesis

Number of cycles	Temperature (°C)	Time	Step
1	95	1 min	Denaturation and activation
23	95	30 s	Denaturation
	55	1 min	Annealing
	68	10 min	extension
1	4	∞	pause

After the PCR, 1 µl of the Dpn1 restriction enzyme (10 U/µl) was added to the amplification product and the sample was mixed thoroughly. The mixture was spun down in a microcentrifuge for 1 min and immediately incubated at 37 °C for 1 hour to digest the parental

supercoiled dsDNA. Then the DNA was precipitated by adding 20 µl of sodium acetate and 150 µl 95% ethanol and was incubated at -20 °C overnight. The sample was centrifuged at 14000 x g for 30 min at 4 °C, the supernatant was discarded carefully and the pellet was dried for 1 hour at room temperature. The pellet was then dissolved in 10 µl of ddH₂O. The plasmids were transformed in XL1-Blue Supercompetent Cells as is indicated in **Section 2.4**. The pcDNA plasmids containing the DNA coding for Wnt3a S209A, Wnt11 C80A, Wnt11 S215A and the double mutant Wnt11 C80A/S215A were provided by the lab of M. Boutros (DKFZ, Heidelberg).

2.4 Bacterial transformation

Competent bacteria were thawed in ice and carefully mixed with 100 pg of the plasmid of interest. After 30 min incubation in ice, heat-shock was performed by placing cells at 42 °C for 30 s followed by an incubation of 5 min in ice. Then, 1 mL of prewarmed (37 °C) super optimal broth with catabolite repression (S.O.C) medium was added to cells and samples were incubated for 1 h at 37 °C while shaking at 300 rpm in a thermoblock (Eppendorf). Two hundred microliters of this pre-culture were plated on selective LB agar plates using glass beads or hassa and incubated at 37 °C overnight. The next day, single bacteria colonies were picked to inoculate 5 mL of liquid LB medium with the respective antibiotic for selection and cells were incubated for 12 hours in a shaker incubator at 180 rpm and 37 °C.

2.5 Plasmid DNA amplification

Following bacterial transformation, the bacterial culture was centrifuged, and the bacterial pellet was used to isolate plasmid DNA using a QIAGEN Plasmid Mini kit (Minipreps). For maxipreps, 500 mL of LB media were inoculated with 5 mL of the pre-culture at 37°C with the respective antibiotic for selection. After 8-12 hours culturing, the bacterial culture was centrifuged and the pellet was used to isolate plasmid DNA using the QIAGEN Plasmid Maxi kit. The plasmid DNA was eluted with ddH₂O and concentration and purity were measured using a NanoDrop ND-1 000 spectrophotometer. Plasmid DNA was stored at -20 °C. The list of plasmids is indicated in **Table 2.10**.

2.6 DNA sequencing

DNA sequencing was outsourced to Eurofins Genomics using SupremeRun Tube Sanger Sequencing (formerly GATC) or Microsynth using Economy Run Sanger Sequencing. Primers for sequencing were provided directly by Eurofins Genomics or generated in silico using SerialCloner, Primer3web tool, or Sequencing Primer Design Tool. The sequences obtained were analyzed with SnapGene.

2.7 Plasmid transfection

Plasmid transfection was performed using TransIT-LT1 or FuGENE HD transfection reagent. A mixture of transfection reagent, transfection medium and amount of plasmid was prepared according to the **table 2.9**. The mixture was incubated for 15 minutes to allow the transfection reagent to interact with the plasmids. Then, the mixture was carefully added to the cells. In the case of RPMI-7951 cells, only FuGENE HD was used as transfection reagent.

Table 2.9: Mix for plasmid transfection

Type of Plate	TransIT-LT1			FuGENE HD		
	24 well	6 well	10 cm	24 well	6 well	10 cm
RPMI medium	100 µl	250 µl	500 µl			
OptiMEM medium				25 µl	450 µl	900 µl
Plasmid DNA	200 ng	750 ng	2250 ng	250 ng	1000 ng	3000 ng
Transfection reagent	2 µl	7.5 µl	20 µl	2.5 µl	10 µl	30 µl

Table 2.10: List of plasmids

Short name	Name	Source
px459	pSpCas9(BB)-2A-Puro (PX459)	Addgene #48139
pcDNA	pcDNA 3.1	Addgene V790-20
Wnt3a	pcDNA3 Wnt3a	Addgene Plasmid #35908
Wnt3a C155A	pcDNA3 Wnt3a C155A	Brügger lab
Wnt3a S209A	pcDNA3 Wnt3a S209A	Brügger lab
Wnt3a S300A	pcDNA3 Wnt3a S300A	Brügger lab
Wnt3a S301A	pcDNA3 Wnt3a S301A	Brügger lab
Wnt3a S338A	pcDNA3 Wnt3a S338A	Brügger lab
Wnt3a T343A	pcDNA3 Wnt3a T343A	Brügger lab
Wnt3	pcDNA3 Wnt3	Addgene Plasmid #35909
Wnt3 ¹⁻⁴⁸ -Wnt11	pcDNA3 Wnt3 ¹⁻⁴⁸ -Wnt11	Boutros lab
Wnt11	pcDNA Wnt11	Addgene #35922
Wnt11 N40Q	pcDNA Wnt11 N40Q	Boutros lab
Wnt11 T42P	pcDNA Wnt11 T42P	Boutros lab
Wnt11 C80A	pcDNA Wnt11 C80A	Boutros lab
Wnt11 C157A	pcDNA Wnt11 C157A	Brügger lab
Wnt11 S215A	pcDNA Wnt11 S215A	Boutros lab
Wnt11 S217A	pcDNA Wnt11 S217A	Brügger lab
Wnt11 S219A	pcDNA Wnt11 S219A	Brügger lab
Wnt11 K332A	pcDNA Wnt11 K332A	Brügger lab
Wnt11 T340A	pcDNA Wnt11 T340A	Brügger lab
Wnt11 S215A/C80A	pcDNA Wnt11 S215A/C80A	Boutros lab
Wnt11 ¹⁻⁴⁸ -Wnt3	pcDNA3 Wnt11 ¹⁻⁴⁸ -Wnt3	Boutros lab
Wnt5a	pcDNA Wnt5a	Addgene # 35911
Wnt5b	pcDNA Wnt5b	Addgene # 35912
TCF4/Wnt luciferase reporter	6xKD; pGL4.26 6xTcf-Firefly luciferase	K. Demir (Boutros lab)
Renilla reporter	pAct-RL (Renilla luciferase)	D. Nickles (Boutros lab)

2.8 Silencing of the acyltransferases ZDHHC5, ZDHHC6 and CPT1A by siRNA

HEK293T cells were seeded in 6 well plates (5×10^5 cells/well) and transfected in parallel with siRNAs (siRNA reverse transfection) to silence the ZDHHC5, ZDHHC6 and CPT1A genes. For this purpose, Dharmacon siGENOME Human siRNAs were used **Table 2. 11**. The siRNAs targeting

ZDHHC5 (catalog ID: MQ-026577-01-0002), ZDHHC6 (catalog ID: MQ-014101-01-0002), CPT1A (catalog ID: MQ-009749-02-0002), UBC (positive silencing control, catalog ID: MU-019408-01-0002), and untargeted control siRNAs (catalog ID: D-001210-01-05) were diluted to obtain a 20 μ M stock solution using 1 \times Dharmacon siRNA Buffer. In a new vial, the siRNAs were diluted 1/8 with ddH₂O, resulting in a working solution with a concentration of 2500 nM.

Table 2.11: List of siRNAs

Target gene	Supplier	Reference
siGENOME siRNA Human ZDHHC5	Dharmacon TM	Catalog ID: MQ-026577-01-0002
siGENOME siRNA Human ZDHHC6	Dharmacon TM	Catalog ID: MQ-014101-01-0002
siGENOME siRNA Human CPT1A	Dharmacon TM	Catalog ID: MQ-009749-02-0002
siGENOME siRNA Human UBC	Dharmacon TM	Catalog ID: MU-019408-01-0002
siGENOME siRNA Human Non targeting siRNA #1	Dharmacon TM	Catalog ID: D-001210-01-05

2 μ l of Lipofectamine RNAiMAX transfection reagent was diluted in 250 μ l of RPMI medium for each well to be transfected. To the diluted RNAiMAX/RPMI mixture, 2 μ l of the respective siRNA working solution was added to achieve a final concentration of 20nM siRNA in the mix. The new RNAiMAX/RPMI/siRNA mixture was added to each well of a 6 well plate and incubated for 20-30 min. After incubation, HEK293T cells were seeded onto the RNAiMAX/RPMI/siRNA mixture in the 6 well plate at a density of 3x 10⁵ cells/well. The cells were incubated for 72 hours.

In experiments requiring Wnt11 overexpression, plasmid transfection was performed 24 hours after seeding (see **section 2.7**).

2.9 Confirmation of silencing of acyltransferases candidates by RT-qPCR

To validate the silencing of acyltransferase candidates involved in Wnt11 secretion, RT-qPCR was used.

2.9.1 RNA extraction

RNA extraction was performed 72 hours after HEK293T cells were treated with siRNA (in the same manner as in **section 2.8**). The cell culture medium was removed, and the cells were washed carefully with PBS. The cells were then lysate and treated for RNA extraction as it is described in the QIAGEN RNeasy Mini Kit with on-column DNase digestion kit together with the QIAGEN RNase-Free DNase Set to reduce DNA contamination (both procedures according to the manufacturer's instructions, HB-0435-005, HB-0456-004, cat. no. 74004, cat. no. 79254). After RNA extraction the RNA concentration was measured with Nanodrop.

2.9.2 Synthesis of complementary DNA (cDNA)

The cDNA synthesis was performed with the RevertAid H minus first-strand cDNA synthesis kit (Fermentas Thermo Scientific). The following components were added to a 1.5 mL nuclease-free tube: 1 μ g of total RNA, 1 μ l of oligo(dT)20 (10 μ M) and RNase-free water up to 12 μ l. Samples were placed at 70 °C for 5 min in a thermocycler, then cooled to 4 °C. A transcriptase

mix was prepared using 4 µl of RT buffer, 1 µl of RiboLock, 2 µl of dNTP, and 1 µl of M-MuLV for each sample. Next, 8 µl of transcriptase mix was added to the RNA +oligo(dt) samples. The sample was mixed by gently pipetting up and down and then centrifuged. Next, the mixture was then incubated at 37 °C for 5 min, followed by incubation at 42 °C for 60 min. The reaction was inactivated by heating at 70 °C for 10 min.

2.9.3 RT-qPCR

RT-qPCR was performed in 384-well plates in a Roche LightCycler 480 Instrument II with Universal ProbeLibrary dual hybridization probes (Table 2.12). The cDNAs were diluted to 5 ng/µl. Subsequently, 5.5 µl of cDNA per well was added to the LC 384 plate (25 ng/well). Then, 5.5 µl of the following master mix was added to each well:

Table 2.12: Master mix qPCR

Components mastermix:	Final concentration	Amount per well
LC-480 Mix (2x)	1x	5 µl
for/rev-primer mix (each primer: 20 µM)	0.6 µM (each primer)	0.33 µl
Universal library probe (10 µM)	0.15 µM	0.17 µl

Table 2.12: Primers and probes for RT-qPCR

Target mRNA	Name primers for qPCR	Primers	Sequence 5' to 3'	Tm	%GC	Probe	Probe Reference
CPT1A	CPT1A#29_for	Forward	cctccgtagctgactcggta	56	60	#29	4687612001
	CPT1A#29_rev	Reverse	cggagtgcacctgaactga	53	58		
	CPT1A#55_for	Forward	cagtgggagcggatgttta	51	53	#55	
	CPT1A#55_rev	Reverse	tctcatgtgctggatgggtgt	52	50		
ZDHH6	ZDHH6#40_for	Forward	aaaaagcagataagagagtcagaagtg	55	37	#40	4687990001
	ZDHH6#40_rev	Reverse	gaaggttttgattcctttattcagag	53	35		
	ZDHH6#74_for	Forward	aaagcagataagagagtcagaagtgtt	55	37	#74	
	ZDHH6#74_rev	Reverse	gaagaaggttttgattcctttattca	52	31		
ZDHH5	ZDHH5#46_for	Forward	gacgcacaaccaatgaacag	52	50	#46	4688066001
	ZDHH5#46_rev	Reverse	tcagagagaacacggctga	50	56		
	ZDHH5#73_for	Forward	catggaccagggttttc	51	53	#73	
	ZDHH5#73_rev	Reverse	gggagctcggaaatcatctt	52	50		
UBC	UBC_#11_rev	Forward	ctgatcagcagaggttgatcttt	53	43	#11	4685105001
	UBC_#11_for	Reverse	tgtttagtcagacagggatcga	55	48		

The qPCR was run under the following settings:

Table 2.13: settings qPCR

Cycle	Time	Temperature
1	10min	95°C
45	10s	95°C
	20s	55°C
	1s	72°C
1	10s	40°C

Threshold or quantification cycles (Cq) were calculated using the LightCycler 480 software.

2.10 Short-guide (sg) RNA design, cloning and generation of knockout cells

All the pools of cells treated with sgRNAs or knockout cell lines were generated by O. Voloshanenko (M. Boutros group, DKFZ, Heidelberg) according to [55, 106]. The sgRNAs were designed using the E-CRISP tool (<http://www.e-crisp.org/E-CRISP>, Table 2.13) [107]. Oligonucleotides were purchased from Eurofins (Ebersberg, Germany), annealed, and cloned into px459 vector (Addgene #48139) as it is described in [106]. The vectors px459 with the respective sgRNAs were transfected in HEK293T and HCT116 as described in the section 2.7. As a control of transfection efficiency, in a separate well, cells were transfected with sgRNA targeting the UBC gene, knockout of this gene induces cell lethality. Forty-eight hours after, transient transfection selection was performed with 1 µg/mL of puromycin for 48-72 hrs. As a control of the efficacy of antibiotic selection, the death of untransfected cells was checked. After antibiotic selection, cells were cultured with fresh medium without antibiotics until 80% confluence was reached. The cells were then split for selection of single-cell clones*, whereby the cells were diluted to a concentration of 500 cells/ml and seeded in 220 µl of medium per well in a 96-well plate following four serial dilution steps (1:10). Single clones were checked by microscope and expanded. In the case of HCT116^{ΔEvi} clones were expanded in the presence of recombinant mouse Wnt3a (50 ng/mL, Peprotech, Hamburg, Germany) or 20% filtrated medium of wild type HCT116 cells. Knockout clones were validated using mutation analysis by indel-nested PCR as described [108].

***Note:** For lipidomic experiments, some samples came from pools of cells treated with sgRNAs without single-cell cloning selection. In this case the cell pool was cultured only one week after the end of antibiotic selection and submitted directly to lipidomic analysis.

Table 2.13: sequence sgRNAs

guide RNA	sequence
sg_Evi1	TGGACGTTTCCTGGCTTAC
sg_Evi2	AATCAGTTAAGTGTACTCTC
sgPORCN_11	TGACATGGCACAAGATGCG
sgPORCN_35	GTGCTTGCATGCTTCAGGT
sgPORCN_192	GGAGCAGCCAGATCTGGTCA

2.11 Cell lysate and determination of protein concentration

Cells were washed carefully once with prewarmed PBS at 37 °C, and the plates were placed on ice. Cells were detached using cold PBS and pipetting up and down. The resuspended cells were transferred into a 2 mL or a 15 mL Falcon tube (depending on the experiment) and centrifuged at 300 x g for 10 min and at 4 °C. The supernatant was discarded and the cell pellet was resuspended in the respective lysis buffer (lysis buffer depends on the type of experiment, see Table 2.4) 150 µl per well for 6-well plates or 450 µl for 10 cm plates. The suspension was transferred into a 1.5 mL tube, and incubated on the rotor wheel for 1 h at 4 °C. The cell lysate was centrifuged at 16000 x g, 4 °C for 30 min, and the supernatant was divided into a new 1.5 mL tube *. The cell lysate was snap frozen or used directly. The protein concentration of the cell lysate was measured with the Pierce™ bicinchoninic acid (BCA) protein assay kit according to the manufacturer's instructions (96-well plate).

***Note:** For SDS-PAGE or immunoprecipitation experiments, the cell lysate was divided into 3 vials, 50 µL as input for western blot, 20 µL for protein quantification with BCA and the rest for

immunoprecipitation. After protein quantification, the required sample volume was calculated taking into account that the amount of protein for immunoprecipitation or SDS-PAGE were the same for all treatments.

2.12 Immunoprecipitation

A premix to coat magnetic Protein G Dynabeads (Thermo Fisher) with respective antibodies was prepared at least 2 hours prior to immunoprecipitation of Wnt proteins. For this purpose, the total amount of magnetic beads and antibody needed for pulldown was calculated by multiplying the volume needed for 1 sample by the total number of samples (30 μ l of magnetic beads and 1 μ l of Wnt antibody per sample). To prepare the premix, using a magnetic rack, the beads were washed four times with wash buffer (see **Table 2.4**). The wash buffer was then discarded and the beads were resuspended in 100 μ l of lysis buffer per sample. The calculated total amount of Wnt antibody was then added to the beads. The premix was incubated in rotation at 4 °C for at least 2 h before addition to the cell lysate.

100 μ l of the bead plus antibody premix was added to new vials. The cell lysate was then added, taking into account the volume previously calculated by BCA to have equal amounts of protein (**section 2.11**). The mixture of cell lysate, antibody, and magnetic beads was incubated in rotation at 4 °C overnight.

After overnight incubation, the beads were separated from the cell lysate using a magnetic rack. An aliquot of the lysate was taken as a control of the material that did not bind to the beads. The lysate was then discarded, and the beads were washed three times with wash buffer three times. Finally, the protein was eluted from the beads with Laemmli buffer.

2.12.1 Wnt-Evi interaction by co-immunoprecipitation

HEK293T cells were seeded in 10 cm plates at a density of 1×10^6 cells/plate. 24 h later, cells were transfected with constructs for overexpression of either Wnt11 wild type, the chimera Wnt3¹⁻⁴⁸-Wnt11, the Wnt11 N40Q or Wnt11 T42P. Immunoprecipitations were performed by pull down of Wnt11 as described above. The samples were run by western blot, and the membranes were probed for the presence of Evi and Wnt11 using the respective antibodies from **table 2.2**.

2.13 SDS-PAGE and Western Blot

2.13.1 Electrophoresis

Protein samples were run on precast NUPAGE 4-12% BisTris gels from Life Technologies GmbH on XCell SureLock Mini-Cell XCell electrophoresis system. The system was assembled as described in [109]. Briefly, the gel was removed from the plastic bag and washed with water. The comb was slowly removed, and the gel was stripped at the base. The gel was mounted in the cassette and electrophoretic chamber. 1x MOPS buffer (stock 20x MOPS buffer: 1 M MOPS, 1 M Tris-Base, 20 mM EDTA, 69.3 mM SDS in ddH₂O) was added to the center of the cassette until it filled the cassette, spilled over, and covered the base of the chamber. The wells were carefully washed with MOPS using a syringe.

For 12-well gels, 10 μ l of standard molecular marker or 6 μ l of fluorescent molecular marker (depending on the detection system to be used*) was loaded. In the case of the

immunoprecipitation eluate, 20 μ l of sample per well was loaded. For the input samples or cell lysate, the volume to be loaded was calculated respecting the protein concentration in such a way to have the same amount of proteins per well. After loading the samples, the electrophoretic chamber was closed and operated for 20 min at 80V to allow the samples to enter the stacking gel. The voltage was then changed to 120V for 90 min or more until the loading dye exited the gel.

* Note: When the signal of the membranes was detected with films and developer machine, 10 μ l of Seebblue plus2 standard was used as standard molecular marker. When the signal was detected in the Lycor system, 6 μ l of Precision plus protein standards, BIO-RAD was used as fluorescent molecular marker.

2.13.2 Incubation with antibodies and membrane developing

After blotting, the membranes were blocked with 5% milk or 5% BSA in TBST for 1 hour. The membranes were then washed with TBST three times for 5 min on a shaker. These were then incubated with the primary antibody overnight at 4 °C or for 2 hours at room temperature (see **Table 2.2**, typically 5 mL total volume in a 50 mL Falcon tube), incubation in Roller Falcon Tube Mixer. The membranes were then washed with TBST five times for 5 min on a shaker.

The membranes were incubated for one hour with horseradish peroxidase (HRP)-coupled secondary antibodies at room temperature to detect proteins by chemiluminescent system. The membranes were then washed 5 times for 5 min on a shaker and incubated with enhanced chemiluminescence (ECL) substrates. HRP induced light emission, which was captured with Amersham Hyperfilm ECL and made visible with the COMPACT 2 X-ray film processor. When signal amplification was required, the membranes were incubated with the highly sensitive substrate SuperSignal West Femto **Table 2.1**.

To detect proteins using the fluorescence system, the membranes were incubated for two hours at room temperature with secondary antibodies coupled to fluorescent dyes emitting at 680 nm or 800 nm **table 2.2**. The membranes were then washed 5 times for 5 min on a shaker and then scanned on the Odyssey CLx-1014 LI-COR fluorescence imaging system controlled with ImageStudio Ver 5.0.

To detect biotin by a chemiluminescent detection system, HRP-conjugated streptavidin (Rockland; S000-03) was used at a 1:10000 dilution in BSA by incubating the membranes for one hour. To detect biotin using a fluorescent imaging system, IRDye 800CW streptavidin (LI-COR; 925-32230) was used at a 1:5000 dilution in BSA by incubating the membranes for two hours.

2.14 Detection of covalent lipid modification of Wnt11 or Wnt11 mutants by immunoprecipitation and alkyne-azide-cycloaddition click reaction

Click chemistry refers to a group of reactions that allow the union of two modified biomolecules containing a specific functional group. One of these reactions is the alkyne-azide-cycloaddition click reaction, which links a molecule containing an azide group to another molecule that has an alkyne group [110]. Here, this reaction was employed to label chemically modified lipids that contain an alkyne group to a biotin molecule with an azide group (I used

the term click labeling to refer to the lipid-alkyne biotin-azide click reaction, **Figure 2.1**). The modified lipids used were palmitic acid alkyne (cC16:0) and palmitoleic acid alkyne (cC16:1n-7) fatty acids. For the detection of lipidation of Wnt proteins, click labeling approach in conjunction with protein immunoprecipitation was used (**Figure 2.1**). The detection of Wnt lipidation through click labeling was established based on the articles [49, 51, 59, 110, 111]. The procedure has eight general steps, which are: seeding of cells, transfection for Wnt protein expression (depending on the cell type if transfection is required), lipid incubation of cells with cC16:0 or cC16: 1n-7 alkyl fatty acids, cell lysis and measurement of protein concentration, the capture of Wnt proteins by immunoprecipitation using antibodies and magnetic beads, alkyne-biotin-cycloaddition click reaction on beads, elution of proteins from beads, and Western blot of eluted samples (**Figure 2.2**).

2.14.1 Seeding and incubation of cells with cC16:0 or cC16:1n-7 alkyne fatty acids

HEK293T, HEK293T^{ΔPORCN} cells or stable cells lines HEK293T^{Wnt11}, HEK293T^{ΔPORCN_1-Wnt11} were seeded with complete DMEM in six-well plates, 3x10⁵ cells per well or in 10 cm plates 1x10⁶ cells per plate. 24 h after seeding, a mixture of lipid-labeling medium containing DMEM medium, 10% charcoal-depleted FBS, 0.5% DMSO, 100 μM cC16:0 or cC16:1n-7 alkyl fatty acids (depending on treatment) was prepared. The mixture was sonicated for 15 min to allow better homogenization of the lipids in the medium. After sonication, the lipid-labeling media mixture was heated for 10 min at 37 °C in a water bath.

Medium of cells was discarded and a first dose of warm lipid-labeling medium were added, 2 ml for 6 well plate (0.2 μmol/well of clickable fatty acid) or 10 ml for 10 cm plate (1 μmol/plate of clickable fatty acid). A second dose was carefully added on top of the cell medium 24 hours after the first dose. For the second dose, the lipid-labeling media mixture was again prepared using the same amount of DMSO, cC16:0 or cC16:1n-7 as the first dose, but in a smaller volume, 500 μl per well or 1 mL per plate, of DMEM, 10% charcoal-depleted FBS. After adding the second dose, the cells were incubated for another 12 hours, making a total of 36 hours of incubation with the lipid-labeling media mixture.

2.14.2 Transient transfection of Wnt3a, Wnt11 or the mutants

After 24 hours of seeding cells, and immediately after adding the first dose of lipid-labeling media mix, HEK293T or HEK293T^{ΔPORCN} cells were transfected, with one of the following plasmids: pcDNA Wnt11, pcDNA Wnt11 N40Q, pcDNA Wnt11 T42P, pcDNA Wnt11 C80A, pcDNA Wnt11 C157A, pcDNA Wnt11 S215A, pcDNA Wnt11 S217A, pcDNA Wnt11 S219A, pcDNA Wnt11 K332A, pcDNA Wnt11 T340A or pcDNA Wnt11 C80A/S215A. A mix per well was prepared for the transfection and added to the cells as it is described in **section 2.7** and **Table 2.9**. The transfection was skipped for the stable cell lines HEK293T^{Wnt11}, HEK293T^{ΔPORCN_1-Wnt11} which have the constitutive expression of Wnt11.

Thirty-six hours after the incubation with the lipid-labeling media mix, the cells were lysed as described in **section 2.11**. The pulldown of the protein was made as it is described in the **section 2.12** by immunoprecipitation. After the immunoprecipitation click labelling was performed.

2.14.3 Click labeling

After overnight incubation of lysed cells with antibody coated beads, supernatant was separated from beads using a magnetic rack. Supernatant was snap frozen and stored for WB analysis. The magnetic beads were washed with PBS + 1% Triton X100 for 15 min in cold room.

Stock solutions of CuSO₄, TBTA, and TCEP were prepared in 2mL tubes to get 50 mM CuSO₄ dissolved in water, 50 mM TCEP (tris(2-carboxyethyl)phosphine) dissolved in water, 5mM TBTA (Tris[(1-benzyl-1H-1,2,3-triazol-4-yl) methyl] amine, Sigma-Aldrich) dissolved in DMSO, and 10 mM Picolyl-Azide-PEG4-Biotin (Jena Bioscience) dissolved in DMSO. A master mix containing 200 μM CuSO₄, 200 μM TCEP, 20μM TBTA, 10 mM Picolyl-Azide-PEG4-Biotin in water was prepared, first it was added CuSO₄, TCEP, and Picolyl-Azide-PEG4-Biotin, briefly vortexed, and after 2 min it was added the TBTA. The master mix was split into new vials, 100 μl per sample. Next, 100 μl of the mix of beads with the immunoprecipitated protein was added to 100 μl of click mix and incubated for 2 hours at 37 °C without light, shaking at 850 rpm. After 2 hours, the beads were washed two times with 1 mL of PBS + 1% Triton x100, using magnetic rack. Finally, the protein was eluted with 50 μl of 2X Laemmli buffer without DTT with 1% beta-mercaptoethanol, incubating at 65 °C, 850 rpm shaking for 15 min. The eluate was spun down and, with the help of a magnetic rack, transferred to new vials and used for western blot.

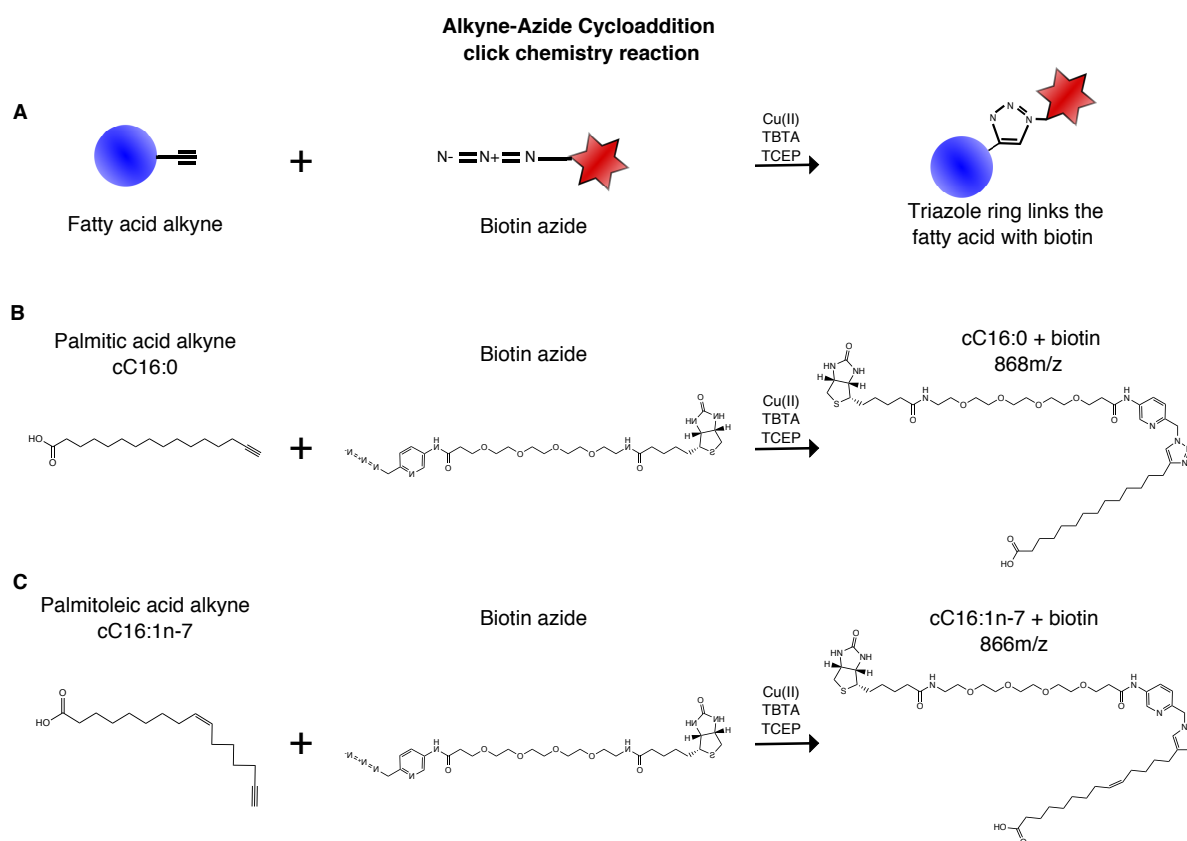


Figure 2.1: Click labeling reaction between cC16:0 or cC16:1n-7 and biotin azide.

A. General scheme of alkyne-azide cycloaddition click chemistry reaction. A complex between Copper (II) and TBTA is reduced with TCEP to form Copper (I), catalyzing the click reaction. **B.** Click reaction with palmitic acid alkyne (cC16:0) and biotin azide react to form an adduct through a triazole ring link. **C.** Click reaction with palmitoleic acid alkyne (cC16:1n-7) and biotin azide.

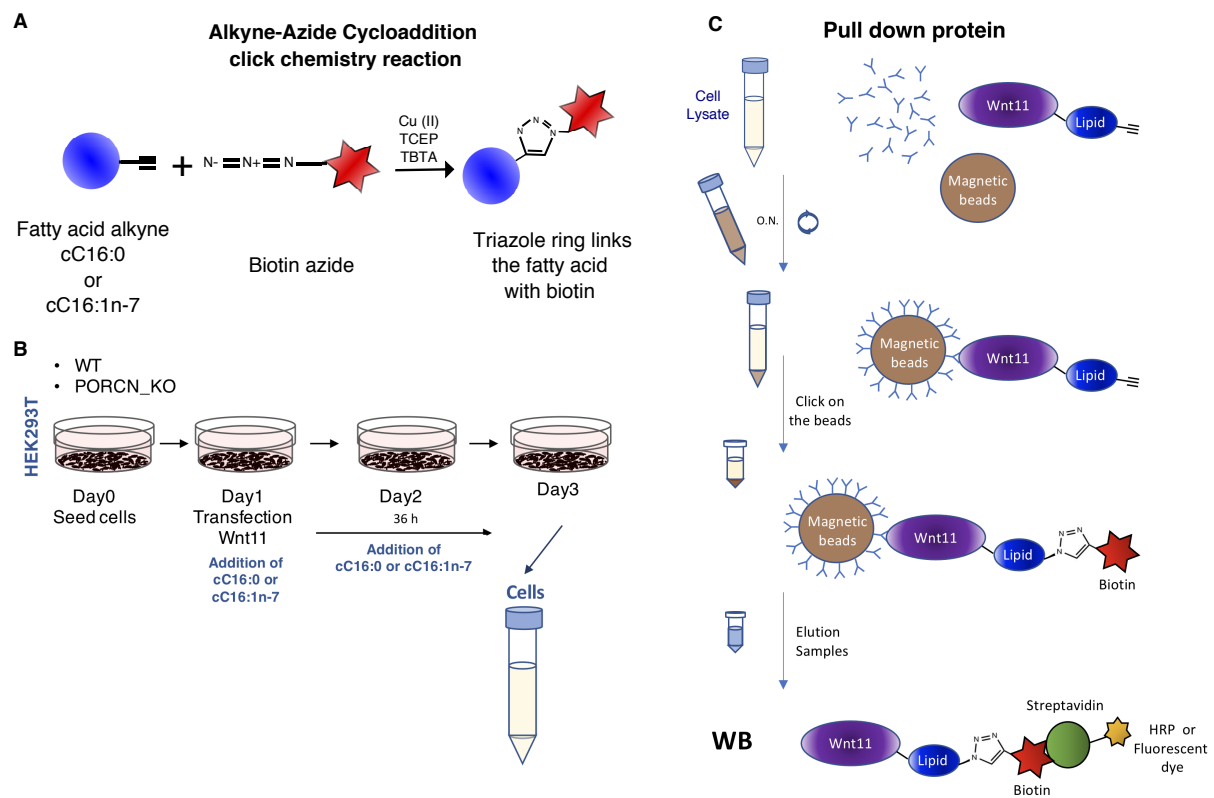


Figure 2.2: Detection of lipid modification on Wnt proteins.

A. Principle of the alkyne-azide click chemical reaction (click labeling). Here palmitic acid alkyne (cC16:0) or palmitoleic acid alkyne (cC16:1n-7) and biotin azide react to form a covalent bond between the fatty acid and biotin via a triazole ring bond. A complex between Copper(II) and TBTA is reduced with TCEP to form Copper(I), catalyzing the click reaction. **B.** Scheme of the protocol for metabolic incubation of cells with palmitic acid alkyne (cC16:0) or palmitoleic acid alkyne (cC16:1n-7). HEK293T cells were seeded in 6-well plates or 10 cm plates as indicated in **section 2.14.1**. One day later, 100 μ M of cC16:0 or cC16:1n-7 was added to the cells. On the same day, cells were transfected with plasmids to overexpress wild-type Wnt11 or Wnt11 mutants. On the following day (day 2), a second dose of cC16:0 or cC16:1n-7 was added to the cells and incubated for a total of 36 hours of incubation with the clicked fatty acids. On day 3, cells were collected for immunoprecipitation and click labeling. **C.** Pull down of Wnt11 protein from the cell lysate was performed by immunoprecipitation with magnetic beads and specific antibodies for Wnt11 (see **section 2.11** and **2.12**). Next, click labeling was performed on the beads (see **section 2.14.3**). Samples eluted from the beads were then analyzed by western blot to identify the Wnt11 protein and its lipid modification. The protein was detected using specific antibodies for Wnt11 and its lipid modification was detected using streptavidin conjugated to HRP or to a fluorescent dye.

2.15 Deglycosylation assay

The assay uses a cocktail of deglycosylation enzymes to remove almost all N-linked or O-linked oligosaccharides, which are post-translationally bound to proteins. The assay readout assesses the molecular weight difference, corresponding to the loss of glycans, and is detected by signal band mobility shifts in immunoblots corresponding to proteins with and without glycans. For the assay, 1×10^6 HEK293T cells were seeded in 10 cm plates. Twenty-four hours after the seeding, cells were transfected, as indicated in **section 2.3**, with the respective plasmids for Wnt3 or the chimera protein Wnt11¹⁻⁴⁸-Wnt3 expression. The procedure continues depending on whether it is on secreted proteins to cell culture media or proteins of the cell lysate.

2.15.1 Procedure to assess glycosylation in proteins from cell lysates

After removal of the culture medium, the cells were carefully washed with PBS, detached from the plate with cold PBS and scraper, and transferred to a 15 mL falcon tube. The cells were

then pelleted by centrifuging at 300 x g for 5 min at 4 °C. To each pellet, 200 µL of lysis buffer (with 1% Triton X100 and phosphatase inhibitors) was added and mixed up and down with a pipette. Samples were incubated with rotation for 1 hr at 4 °C, and then centrifuged at 14000 rpm for 30 min at 4 °C. The supernatant (cell lysate) was transferred to a new 2 mL tube.

Then, 50 µL of cell lysate was transferred to a new tube and the deglycosylation was performed. 5 µl of deglycosylation Mix buffer 2 was added and samples were incubated at 75 °C for 10 min. The samples were cooled to room temperature, and 5 µl of protein deglycosylation Mix II was added and mixed gently. The reaction was incubated at 25 °C for 30 min, shaking in a ThermoMixer at 650 rpm. The reaction temperature was then increased to 37 °C and samples were further incubated for 2 hours, shaking in the thermoMixer 650 rpm. 25 µl of 5x Laemmli buffer was added to the cell lysate and incubated at 75 °C for 15 min with shaking on the ThermoMixer 650 rpm. Samples were then centrifuged and analyzed by SDS-PAGE and immunoblot as explained in section 2.14. Blots were probed with antibodies against Wnt11, Wnt3 and HSC70.

2.15.2 Procedure to assess glycosylation in proteins from extracellular medium

Forty-eight hours after transfection, 10 mL of culture medium was collected in a 15 mL falcon tube. To remove debris, the medium was centrifuged at 300 x g 4 °C for 10 min, and then the medium was transferred to a new falcon tube, and the pellet was discarded. 50 µl of the medium was taken as input sample for the immunoblot. Next, 150 µl of pre-washed blue sepharose beads were added to the culture medium. Triton X100 was added to the medium to get a final concentration of 1%. The mixture of medium with beads was incubated rotating overnight at 4 °C. The next day, the blue sepharose beads were centrifuged at 100 x g for 5 min at 4 °C and the supernatant was discarded. The beads were washed 4 times with PBS + 1% Triton X100 for 5 min at 4 °C each time. The beads were centrifuged at 100 x g for 5 min at 4 °C and the remaining wash buffer was discarded. The following steps were performed according to the Protein Deglycosylation Mix II protocol [112]. The beads were resuspended in 50 µl of lysis buffer. Then, 5 µl of deglycosylation buffer 2 was added and incubated at 75 °C for 10 min. The samples were cooled to room temperature, and 5 µl of Protein deglycosylation Mix II was added and mixed gently. The reaction was incubated at 25 °C (room temperature) for 30 min, shaking in the ThermoMixer at 650 rpm. The reaction temperature was then increased to 37 °C and set for 2 hours*, stirring in the thermoMixer at 650 rpm. 25 µl of 5x Laemmli buffer was added to the beads and incubated at 75 °C for 15 min by shaking on the thermoMixer 650 rpm. The beads were then centrifuged, and the eluted sample was transferred to new tubes. Samples were analyzed by SDS-PAGE and immunoblot, as explained in **section 2.13**. Blots were probed with antibodies against Wnt11, Wnt3, and HSC70.

2.16 Wnt secretion assay with Blue Sepharose beads

To qualitatively assess the amount of Wnt secreted into the extracellular medium, Wnt proteins were enriched from cell culture supernatants using Blue Sepharose 6 Fast Flow beads and analyzed by Western blotting as described in [113]. HEK293T cells were seeded in 6-well plates, 2 mL of medium per well and 2 wells per condition at a seeding density of 3×10^5 cells/well were used. Medium was collected from 6-well and transferred to 15 mL Falcon tubes, 4 mL per condition. The debris in the extracellular medium were pelleted and discarded by centrifugation at 300 x g 4 °C for 10 min. The supernatant was transferred to new 2 mL vial tubes or 15 mL Falcon tubes. 30µl of Blue Sepharose beads were used per 2 mL of medium.

Blue Sepharose beads were washed 4 times in PBS before use. The beads were centrifuged and the remaining PBS was removed. The beads were resuspended again in 30µl of PBS per condition and added to the extracellular medium. Triton X100 was added to the medium to give a final concentration of 1%. The mixture of beads + media was incubated overnight at 4 °C with rotation. The Blue Sepharose beads were then washed once with PBS + 1% Triton X100 for 10 min and the proteins were eluted with 1X Laemmli buffer with DTT at 65 °C for 15 min by shaking on the thermoMixer 650 rpm. Eluted samples were analyzed by SDS-PAGE and Western Blot.

2.17 Analysis of lipidation sites on Wnt3a and Wnt11 by mass spectrometry

For an independent approach towards studying Wnt acylation, our group teamed up with the group of Prof. Carsten Hopf (Center for Mass Spectrometry and Optical Spectroscopy-CeMOS, Mannheim) to establish a mass spectrometric analysis of commercially available purified Wnt proteins and determine possible lipid modification sites on Wnts. The results were obtained by Dr. Diego Yepes in the CeMOS group.

5 µg of commercially purified recombinant Human Wnt3a and recombinant Human Wnt11 proteins (from CHO cells, R&D system Catalog#: 5036-WN-010/CF and Catalog#: 6179-WN-010/CF) were run by SDS page in 16% Tricine-Glycine gels. Bands were cut out from gel and in-gel digestion was performed. First, a deglycosylation step was performed using PNGaseF 1000 U + 0.1% RapiGest in 100 mM ammonium bicarbonate in 97% H₂¹⁸O, incubated at 37 °C for 24 h. Then reduction and alkylation of the samples were made, by adding 10 mM TCEP in 97% H₂¹⁸O followed by the addition of 100 mM iodoacetamide (IAA) in 97% H₂¹⁸O. For trypsin digestion, 1 µg trypsin (50 mM in 97% H₂¹⁸O) was added to the gel pieces and incubated at 37 °C for 18 h. Then, the peptides were extracted from gel adding first 5% acetonitrile (ACN) in 97% H₂¹⁸O; 0,1% formic acid (FA), then adding 60% ACN in 97% H₂¹⁸O (x2); 0,1% FA, and finally adding 90% ACN in 97% H₂¹⁸O.

Samples were analyzed by LC-MS/MS. The liquid chromatography (LC) was run on an Agilent 1260 Infinity CapLC instrument with the following settings: Column: ZORBAX SB-C18, gradient: from 3-60% in 70 min (A: 0,1% FA; B: ACN with 0,1% FA). The column temperature was set up at 40 °C with a flow rate of 12 µL/min (+/-). 120 ng of the sample were loaded. The mass spectrometry measures were made using a Q-ToF ImpactII Bruker system. The samples were run in the positive mode under the following conditions: AutoMSMS Top10 Method. Capillary 4500 V Nebulizer: 0.7 bar. Dry gas 6 l/min. Dry temperature: 150 °C. Mass range 150-2200 m/z Spectra rate: 5 Hz.

The data analysis of the mass spectra was made with the software PEAKS [114]. The search settings to find post-translational modifications were: Parent Mass Errors Tolerance: 10 ppm Fragment. Mass Error Tolerance: 0,05 Da. FDR: 1%. Precursor Mass Search Type: monoisotopic. Enzyme: Trypsin (Semi). Max. Missed Cleavages: 3. Digesting Mode: Semi-specific. Fixed Modification: Carbamidomethyl (C) (+57,021) Variable Modifications; Palmitoylation (N) (+238,23); Oxidation (M) (+15,99); 18O Deamidation (N) (+2,99); 18O Labeling (C-term) (+2,00); Max. Variable PTM per Peptide: 3.

2.18 Incorporation of cC16:0 and cC16:1n-7 into lipid species

2.18.1 Thin Layer Chromatography assays (TLC)

This assay was used to track fatty acid metabolism by click chemistry. Employing thin layer chromatography (TLC), lipid extracts were separated on a silica glass plate support. The protocol was adopted from Thiele et al [110].

5x10⁵ HEK293T cells were seeded in 6 well plates and incubated with 100 μM of cC16:0 or cC16:1n-7 for 36 h, maintaining the same incubation conditions used to detect lipidation at Wnt11 (Figure 2.2B). After incubation time, cells were washed twice with PBS at room temperature. Around 1x10⁶ cells were collected to 1.5 mL vials using scraper and 1 mL of PBS. The cells were pelleted at 300 x g for 5 min and the PBS was removed. The pellet was resuspended in 330 μl of ddH₂O. 600 μl MeOH was added to the resuspended pellet and vortexed for 10 seconds. Next, 150 μl of CHCl₃ were added and vortexed for 10 seconds. The vortexed extract was cleaned by centrifugation (14000 rpm for 5 min), the supernatant was transferred to 2 mL vials and the pellet was discarded. Next, 300 μL of CHCl₃ were added to the supernatant and vortexed for 10 sec. Next, 600 μL of 0.1% acetic acid in H₂O (v/v) was added and vortexed for 10 seconds. The mixture was centrifuged at 14,000 rpm for 5 min. The upper phase was discarded and the lower phase was carefully transferred to a new vial tube. The solvent was removed in speed vac for 20 min at 30 °C.

Lipid extracts were subjected to a click reaction with 3-Azido-7-hydroxycoumarin and thin layer chromatography analysis was performed comparing the samples with standards of different lipid classes. 0.5 nmol of each standard was used (pacFA-18:1 PC, Avanti 900408, pacFA Ceramide; Avanti 900404, pacFA Glucosylceramide, Avanti 900405, and clickable SM (synthesized in house)). For the click reaction, a click master mix was prepared with 2.5 μL of 3-azido-7 hydroxycoumarin (44.5 mM), 250 μL of [MeCN]₄CuBF₄ (10 mM) and 1 mL of EtOH (100%). The extracted lipids were dissolved in 7 μl CHCl₃ and 30 μL of the master mix was added. The reaction was carried out in speed-vac at 45 °C for 20 min. The lipids were then redissolved in 30 μL of MeOH and applied with CAMAG Linomat 5 on an HPTLC plate (105641 - HPTLC Silica gel 60 (Merck 1.05641.0001)).

The plate was developed in CHCl₃/MeOH/H₂O/AcOH 65/25/4/1 to 60% of the plate height. It was dried for 5 min and re-developed with 1:1 ethyl acetate/hexane to 100% of the plate height. The plate was sprayed with 4% (v/v) N,N-diisopropyl ethylamine in hexane for sensitive detection of deprotonated coumarin. It was then dried again in the hood for 1 min to evaporate excess solvent. Fluorescent imaging of the plate was performed on an AmershamTM imager 600 (GE Healthcare) with excitation at 460nm and emission at 488nm. For sulfuric acid staining, the plate was soaked with 20% sulfuric acid in water and incubated for 10 to 20 min at 125 degrees until charred lipids appeared on the plate. The plate was then immediately scanned.

2.18.2 Lipidomic analysis of incorporated cC16:0 and cC16:1n-7

Lipid extraction was done by Iris Leibrecht, Christian Luchtenborg and Timo Sachsenheimer. The samples were measured with a high-resolution mass spectrometer by Timo Sachsenheimer. Lipidome data was analyzed and provided by Christian Luchtenborg and Timo Sachsenheimer (Brügger lab).

HEK293T cells were seeded in 6 well plates (3×10^5 cells per well) and incubated with $100 \mu\text{M}$ of cC16:0 or cC16:1n-7, keeping the same incubation conditions used to detect lipidation on Wnt11 (see **section 2.14.1** and **Figure 2.2B**). After the incubation, the cells were washed twice with room temperature PBS. Then the cells were scraped in PBS and transferred to 1.5 mL Eppendorf vials. For each sample, approximately 1×10^6 cells were collected from cell cultures. Cells were pelleted at $300 \times g$ for 5 min, and the PBS was removed. Then the pellet was resuspended in 100 μl of ammonium bicarbonate ($(\text{NH}_4)\text{HCO}_3$, 155 mM) methanol 1:1 (v/v). Then the samples were subjected to acidic Bligh and Dyer lipid extraction (SBD-extraction) as is described in [115, 116]. A mix of the lipid standards PC di 17:0, PC di 18:3, and PE di 17:0 was included (all of them from Avanti Polar Lipids). Then the lipid extracts were resuspended in 60 μl of a buffer solution of 7.5 mM ammonium-formate in Isopropanol/MeOH/ CHCl_3 (4:2:1). 5 μl of the resuspended sample was transferred into Eppendorf twin tec 96-well plates followed by the addition of 15 μl of buffer solution (5 mM ammonium-formate in Isopropanol/MeOH/ CHCl_3 (4:2:1)) to get a dilution of 1:3. The resuspended extracts were submitted to high-resolution mass spectrometry analysis.

Mass spectrometric measurements were performed with negative ion mode on a Q Exactive mass spectrometer equipped with chip-based (HD-D ESI Chip, Advion Biosciences) nano-electrospray infusion and ionization (TriVersa NanoMate, Advion Biosciences). The samples were measured first in a survey full scan MS in an m/z range from 650 to 950. Then the targeted MS^2 with m/z corresponding to PC and PE ions for fragmentation was measured. Phosphatidylcholine (PC) lipid species were measured as formate adducts $[\text{M}+\text{HCOO}]^-$ and phosphatidylethanolamine lipid species were measured as deprotonated ions $[\text{M}-\text{H}]^-$. Then it was performed targeted selected ion monitoring mass spectrometry (SIM) with 20 Da windows with an acquisition time of 20 to 30 min. The acquired data were preprocessed with the software PeakStrainer to exclude signals which were not present in 70% of the cases during the repetition of the scans. After the preprocessing of the spectra with PeakStrainer, the preprocessed data was imported and analyzed with the software lipidXplorer 1.2.8 to obtain the MS and MS^2 precursor and fragment data, followed by the selection of intensities for PC and PE lipid species from the targeted SIM and targeted MS^2 [117, 118]. The mol percentage for each PC and PE lipid species was calculated based on the concentration and the intensities of the lipid standards.

2.19 Lipidomics analysis of HEK293T and HCT116 cells

Lipidomics uses mass spectrometry methods to quantitatively analyze cellular lipidomes from different biological sources [119]. Here we used lipidomics to analyze the lipid composition of HEK293T and HCT116 cells either overexpressing Wnt proteins, or that lack of PORCN or Evi by knockout, or were inhibited from PORCN activity by a small molecule inhibitor. The process consists of three steps, the first is the extraction of lipids, the second is the measurement by mass spectrometry and the third is the data analysis by software. Lipidomics analyses were performed together with Iris Leibrecht, Timo Sachsenheimer and Christian Luchtenborg from the CellNetworks Lipidomics Platform Heidelberg (B. Brügger lab, BZH, Heidelberg University).

For each sample, approximately 1×10^6 cells were collected from cell cultures of the stable cell lines HEK293T, HEK293T ^{Δ PORCN}, HEK293T ^{Δ Evi}, HCT116, HCT116 ^{Δ Evi} cells; or from HEK293T and HCT116 cells treated either with LGK974 as described in **section 2.2**; or HEK293T cells treated

either with sgRNAs to induce depletion of Porcupine as described in **section 2.10**, or transfected with plasmids to overexpress Wnt3a, Wnt5a, Wnt5b or Wnt11 as described in **section 2.7**. Cells were pelleted at 300 x g for 5 min at 4 °C.

2.19.1 Lipid extraction

The pellet was resuspended in 100 µl ammonium bicarbonate ((NH₄)HCO₃, 155 mM). Then, 100 µl of methanol was added. A 1:20 dilution was made in the same buffer bicarbonate/methanol 1:1. Samples were subjected to Bligh and Dyer acid lipid extraction (SBD extraction) or neutral extraction as described by Ozbalci et al [115, 116]. SBD extraction was performed in the presence of an internal lipid standard mixture containing 50 pmol phosphatidylcholine (PC, 13:0/13:0, 14:0/14:0, 20:0/20:0; 21:0/21:0, Avanti Polar Lipids), 50 pmol sphingomyelin (SM, d18:1 with N-acylated 13:0, 17:0, 25: 0, semi-synthesized77), 100 pmol deuterated cholesterol (D6 cholesterol or D7 cholesterol, Cambridge Isotope Laboratory), 30 pmol phosphatidylinositol (PI, 17:0/20: 4, Avanti Polar Lipids), 25 pmol phosphatidylethanolamine (PE, 14:1/14:1, 20:1/20:1, 22:1/22:1, semi-synthesized77), 25 pmol phosphatidylserine (PS, 14:1/14:1, 20:1/20:1, 22:1/22:1, semi-synthesized77), 25 pmol diacylglycerol (DAG, 17:0/17:0, Larodan), 25 pmol cholesterol ester (CE, 9: 0, 19:0, 24:1, Sigma), 24 pmol triacylglycerol (TAG, LM-6000/D5-17:0,17:1,17:1, Avanti Polar Lipids), 5 pmol ceramide (Cer, d18:1 with N-acylated 14:0, 17:0, 25: 0, semi-synthesized77 or Cer d18:1/18:0-D3, Matreya), 5 pmol Glucosylceramide (HexCer, d18:1 with N-acylated 14:0, 19:0, 27:0, semi-synthesized or GlcCer d18: 1/17:0, Avanti Polar Lipids), 5 pmol lactosylceramide (Hex2Cer, d18:1 with N-acylated C17 fatty acid), 10 pmol phosphatidic acid (PA, 17:0/20: 4, Avanti Polar Lipids), 10 pmol phosphatidylglycerol (PG, 14:1/14:1, 20:1/20:1, 22:1/22:1, semi-synthesized77), and 5 pmol lysophosphatidylcholine (LPC, 17:1, Avanti Polar Lipids). Neutral extraction was performed in the presence of an internal lipid standard mixture containing phosphatidylethanolamine-plasmalogen (PE P-) standard mix was spiked with 16. 5 pmol PE P-mix 1 (16:0p/15:0, 16:0p/19:0, 16:0p/ 25:0), 23.25 pmol PE P-mix 2 (18:0p/15:0, 18:0p/19:0, 18:0p/25:0), and 32.25 pmol PE P-mix 3 (18:1p/15:0, 18:1p/19:0, 18:1p/25:0).

2.19.2 Mass spectrometry measurements

The lipid extracts were resuspended in 50 µl of ammonium acetate 10 mM in methanol, diluted 1:10, and transferred into Eppendorf twin-tec 96-well plates. Mass spectrometric measurements were performed in positive ion mode on an AB SCIEX QTRAP 6500+ mass spectrometer equipped with chip-based (HD-D ESI Chip, Advion Biosciences) nano-electrospray infusion and ionization (TriVersa NanoMate, Advion Biosciences) as described Özbalci et al. [115, 116]. The following precursor ion scanning (PREC) and neutral loss scanning (NL) modes were used for the measurement of the various lipid classes:

Table 2.14: List of scanning modes for each lipid class

Lipid class	Polarity	Scan type	m/z (Da)	Mass range
PA	Positive	Neutral loss	115	600-900
PC	Positive	Precursor	184	644-880
LPC	Positive	Precursor	184	644-880
PE	Positive	Neutral loss	141	620-860
PE P-	Positive	Precursor	364.2, 390.3, 392.3	650-850
PS	Positive	Neutral loss	185	670-910
PG	Positive	Neutral loss	189	670-910

PI	Positive	Neutral loss	277	800-950
SM	Positive	Precursor	184	644-880
Cer	Positive	Precursor	264.3	500-670
HexCer	Positive	Precursor	264.3	670-860
Hex2Cer	Positive	Precursor	264.3	830-1020
Cholesterol	Positive	Precursor	369	500-800
CE	Positive	Precursor	369	500-800
DAG	Positive	Neutral loss	217.3-345.3	500-750
TAG	Positive	Neutral loss	217.3-345.3	750-1000

Mass spectrometry settings: resolution: unit, low mass configuration; data accumulation: 400 MCA; curtain gas: 20; Interface heater temperature: 60; CAD: medium.

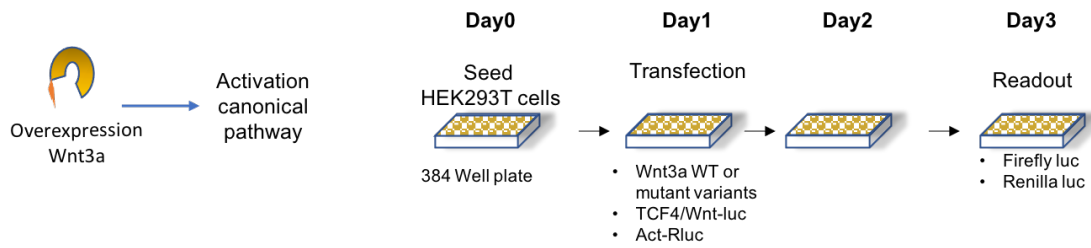
Data evaluation was done using LipidView (Sciex) and ShinyLipids, a software developed in house.

2.20 Canonical and non-canonical TCF4/Wnt-reporter activity assay

For the canonical TCF4/Wnt-reporter activity assay (implemented in the group of M. Boutros at DKFZ, [120, 121], **Figure 2.3**), HEK293T cells were seeded into a 384-well format using white flat-bottom polystyrene plates, the final volume per well 50 μ l at a concentration 5×10^4 cells/ml. After 24 h cells were transfected with 20ng TCF4/Wnt firefly luciferase reporter, 10ng actin-Renilla luciferase reporter, 10ng of pcDNA Wnt3a, or their respective mutants, see **Table 2.10** and **Figure 2.3A**. Forty-eight hours post-transfection, the canonical pathway activity was measured by the luminescence of luciferase with a Mithras plate reader. TCF4/Wnt-luciferase signals are normalized to the actin-Renilla luciferase reporter.

For the non-canonical TCF4/Wnt-reporter activity assay (implemented in the group of M. Boutros at DKFZ, [120, 121], **Figure 2.3**), HEK293T cells were seeded into a 384-well format using white flat-bottom polystyrene plates, the final volume per well 50 μ l at a concentration 5×10^4 cells/ml. After 24 h cells were transfected with 20 ng TCF4/Wnt firefly luciferase reporter, 10 ng actin-Renilla luciferase reporter, 10 ng of pcDNA Wnt11 (inhibitory effect on the Wnt pathway, **Figure 2.3B**), or their respective mutants, see **Table 2.10**. Forty-eight hours post-transfection, the luminescence was measured with a Mithras plate reader. Paracrine induction of Wnt signaling was performed adding recombinant mouse Wnt3a (PeproTech, Hamburg, Germany), 16 h prior to the luciferase read out. Luminescence was measured with a Mithras plate reader. TCF4/Wnt-luciferase signals are normalized to the actin-Renilla luciferase reporter.

A. Canonical TCF4/Wnt-reporter activity assay



B. Non-canonical TCF4/Wnt-reporter activity assay

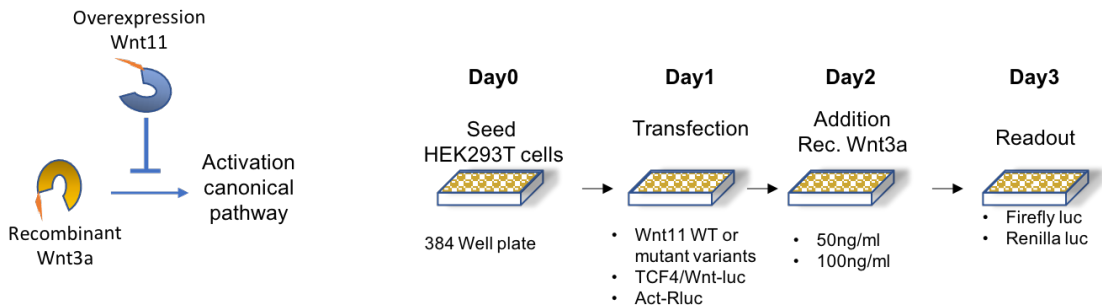


Figure 2.3: Set-up of canonical and non-canonical TCF4/Wnt reporter activity assay

A. Activation of canonical Wnt pathway after overexpression of Wnt3a in HEK293T cells. **B.** The paracrine activation of the canonical Wnt pathway with recombinant Wnt3a is inhibited after Wnt11 overexpression in HEK293T cells. The readout measures the luminescence emitted by firefly-luciferase expressed under the control of the TCF4 transcription factor. The signal is normalized with respect to the Actin-Renilla-luciferase reporter.

2.21 Gelatin degradation assay

The gelatin degradation assay was performed in collaboration with L. Wolf (M. Boutros group, DKFZ, Heidelberg). The steps were followed as it is described in [25]. The assay mimics in vitro the process of remodeling the extracellular matrix during the invasion and metastasis of melanoma cells. For the assay, gelatin-coated slides were prepared using the QCM™ Gelatin Invadopodia Assay (Green) following the manufacturer's instructions (ECM670, Merck Milipore). RPMI-7951 melanoma cells (1.5×10^5 cells) were transfected with plasmids that codified either for Wnt11, the mutant Wnt11 S215A, or Wnt5a, as is indicated in **section 2.3**. 72 hrs later, cells were dissociated from the plate and seeded on gelatin-coated coverslips (3×10^4 cells per 12 mm coverslip per condition). Gelatin coated slides were prepared using the QCM™ Gelatin Invadopodia Assay (Green) following the manufacturer's instructions (ECM670, Merck Milipore). Additionally, Wnt protein expression in the lysate and supernatant was checked. Twenty-four hours after seeding on gelatin slides, cells were fixed using 4 % paraformaldehyde for 10 min at room temperature. For immunofluorescence staining of coverslips, cells were permeabilized using 0.2% Triton X100/ PBS (v/v, T8787, Sigma-Aldrich) for 10 min and then blocked with blocking solution (3% FCS (v/v), 1% goat serum (v/v), 0.1% Triton X100 (v/v) in PBS) for 30 min. Staining of the actin cytoskeleton was performed using Phalloidin-TRITC (dilution 1/500, provided with QCM™ Gelatin Invadopodia Assay (Green)) for 1 hour followed by three washes in PBS. Coverslips were mounted using ProLong® Diamond Antifade Mountant with DAPI (P36962, Life Technologies GmbH).

Cells were imaged using a wide field Zeiss Cell Observer with a 20x objective. Eight randomly chosen fields of view with a minimum of 100 cells per condition were analyzed. Cell numbers

were counted based on DAPI and actin staining. Gelatin degradation quantification analysis was performed using Fiji (ImageJ) software. The area of gelatin degradation was assessed after thresholding, and the ratio between this area and the cell number was calculated. The “gelatin degradation capacity per cell” of each condition was then normalized to its control treatment per replicate (values close to 1 indicate a small difference between treatment and control). At least six biological replicates were performed per condition. The resulting values were tested against 1 using the Wilcoxon signed-rank test and software R, version 3.6.0, and R Studio.

3 Results

A. Alternative acylation sites and types of fatty acid modification of Wnt11

3.1 Role of serine 215, cysteine 80 and Porcupine in Wnt11 palmitoylation

Serine 215 and cysteine 80

Wnt11 is a non-canonical Wnt protein, which is key for the development of mammalian heart, liver, and kidney [86-93]. In polarized cells, its apical and basolateral secretion and subsequent function has been linked to the acylation of the residue serine 215 [35]. However, the recent experiments of O. Voloshanenko (M. Boutros group, DKFZ, Heidelberg) revealed that mutation of serine 215 in Wnt11, impeding its acylation, does not abolish its secretion. In turn, the protein partially keeps its hydrophobic character (section 1.3.5). These findings suggest that besides the earlier-proposed regulation mechanism [35], other putative acylation types and lipid-modified amino acids could be at place.

Firstly, I addressed the question whether lipidation of Wnt11 occurred at serine 215 and/or cysteine 80, as it has been pointed out before [42, 43]. To this end, HEK293T cells were incubated with palmitic acid alkyne (cC16:0) and transfected with wild type Wnt11 plasmid or with the Wnt11 S215A and C80A mutants (Figure 3.1A). The cC16:0 acyl chain attached to Wnt11 was then detected using Wnt11 pull-down assays in combination with click chemistry reactions targeting the alkyne fatty acid (see methods of Figure 2.1, 2.2).

Lipidation with the c16:0 fatty acid was observed for the Wnt11 wild type protein for nine out of ten experimental replicates (Figure 3.1 and Appendix Figure 5.1). Strikingly, lipidation was also observed for the mutants C80A and S215A, with the latter one lacking the canonical Wnt lipidation site (Figure 3.1B-C). In the case of Wnt11 S215A, four out of five replicates showed lipidation, while for C80A, three out of four experiments displayed lipidation (Figure 3.1E and Appendix Figure 5.1). A double mutant C80A/S215A, with both acylation sites removed, showed a signal of lipidation in one out of three cases (Figure 3.1D). The results indicate that there is an alternative lipidation site when either C80 and S215 are removed.

Porcupine

Porcupine was identified as the acyltransferase catalyzing the O-acylation of Wnt proteins [33, 43-45]. To test for the role of Porcupine in lipidation of Wnt11, HEK293T Porcupine knockout cells (HEK293T^{ΔPORCN}) were incubated with cC16:0 and transfected with wild type Wnt11 plasmid. Lipid modification was observed for Wnt11 expressed in the HEK293T^{ΔPORCN} cells in half of the replicates (5 out of 10 experiments, Figure 3.1 and Appendix Figure 5.1). These results suggest that, besides PORCN, another acyltransferase could be involved in Wnt11 lipidation.

Due to the variability between replicates the results obtained for both Wnt11 S215A/C80A and HEK293T^{ΔPORCN} cells did not allow to make a definite statement on acylation of Wnt 11. I thus next attempted to identify the factors responsible for the low experimental reproducibility.

One parameter that may contribute to varying results is the metabolic conversion of palmitic acid alkyne cC16:0 to palmitoleic acid alkyne cC16:1n-7, which might take place before the fatty acid is transferred to the Wnt protein. In fact, several reports have suggested a preference of Wnts for the monounsaturated palmitoleic acid C16:1n-7 instead of the saturated palmitic acid C16:0 [36, 43, 45, 55, 60]. Accordingly, the use of cC16:0 in the assay may have affected the labeling efficiency and thereby may have rendered an unspecific lipidation pattern. Next, the relevance of the saturation of the fatty acid for Wnt11 lipidation was also investigated (see section 3.2 below).

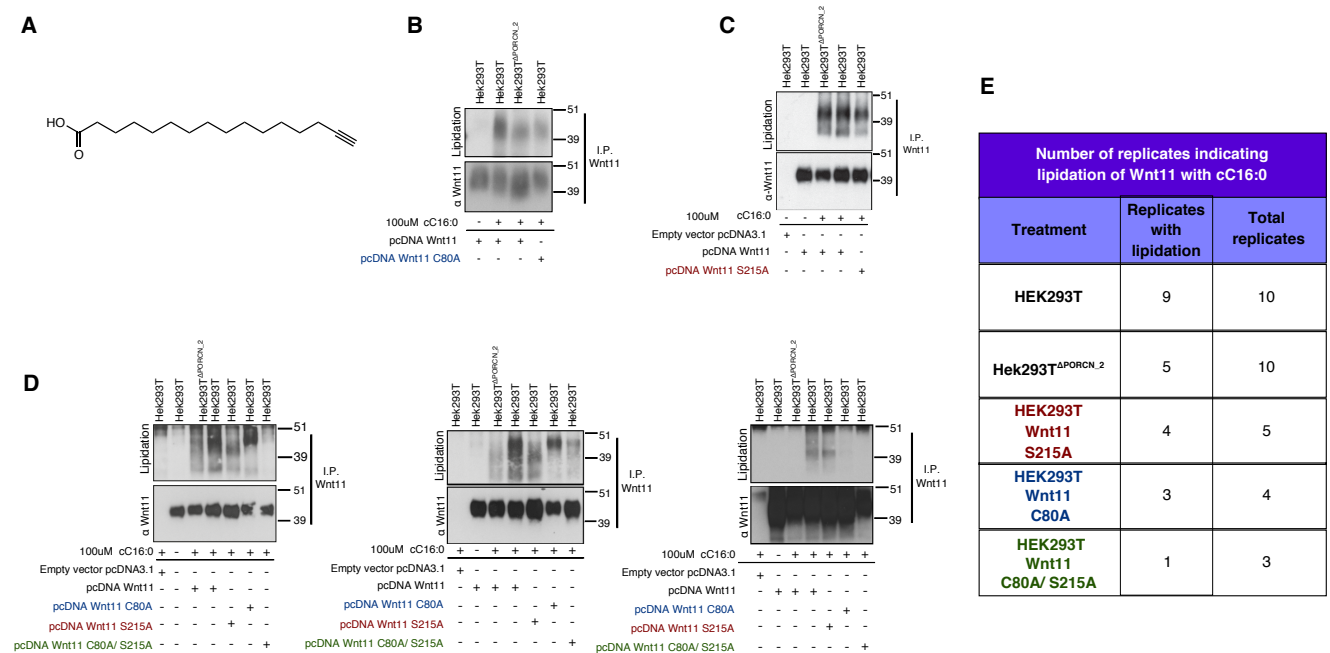


Figure 3.1: Detection of lipid modification of Wnt11 and Wnt11 mutants with cC16:0

HEK293T and HEK293T^{ΔPORCN_2} cells were seeded in 10 cm plates as indicated in section 2.14.1. 24 h later, 100 μM of cC16:0 was added to the cells. On the same day, the cells were transfected with the indicated overexpression constructs for either Wnt11 wild type or Wnt11 mutants. On the following day, a second dose of cC16:0 was added to the cells and incubated to reach a total of 36 hours of incubation with the clickable fatty acid. On day 3, cells were collected for immunoprecipitation and click labeling as outlined in sections 2.11, 2.12, and 2.14.3. Samples were eluted from the beads and analyzed by western blot. Antibodies specific for Wnt11 were used for protein detection and its lipid modification was detected using HRP-conjugated streptavidin. The blots were analyzed by a chemiluminescent system using ECL substrates and a COMPACT 2 X-ray film processor.

A Chemical structure of palmitic acid alkyne cC16:0. **B-C.** Detection of the lipid modification of Wnt11 using cC16:0 in HEK293T and HEK293T^{ΔPORCN} cells. The lipid modification was also detected in the mutants Wnt11 C80A **B** (see the lane four), Wnt11 S215A **C** (see the lane five), but was not clearly observed in the double mutant Wnt11 C80A/S215A **D** (see the lane seven). **D** Variation of experimental replicates with respect to lipidation of Wnt11 in HEK293T^{ΔPORCN} cells or Wnt11 mutants in HEK293T cells. **E** Summary of the number of replicas with a positive signal, indicating lipidation relative to the total number of replicas. **B-D:** α: indicates the protein to which the primary antibody is directed. **I.P.:** Immunoprecipitated protein.

3.2 Click metabolic labeling with cC16:1n-7 fatty acid: Wnt11 lipidation occurs at the serine 215 residue and is critically mediated by porcupine

The works from Takada et al. [43], Rios-Esteves et al. [45] and Tuladhar et al. [55] demonstrated that Wnts are lipidated with the monounsaturated palmitoleic acid (C16:1n-7). Therefore, as an alternative to overcome poor labeling efficiency and subsequent low reproducibility of our assays, I conducted experiments with C16:1n-7 instead of cC16:0. A clickable monounsaturated cC16:1n-7 alkynylated palmitoleic acid was synthesized, following the procedures established by Tuladhar, Lum, et al. [55, 59] (kindly provided by B. Pokrandt, member of the group of Prof. Britta Brügger, BZH, Heidelberg, Germany) kindly produced the fatty acid and shared them with us for our experiments. With this monosaturated lipid at hand, I checked distinct putative lipidation sites and the role of porcupine for lipidation of Wnt11.

3.2.1 Lipidation of serine 215 of Wnt11 with cC16:1n-7

I investigated whether the metabolic labeling improved with the synthesized palmitoleic acid alkyne cC16:1n-7 in a way that the lipidation of serine 215 could be clearly detected. To this end, HEK293T cells were incubated with cC16:1n-7 and treated to overexpress Wnt11, either in its wild type form or with the residues S215 mutated to alanine (**Figure 3.2B**). A strong lipid modification signal was observed for Wnt11 in HEK293T cells (**Figure 3.2B**). A similar result was observed using stable cell lines with constitutive expression of Wnt11 (compare **Figure 3.2B** with HEK293T^{Wnt11}, **Figure 3.2C**). Remarkably, in contrast to our previous results using palmitic acid alkyne cC16:0 (**Figure 3.1**), the mutant Wnt11 S215A did not display any lipidation with the cC16:1n-7 fatty acid (in n = 7 replicates; **Figure 3.2B**). These data suggest that serine 215 of Wnt11 is specifically acylated by the monounsaturated fatty acid 16:1n-7, consistently as previously reported Yamamoto et al. [35]. Our results also highlight the strict role lipid unsaturation plays in the acylation process of Wnt11.

3.2.2 cC16:1n-7 lipidation mediated by Porcupine

I also checked the role of Porcupine in the lipidation of Wnt11 with cC16:1n-7. Contrary to the data obtained with cC16:0 fatty acid (**Figure 3.1**), lipidation of Wnt11 in HEK293T^{ΔPORCN} cells by cC16:1n-7 was completely absent (n = 2 replicates; **Figure 3.2B**). Similar results were observed using Porcupine knockout cells constitutively expressing Wnt11 (HEK293T^{ΔPORCN_1-Wnt11}, n = 5 replicates **Figure 3.2C**). These results suggest that the lipidation of Wnt11 with the monounsaturated cC16:1n-7 fatty acid is critically dependent on Porcupine, which is consistent with previous reports [33, 43, 44, 46, 55, 67].

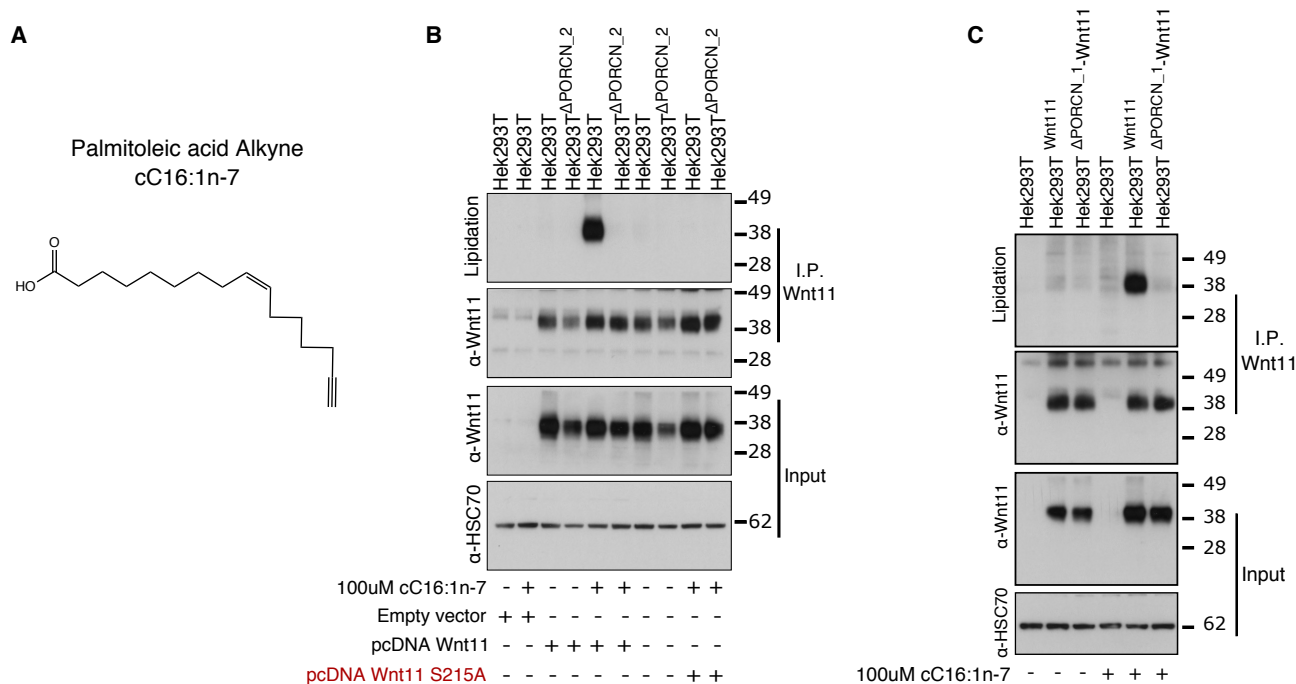


Figure 3.2: Mutation of serine 215 of Wnt11 or knockout of PORCN impairs Wnt11 lipidation with cC16:1n.7

A. Chemical structure of palmitoleic acid alkyne cC16:1n-7. **B-C.** HEK293T, HEK293T^{Wnt11}, and HEK293T^{ΔPORCN_2} cells were seeded in 10 cm plates as indicated in **section 2.14.1**. 24 h later, 100 μM of cC16:1n-7 was added to the cells. On the same day, HEK293T and HEK293T^{ΔPORCN_2} cells were transfected with the indicated overexpression constructs for either Wnt11 wild type or Wnt11 S215A mutant. On the following day, a second dose of cC16:1n-7 was added to the cells and incubated to reach a total of 36 hours of incubation with the clickable fatty acid. On day 3, cells were collected for immunoprecipitation and click labeling as outlined in **sections 2.11, 2.12, and 2.14.3**. Samples were eluted from the beads and analyzed by western blot. Antibodies specific for Wnt11 were used for protein detection and its lipid modification was detected using HRP-conjugated streptavidin. The blots were analyzed by a chemiluminescent system using ECL substrates and a COMPACT 2 X-ray film processor. HSC70 was used as loading control. *α*: indicates the protein to which the primary antibody is directed. I.P.: Immunoprecipitated protein. Western blots are representative of three independent experiments. **B.** Lipidation with palmitoleic acid alkyne cC16:1n-7 was observed in HEK293T cells transfected with a pcDNA plasmid coding for Wnt11 (see the lane five). In contrast, either PORCN knockout cells or HEK293T cells transfected with a pcDNA plasmid coding for the mutant Wnt11 S215A did not display lipidation (see lanes six and nine). **C.** In HEK293T^{Wnt11} and HEK293T^{ΔPORCN_1-Wnt11} cells with constitutive expression of Wnt11, lipid modification with palmitoleic acid alkyne cC16:1n-7 was observed in HEK293T^{Wnt11} but not in HEK293T^{ΔPORCN_1-Wnt11} cells.

3.2.3 Only mutation of serine 215 impairs cC16:1n-7 dependent lipidation of Wnt11

To test for lipidation additional amino acid residues of Wnt11 sites (some of which had been predicted by mass spectrometry, see **section 3.3**), a set of Wnt variants was generated by substituting the amino acid of interest with alanine (indicated with stars in **Table 3.1**). The lipid modification of these mutants was tested using cC16:1n-7 in click labeling assays. Among all studied Wnt11 variants only Wnt11 S215A impaired the lipidation with cC16:1n-7 (**Figure 3.3**). All other mutants, including Wnt11 C80A, were lipidated with this fatty acid (**Figure 3.3**). These results imply that serine 215 is the only site lipidated with the cC16:1n-7 fatty acid and removal of the other selected amino acids did not affect the lipidation of serine 215. A similar result was observed for Wnt3a, i.e. only mutation of the canonical serine residue (S209A) abolished lipidation with cC16:1n-7 (**Appendix Figure 5.2**), a finding consistent with previous reports [35, 43, 55].

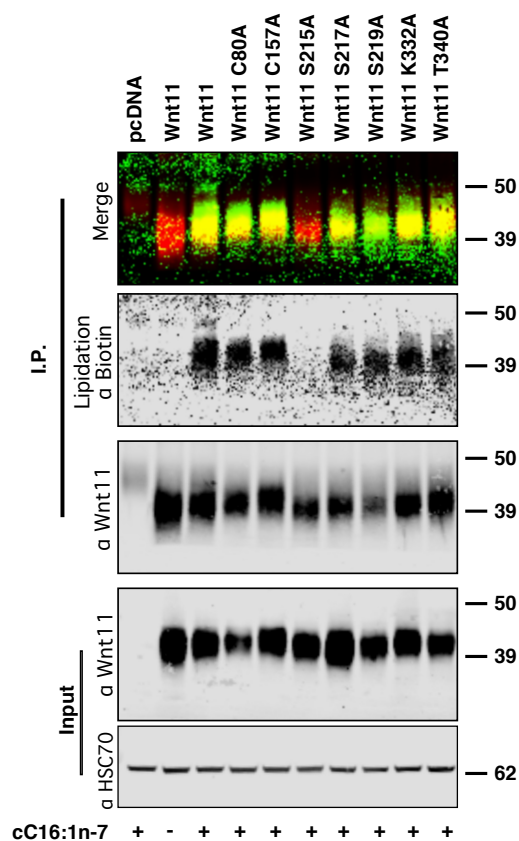


Figure 3.3: Serine 215, and not other mutated residues, impairs lipidation of Wnt11 by cC16:1n-7.

Lipid modification of overexpressed Wnt11 wild type or Wnt11 mutants in HEK293T cells. HEK293T cells were seeded in 10 cm plates as indicated in **section 2.14.1**. 24 h later, 100 μ M of cC16:1n-7 was added to the cells. On the same day, cells were transfected with the indicated overexpression constructs for either Wnt11 wild type or the mutants Wnt11 C80A, Wnt11 C157A, Wnt11 S215A, Wnt11 S217A, Wnt11 S219A, Wnt11 K332A, and Wnt11 T340A. On the following day, a second dose of cC16:1n-7 was added to the cells and incubated to reach a total of 36 hours of incubation with the clickable fatty acid. On day 3, cells were collected for immunoprecipitation and click labeling as outlined in **sections 2.11, 2.12, and 2.14.3**. Samples were eluted from the beads and analyzed by western blot. Antibodies specific for Wnt11 were used for protein detection and its lipid modification was detected using IRDye 800CW streptavidin. The blots were analyzed using Odyssey CLx-1014 LI-COR fluorescence imaging system controlled with ImageStudio Ver 5.0. HSC70 was used as loading control. α : indicates the protein to which the primary antibody is directed. I.P.: Immunoprecipitated protein. Western blot is representative of two independent experiments.

3.3 Additional lipid modifications of Wnt11 beyond the canonical acylation site

3.3.1 Towards mass spectrometric identification of additional acylation sites in Wnt11

I also initiated to identify additional lipid modification sites of Wnts beyond the canonical serine residue using a mass spectrometric approach. To this end, our group teamed up with the group of Prof. Carsten Hopf (Center for Mass Spectrometry and Optical Spectroscopy-CeMOS, Mannheim). Experiments were carried out with commercially available Wnt11 (R&D system, catalog #: 6179-WN-010/CF) and in addition with Wnt3a (R&D system, catalog#: 5036-WN-010/CF), both of them purified from CHO cells. Samples were analyzed by LC-MS/MS (see methods, **section 2.17**). The analysis of tryptic peptides suggested the presence of several other acylation sites in addition to the ones already reported (Serine 209 in Wnt3a [43] and S215 in Wnt11 [35], **Table 3.1**). Most of the residues seemed to be selective to either 16:0 or

16:1n-7 (such as C157, C211, S217, S219, K332 for 16:0, and S162, C218, T222 for 16:1n-7), while few others sites were non-selectively labelled with both fatty acids (e.g. S215 and T340).

Although the analysis of tryptic peptides showed multiple possible modification sites, analyses of the intact mass of the protein suggested only one acylation per molecule (data not shown). Nonetheless, by alanine mutagenesis, I evaluated the role of some of these residues in Wnt lipidation with cC16:1n-7 (**section 3.2**) and in Wnt secretion and signaling activity (**section 3.6 and 3.7**).

Putative Wnt lipidation sites identified by mass spectrometry					
Wnt3a			Wnt11		
C16:0			C16:0		
Residue	Ascore		Residue	Ascore	
S197	Low		★ C157	Low	
C203	Low		★ C211	Low	
C205	Low		★ S215	Low	
S211	Low		★ S217	Low	
C212	Low		★ S219	Low	
K215	Low		★ K332	High	
S220	Low		★ T340	High	
★ S300	High		C16:1n-7		
★ S301	High		★ S215	Low	
★ S338	High		C218	Low	
★ T343	High		T222	Low	
C16:1n-7			S162	High	
S64	Low-Medium		T322	High	
★ S209	Low-Medium		★ T340	High	
S211	Low-Medium				
T296	Low-Medium				
S338	Low-Medium				
C342	Low				
T343	Low-Medium				

Table 3.1. Putative Wnt lipidation sites identified by mass spectrometry.

List of amino acids of Wnt3a and Wnt11 predicted to be lipidated with either palmitic acid C16:0 or palmitoleic acid C16:1, as detected by mass spectrometry. Results were obtained by Dr. Diego Yepes in the Center for Mass Spectrometry and Optical Spectroscopy-CeMOS, Mannheim, from commercially purified recombinant Human Wnt3a and recombinant Human Wnt11 proteins (from CHO cells, R&D system Catalog#: 5036-WN-010/CF and Catalog#: 6179-WN-010/CF). The mass spectrometry measures were made using a Q-ToF ImpactII Bruker system. The prediction of lipid modification is classified based on the Ascore [122, 123]; Ascore calculates an ambiguity score as $-10 \times \log_{10} P$. The p value indicates the likelihood that the peptide is matched by chance, (Low, Ascore ≤ 20 ; Low-Medium, $20 \leq \text{Ascore} \leq 40$; Medium, $40 < \text{Ascore} < 100$, and High, Ascore ≥ 100). Stars indicate the residues selected for further mutagenesis experiments.

3.4 Differences between cC16:0 and cC16:1n-7 with respect to acylation and metabolic labeling

3.4.1 cC16:0 versus cC16:1n-7 acylation

I further analyzed the difference in the lipid labeling efficiency between the two fatty acids, cC16:0 and cC16:1n-7. HEK293T cells were transfected to overexpress Wnt11 and were later treated with either cC16:0 or cC16:1n-7 (**Figure 3.4A**). Wnt11 lipidation with both cC16:0 and cC16:1n-7 was observed (lanes 5 and 7 in **Figure 3.4A**). However, the band corresponding to cC16:1n-7 was more intense than that to cC16:0. When the mutant S215A was overexpressed, instead of wild type Wnt11, lipidation was not detected, neither with cC16:0 nor with cC16:1n-

7 (lanes 4-8, **Figure 3.4B**). Consistently, lipidation was not observed in knockout HEK293T^{ΔPORCN} cells transfected to overexpress Wnt11 wild type or mutant S215A (**Figure 3.4A,B**). These results reinforce the idea of a variable and nonspecific labeling efficiency with the saturated cC16:0 fatty acid (as already pointed out in **Figure 3.1**). Moreover, the data indicate that cC16:1n-7 is more efficient in lipidating Wnt11 than cC16:0.

In addition, Wnt acylation was investigated using stable cell lines that constitutively express Wnt11 (HEK293T^{Wnt11} and HEK293T^{ΔPORCN-Wnt11} cells, **Figure 3.4C-D**). In HEK293T^{Wnt11} cells, cC16:1n-7 labeling was observed to be significantly stronger than cC16:0 labeling (lanes 5 and 8 in **Figure 3.4C**). Lipidation with cC16:1n-7 was observed in HEK293T^{Wnt11} but not in HEK293T^{ΔPORCN-Wnt11} cells (lanes 8-9 in **Figure 3.4C**). On the contrary, for cC16:0 Wnt11 lipidation was observed both in HEK293T^{Wnt11} (lane 5, **Figure 3.4C**) and faintly in HEK293T^{ΔPORCN-Wnt11} cells (lane 6, **Figure 3.4C**). For cC16:0, it is thus unclear whether there was also lipidation in Porcupine knockout cells. In an attempt to improve the signal detection of cC16:0 the exposure time during the detection was increased in a separate gel (using ECL and chemiluminescent detection system, **Figure 3.4D**). Under these conditions, a labeling with cC16:0 in HEK293T^{Wnt11} and HEK293T^{ΔPORCN-Wnt11} cells was observed (lanes 5-6, **Figure 3.4D**).

Taken together, these results suggest a preference of Wnt11 for palmitoleic acid alkyne cC16:1n-7 over palmitic acid alkyne cC16:0. Moreover, serine 215 appears to be the site in Wnt11 where cC16:1n-7 attaches. These results corroborate reports regarding labeling efficiency and lipid modification of Wnt11 [**14, 35, 36, 43, 46, 55, 59-61**]. This explains the variability of the lipidation pattern among the replicates observed for cC16:0.

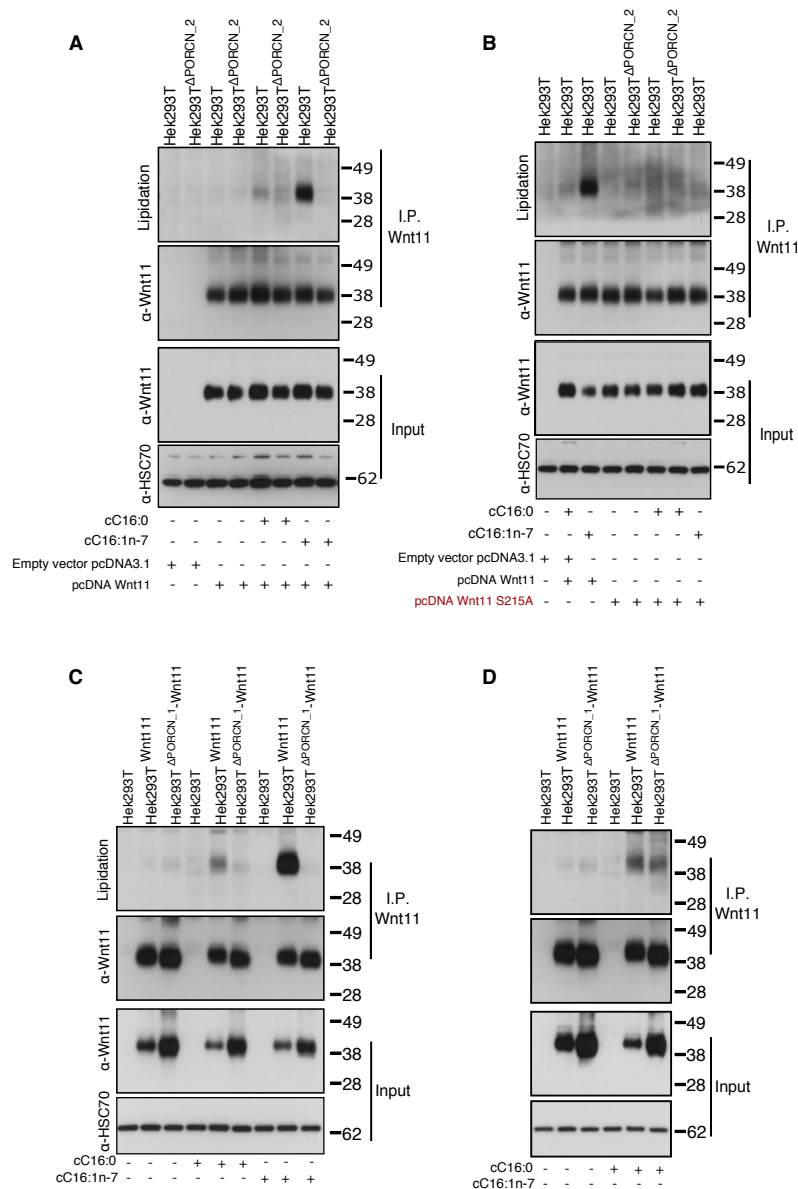


Figure 3.4: Comparison of Wnt acylation using cC16:0 or cC16:1n-7.

HEK293T, HEK293T^{ΔPORCN_2}, HEK293T^{Wnt11}, and HEK293T^{ΔPORCN_1-Wnt11} cells were seeded in 10 cm plates as indicated in **section 2.14.1**. 24 h later, 100 μM of either cC16:0 or cC16:1n-7 was added to the cells. On the same day, HEK293T and HEK293T^{ΔPORCN_2} cells were transfected with the indicated overexpression constructs for either Wnt11 wild type or Wnt11 S215A. On the following day, a second dose of cC16:1n-7 was added to the cells and incubated to reach a total of 36 hours of incubation with the clickable fatty acid. On day 3, cells were collected for immunoprecipitation and click labeling as outlined in **sections 2.11, 2.12, and 2.14.3**. Samples were eluted from the beads and analyzed by western blot. Antibodies specific for Wnt11 were used for protein detection and its lipid modification was detected using HRP-conjugated streptavidin. The blots were analyzed by a chemiluminescent system using ECL substrates and a COMPACT 2 X-ray film processor. HSC70 was used as loading control. *α*: indicates the protein to which the primary antibody is directed. I.P.: Immunoprecipitated protein. **A-B**. HEK293T wild type and PORCN knockout cells were transfected to overexpress either Wnt11 or Wnt11 S215A. Western blots are representative of two independent experiments. **A**. Lipidation of Wnt11 with cC16:0 in HEK293T or HEK293T^{ΔPORCN} cells (lanes five and six). Lipidation of Wnt11 with cC16:1n-7 in HEK293T cells (lane seven). **B**. No lipid modification was detected in Wnt11 S215A (lanes four to eight). **C-D** Lipid labeling with either cC16:0 or cC16:1n-7 in stable cell lines with constitutive expression of Wnt11. **C**. Lipidation of Wnt11 with cC16:0 in HEK293T^{Wnt11} or HEK293T^{ΔPORCN_1-Wnt11} cells (lanes five and six). Lipidation of Wnt11 with cC16:1n-7 in HEK293T^{Wnt11} cells (lane eight). Western blot is representative of three independent experiments. **D**. Samples from cells incubated with cC16:0 (from **C**) run in a separate gel.

3.4.2 cC16:0 and cC16:1n-7 are metabolically incorporated into distinct lipid classes

I next asked if the difference in the lipidation efficiency for cC16:0 and cC16:1n-7 was correlated with the metabolic conversion of cC16:0 into cC16:1n-7. To this end, in a first attempt, the incorporation into HEK293T cells of cC16:0 and cC16:1n-7 fatty acids was measured by using alkyne-azide cycloaddition click chemistry combined with precursor ion scanning mass spectrometry (a technique previously established in the group) [116, 119, 124]. However, it was not possible to detect neither palmitic acid alkyne cC16:0 nor the conversion of cC16:0 to cC16:1n-7 (see **Figure 5.3 in the Appendix**).

Next, I checked if metabolism of cC16:0 and cC16:1n-7 would lead to a differential channeling into different lipid classes. To test this, lipids were extracted from HEK293T cells incubated for 36 h with 100 μ M of cC16:0 or cC16:1n-7, similar to the experimental conditions used to detect lipidation of Wnt11 (**Figure 2.2B**). The lipid extracts were submitted for click reaction with 3-Azido-7-hydroxycoumarin. This was followed by thin layer chromatography (TLC) which was performed in the presence of lipid standards. cC16:0 incorporated mainly into the lipid classes phosphatidylcholine (PC), phosphatidylethanolamine (PE), and triacylglycerol (TAG) (**Figure 3.5**, upper panel). In the case of cC16:1n-7, the overall staining intensity was lower when compared to the results obtained for cC16:0. However, the incorporation of cC16:1n-7 into PC, PE, and TAG lipid classes could still be observed (**Figure 3.5**, upper panel). The observed differences were not due to the amount of sample loaded onto the TLC plate, as a similar amount of total lipids was detected for HEK293T cells, either untreated, treated with 100 μ M cC16:0 or with 100 μ M cC16:1n-7 (see sulfuric acid stain in **Figure 3.5**, in the lower panel). Altogether these results indicate that under the labeling condition used for the detection of lipidation of Wnt11 (**Figure 2.2B**), cC16:0 and cC16:1n-7 were metabolized into complex lipid classes such as PC, PE and TAG. Furthermore, due to the differences in the signal band intensities between the cC16:0 and cC16:1n-7 samples suggest that cellular uptake of cC16:0 and/or its further metabolization into lipid classes occurs more efficiently than for cC16:1n-7.

The lipid species into which the fatty acids cC16:0 and cC16:1n-7 were incorporated, were studied in detail following the same procedure as before (**Figure 2.2B**). Lipid extracts were submitted to MS/MS analysis using a high resolution Q Exactive Plus mass spectrometer to measure PC and PE lipid species (**Figure 1.5**). The alkyne group gave rise to two degrees of unsaturation, i.e. two unsaturations for the fatty acids cC16:0 and three unsaturations for cC16:1n-7. This degree should be reflected in the detected lipid species. Consequently, I grouped the lipid species according to the grades of unsaturation, focusing on the most abundant phosphatidylcholine (PC) and phosphatidylethanolamine (PE) lipid classes, namely those of a length of 16 or 18 carbons (**Figure 3.6**).

For PC the percentage of lipid species containing the saturated fatty acid C16:0 was lower in cells labeled with the clickable fatty acid cC16:0 than in unlabeled cells (**Figure 3.6A**, PC C16:0). The percentage of PC species that contain a C16:1 fatty acid was lower in cells incubated with cC16:0 and cC16:1n-7 compared to unlabeled cells (**Figure 3.6A**, PC C16:1). As expected, PC species with C16:2 fatty acids were observed at a higher level in cells labeled with cC16:0 than in unlabeled cells (**Figure 3.6A**, PC C16:2). Furthermore, the percentage of PC species that contain a C16:3 fatty acid increased in cells labeled with cC16:1 compared to unlabeled cells (**Figure 3.6A**, PC C16:3). Comparing the lipid species containing C16:2 fatty acids in cells incubated with cC16:0 and C16:3 fatty acids in cells incubated with cC16:1, it was observed

that the amount of PC species containing a C16:2 fatty acid was higher than the amount of PC species containing a C16:3 fatty acid (**Figure 3.6A**, PC C16:2 in blue and PC C16:3 in yellow). This points to a higher efficiency of cC16:0, compared to cC16:1n-7, to be incorporated into PC species of 16 carbons.

Regarding the PC species that contain fatty acids with 18 carbons, we did not observe significant changes in the PC species that include saturated fatty acids (**Figure 3.6A**, PC C18:0). However, there was a decrease in the percentage of PC species with unsaturated C18:1 fatty acid when cells were treated with cC16:0 or cC16:1n-7 compared to unlabeled cells (**Figure 3.6A**, PC C18:1). Similar, to the 16 carbon fatty acid containing PC species, an increased amount of PC species with C18:2 in cells incubated with cC16:0 and an increased of the lipid species with C18:3 in cells incubated with cC16:1n-7 was observed (**Figure 3.6A**, PC C18:2, PC C18:3). However, here the amount of PC species containing C18:2 lipid species (in cells incubated with cC16:0) was found to be similar to the amount of PC species containing C18:3 species (in cells incubated with cC16:1n-7). Consequently, the results here suggest that cC16:0 and cC16:1n-7 can be elongated to 18 carbon fatty acids and incorporated into PC.

For phosphatidylethanolamine (PE), a similar behavior was observed as that of PC. The PE species containing fatty acid C16:0 and C16:1 were less common in cells incubated with the clickable fatty acid cC16:0 and cC16:1n-7 than in unlabeled cells (**Figure 3.6B**, PE C16:0 and C16:1). On the contrary, PE species with a C16:2 fatty acid content increased in cells labeled with cC16:0 compared to unlabeled cells (**Figure 3.6B**, PE C16:2). The PE species that contained C16:3 fatty acid also increased in cC16:1-labeled cells (**Figure 3.6B**, PE C16:3). In contrast to the PC species, PE species displayed a similar amount of species containing C16:2 and C16:3 (**Figure 3.6B**, PE C16:2 and PE C16:3).

Regarding the PE species containing 18 carbons fatty acids, saturated PE species containing C18:0, from cells incubated with both clickable fatty acids cC16:0 and cC16:1n-7, were predominantly observed (**Figure 3.6B**, PE C18:0). However, there was a decrease in the percentage of C18:1 species from cells treated with cC16:0 and cC16:1n-7 compared to untreated cells (**Figure 3.6B**, PE C18:1). The opposite was observed for C18:2 species, i.e. an increase of PE C18:2 lipid species from cells incubated with cC16:0 was observed (**Figure 3.6B**, PE C18:2). Interestingly, for the PE species containing C18:3 species, an increase in signal was observed for cells incubated with cC16:0 and cC16:1n-7 (**Figure 3.6B**, PE C18:3). These results suggest the clickable fatty acids cC16:0 and cC16:1n-7 lead to an increase of PE species containing saturated C18:0, unsaturated C18:2, or C18:3 fatty acids. Comparing PE with PC (**Figure 3.6A-B**), the data suggest a preference for PE species containing C18 fatty acids rather than those with 16 carbons, contrary to what was observed for PC.

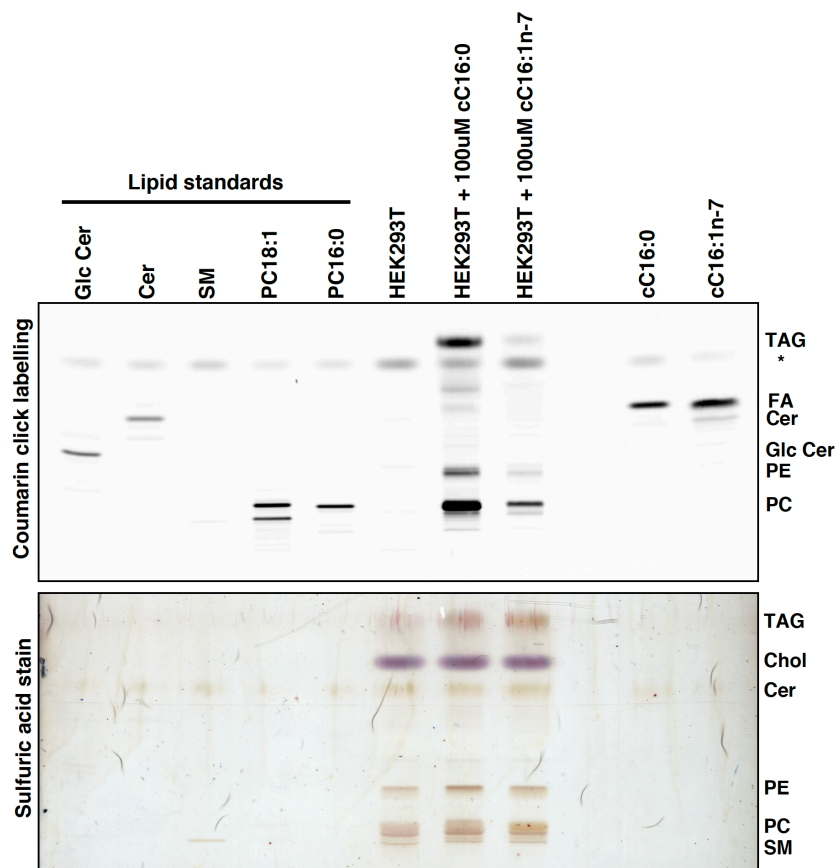


Figure 3.5: Metabolic incorporation of cC16:0 or cC16:1n-7 in HEK293T cells.

HEK293T cells were incubated with 100 μM of cC16:0 or cC16:1n-7 for 36 h. After incubation, 1×10^6 HEK293T cells were collected and submitted to lipid extraction. Lipid extracts were subjected to a click reaction with 3-Azido-7-hydroxycoumarin. 30 μL of lipid extract were applied on an HPTLC plate and separated by thin-layer chromatography. The plate was sprayed with 4% (v/v) N,N-diisopropyl ethylamine in hexane for sensitive detection of protonated coumarin. Fluorescent imaging of the plate was performed with excitation at 460nm and emission at 488nm. For detection of the total lipids on the plate, sulfuric acid staining was performed. Analysis of the TLC was performed comparing the samples with clickable lipid standards of different lipid classes. The **upper panel** shows a fluorescence image of clicked lipids. The **lower panel** displays a sulfuric acid stain. The detail procedure is described in **section 2.18**. Image is representative of three independent experiments.

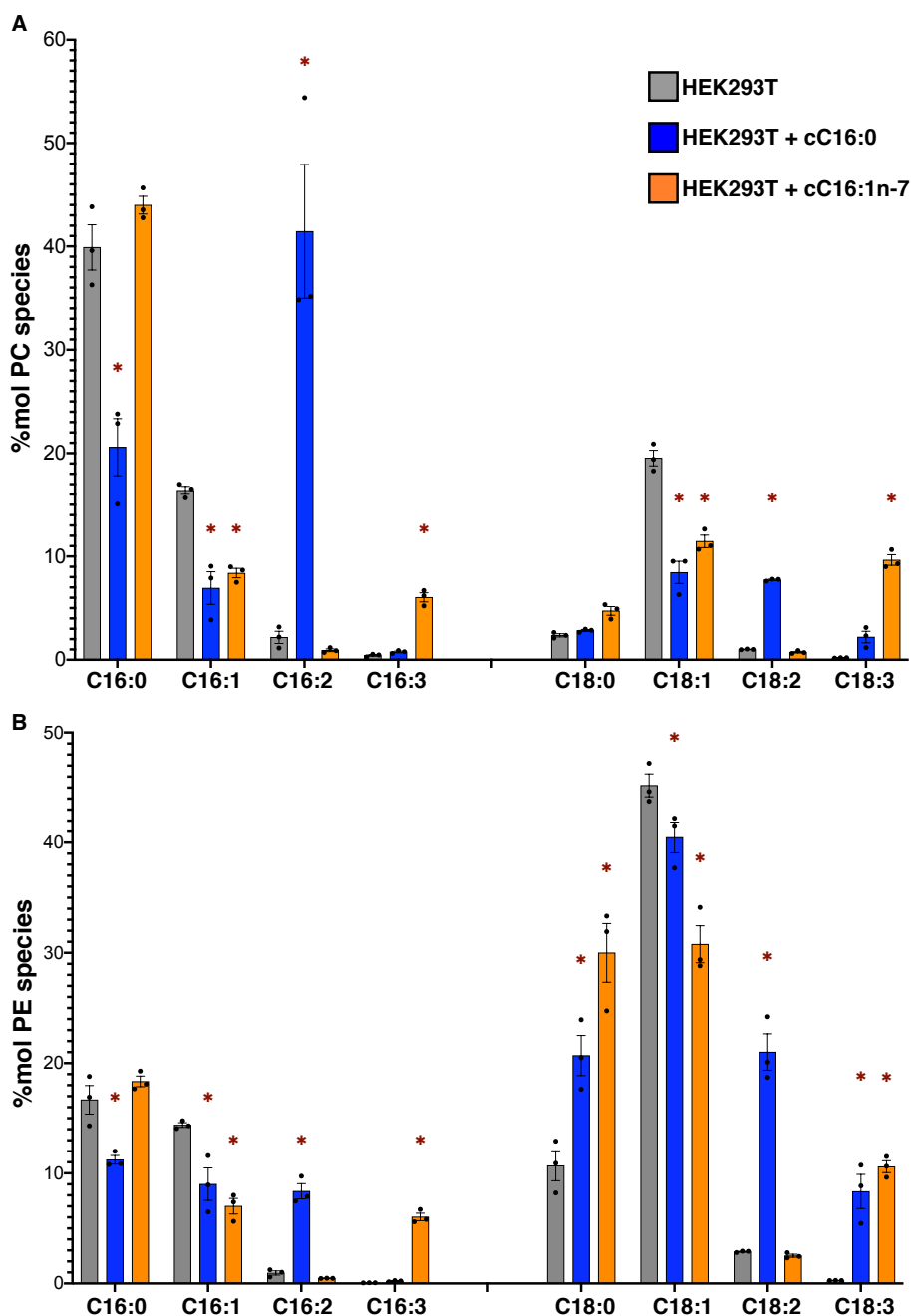


Figure 3.6: Incorporation of cC16:0 and cC16:1n-7 into PC and PE lipid species.

HEK293T cells were seeded in 6 well plates (3×10^5 cells/ well) and treated with either $100 \mu\text{M}$ of cC16:0 (blue bars) or cC16:1n-7 (orange bars), keeping the same incubation conditions used to detect lipidation on Wnt11 (see **section 2.14.1** and **Figure 2.2B**). Untreated HEK293T cells (gray bars) were used as control. After incubation, approximately 1×10^6 cells were collected from cell cultures and pelleted by centrifugation. Then the pellet was resuspended in ammonium bicarbonate ($(\text{NH}_4)\text{HCO}_3$, 155 mM) methanol 1:1 (v/v) and the samples were subjected to acidic Bligh and Dyer lipid extraction (SBD-extraction) as is described in [115, 116]. Mass spectrometric measurements were performed on a Q Exactive mass spectrometer equipped with chip-based (HD-D ESI Chip, Advion Biosciences) nano-electrospray infusion and ionization (TriVersa NanoMate, Advion Biosciences). Mass spectra was processed with the software PeakStrainer and lipidXplorer 1.2.8 to [117, 118]. The mol percentage for each PC and PE lipid species was calculated based on the concentration and the intensities of the lipid standards. Three independent experimental replicates were carried out. Data are presented as mean \pm SE. Statistic analyses were performed using 2-way ANOVA and Dunnet multiple comparison test were used. The Ctrl inside each group was considered as reference for the statistical test. Statistical significance of the changes indicated (*: p-value < 0.05). Lipid extractions were done by Iris Leibrecht, Christian Luchtenborg and

Timo Sachsenheimer. Lipidome data was analyzed and provided by Christian Lüchtenborg and Timo Sachsenheimer (Brügger lab), for details in the procedure see **section 2.18.2**. **A.** Left, phosphatidylcholine (PC) species distribution displaying species with fatty acids of 16 carbons length, being either saturated (PC C16:0), containing one (PC C16:1), two (PC C16:2) or three (PC C16:3) unsaturations. In the right side of the plot: % mol of phosphatidylcholine species with fatty acids of 18 carbons, saturated (PC C18:0), containing one (PC C18:1), two (PC C18:2) or three (PC C18:3) unsaturations. **B.** In the left side of the plot: % mol of phosphatidylethanolamine (PE) species with fatty acids of 16 carbons, saturated (PE C16:0), with one unsaturation (PE C16:1), two unsaturations (PE C16:2) and three unsaturations (PE C16:3). In the right side of the plot: % mol of phosphatidylethanolamine species with fatty acids of 18 carbons, saturated (PE C18:0), with one unsaturation (PE C18:1), two unsaturations (PE C18:2) and three unsaturations (PE C18:3).

3.5 Summary of the part A: alternative acylation sites and types of fatty acid modification of Wnt11

In this part, chemical biology tools and mass spectrometry were used to characterize the lipidation of Wnt11. Unexpectedly, using the palmitic acid alkyne cC16:0, lipidation was detected for Wnt11 variants with the canonical lipidation site S215 removed [35] and in cells that lacked the acyltransferase Porcupine. These results would indicate that, besides serine 215 and Porcupine, there could be another amino acid and another acyltransferase involved in Wnt11 lipidation. However, the experiments could not be fully reproduced across multiple replicas.

In fact, detection of lipidation drastically improved when the monounsaturated lipid cC16:1n-7 was used instead. By using palmitoleic acid alkyne cC16:1n-7, the central role of serine 215 and the importance of the protein partner Porcupine could be recapitulated. These data are consistent with the literature [33, 35, 43, 44, 46, 55, 67] and highlights the importance of a monounsaturated acyl chain for the lipidation of Wnt11.

Why cC16:0 and cC16:1n-7 displayed such a difference in Wnt11 acylation was also investigated. By using a TLC readout, it was observed that both fatty acids were metabolized into distinct lipid classes such as PC, PE, and TAG. My results suggest that cC16:0 is either more efficiently taken by cells or metabolized into other lipid classes than cC16:1n-7. The lipidomics data shows a higher probability for cC16:0 to be incorporated into 16 carbon PC species than cC16:1n-7, although both of them can be elongated to 18 carbon PC fatty acids. cC16:0 and cC16:1n-7 were also incorporated into PE species of 16 carbons, saturated C18:0, unsaturated C18:2, or C18:3 fatty acids. In general, the clickable fatty acids were preferentially elongated resulting in PE C18 species but remained mainly as C16 species in PC.

In summary, our results confirm that the monounsaturated cC16:1n-7 is used for acylation of serine 215 of Wnt11 and that Porcupine is essential for this lipidation process. Wnt11 lipidation with the saturated cC16:0 at another site besides serine 215 and without the assistance of Porcupine, although initially observed, it could not be fully reproduced.

B. Molecular factors that contribute to Wnt11 secretion and function

Wnt11 activity has been linked to the acylation of serine 215 residue by PORCN [35]. However, recent experiments of O. Voloshanenko (unpublished data, M. Boutros group, DKFZ, Heidelberg) revealed that mutation of serine 215 or depletion of PORCN and Evi proteins did not abolish Wnt11 secretion. Based on this, we asked whether other uncharacterized amino acids of Wnts, or other acyltransferases involved in their lipidation, could affect the secretion and functions of Wnts. I selected Wnt11 and Wnt3a to study this. First, by mutagenesis I investigated whether other amino acids affect secretion and function of these two proteins. Second, in a contribution to the project of O. Voloshanenko, we investigated whether the secretion of Wnt11 depend on a specific domain or particular amino acids of Wnt11 by modulating its post-translational modification and interaction with the carrier protein Evi. Third, we explored which other acyltransferases could be involved in the secretion of Wnt11.

3.6 Secretion of Wnt variants

A set of putative lipidation sites was predicted by mass spectrometry (section 3.3). Here, I investigated whether these sites were important for the secretion of Wnt11 and Wnt3a. To this end, the amount of protein that was secreted into the extracellular media was measured qualitatively, using blue sepharose pulldown and western blot assays (see methods section 2.16), using Wnts with the amino acids of interest being replaced by alanine (Figure 3.7A). In these experiments the secretion of the wild type protein was taken as reference. The residual secretion observed for Wnt11 S215A would be consistent with the preliminary data of O. Voloshanenko (M. Boutros group, DKFZ, Heidelberg) in which Wnt11 was secreted independently of the presence of serine 215 (unpublished data, M. Boutros group, DKFZ, Heidelberg).

For Wnt11 the mutants S219A, K332A, and T340A did not affect secretion (Figure 3.7B). I observed a slight reduction for the mutants C157A and S217A and 215A, with the latter displaying the most appreciable decrease (Figure 3.7B). Because neither of the studied mutations fully abolished Wnt11 secretion, these residues seem to be dispensable for Wnt11 secretion.

In the case of Wnt3a, a drastic reduction in the secretion was observed for the mutant S209A (Figure 3.8B). These results are in line with previous experiments [46, 55, 60]. Together with these results, our data strongly suggest that serine 209, and more likely its lipidation, is essential for Wnt3a secretion. All other mutants preserved a qualitatively similar secretion level as the wild type protein, thus implying the targeted amino acids were not relevant for the secretion process (Figure 3.8B).

3.7 Amino acids involved in the activation (Wnt3a) or inhibition (Wnt11) of Wnt/ β -catenin canonical pathway

Wnt11 is associated with the inhibition of the Wnt/ β -catenin canonical pathway [125-127]. Next, I tested whether any of the Wnt variants tested for acylation would be important for Wnt activity (**table 3.2**), i.e. participating in the pathway's inhibition. For this purpose, a non-canonical TCF4 reporter assay (implemented in the group of M. Boutros, at DKFZ, see **section 2.20**) was used.

Using this assay, I found that the Wnt11 mutants S215A and C157A were less efficient in inhibiting the activation of the Wnt/ β -catenin pathway when compared to Wnt11 wild type (**Figure 3.7C**). These results indicate serine 215 is necessary for the inhibitory function of Wnt11 on the canonical pathway, either by directly undergoing acylation [35] or by contributing to acylation at other sites. Cysteine 157 is engaged in a disulfide bond with cysteine 140 (as predicted from Uniprot, UniProtKB - O96014 WNT11_HUMAN, **Figure 3.7A**). Hence, removal of this bond by the introduced mutation in C157, may have altered the protein conformation, and thereby the inhibition of the canonical pathway (**Figure 3.7C**).

Wnt3a, in turn, has been related to the activation of the Wnt/ β -catenin canonical [32, 43, 44, 55]. I followed a similar approach as for Wnt11, to discern important sites in Wnt3a related to the activation process (see **section 2.20**). Consequently, the mutants S209A and C155A were observed to compromise the activation of the Wnt/ β -catenin canonical pathway (**Figure 3.8C**). These results suggest that serine 209, and more specifically its lipid modification, is linked to the activation of the canonical pathway in question, as already reported [32, 43, 44, 55]. The residue cysteine 155 forms a disulfide bond with cysteine 138 (according to Uniprot, UniProtKB - P56704 WNT3A_HUMAN, **Figure 3.8A**), suggesting a similar mechanism as described for Wnt11 when replacing this residue by alanine.

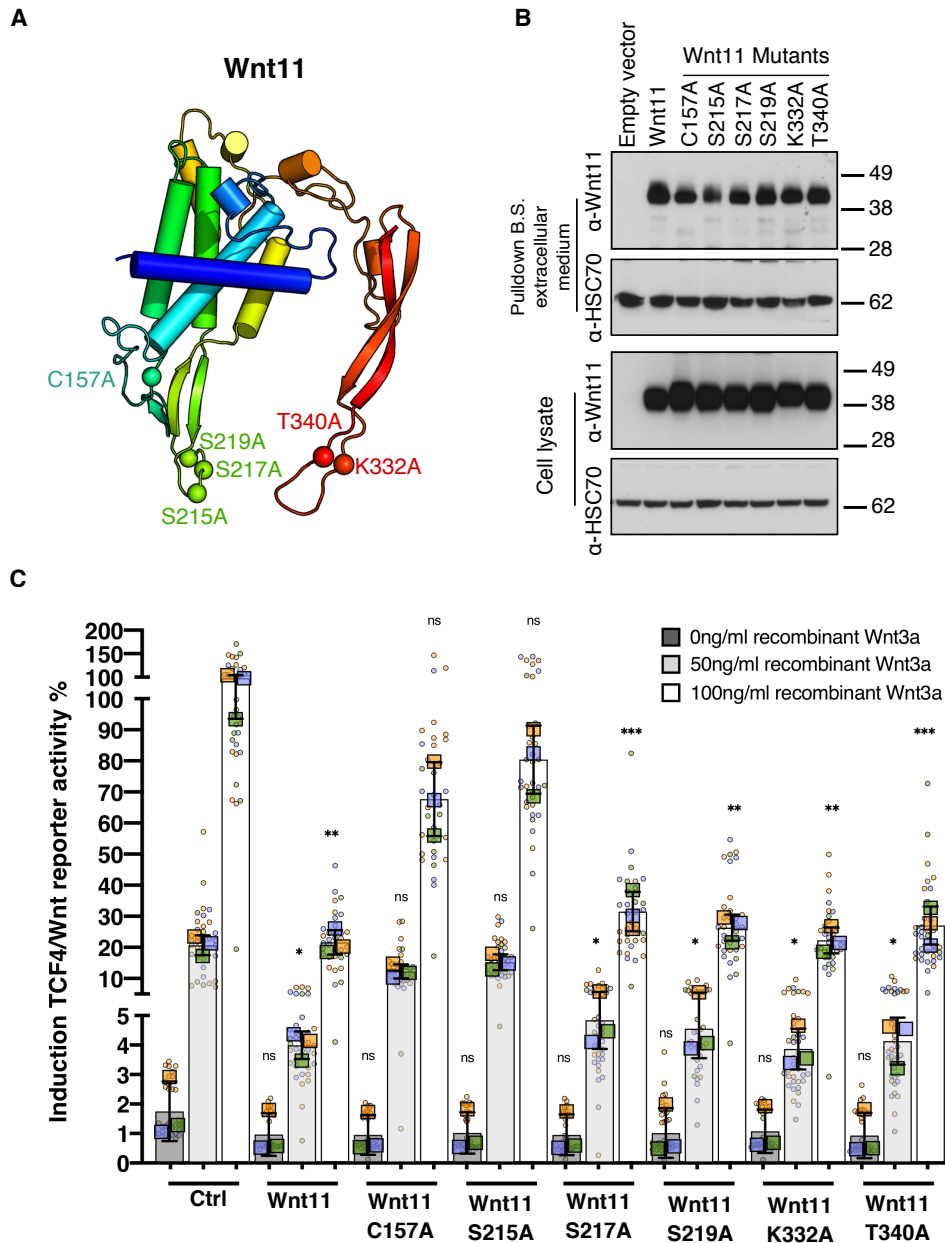


Figure 3.7: Secretion and functional assays of Wnt11 wild type and variants. **A.** 3D structure of Wnt11 (cartoon) showing the residues that have been selected for alanine mutagenesis screen (sphere). The cysteine 157 forms a disulfide bond with cysteine 140 (UniProtKB - O96014). **B.** Western blot shows the secretion of Wnt11 wild type or alanine-mutants into the extracellular medium. HEK293T cells were seeded in 6-well plates, 2 wells per condition at a seeding density of 3×10^5 cells/well. Twenty-four hours later, HEK293T cells were transfected with either Wnt11 wild type or one of the mutants C157A, S215A, S217A, S219A, K332A and T340A plasmids. 48 hrs later extracellular medium and lysates of cells were collected. Wnts were precipitated from the extracellular medium with the help of blue sepharose beads (B.S.). Samples from blue sepharose pull down and cell lysate were run by SDS-PAGE and western blot. HSC70 served as the loading control for lysate and extracellular medium. Western blots are shown as representatives of 3 independent experiments. **C.** Percentage of induction of TCF4/Wnt reporter activity is presented for Wnt11 and the mutants with the indicated residue substituted by alanine. HEK293T cells were seeded into 384-well plates, the final volume per well was 50 μ l at a concentration 5×10^4 cells/ml. After 24 h cells were transfected with 20ng TCF4/Wnt firefly luciferase reporter, 10ng actin-Renilla luciferase reporter, 10ng of pcDNA Wnt11 wild type or the Wnt11 mutants C157A, S215A, S217A, S219A, K332A and T340A plasmids. 16 hrs before the read-out recombinant mouse Wnt3a was added for activation of β -catenin-dependent signalling in three different concentrations: 0ng/ml (dark gray shade bar), 50ng/ml (light gray shade bar) and 100ng/ml (white shade bar). The read-out was performed 48 h after plasmid transfection. HEK293T cells

transfected with empty vector (pcDNA) was considered as control (Ctrl). A reduction in the percentage of induction is indicative of the ability of the studied proteins to inhibit β -catenin-dependent Wnt signalling. Three independent experimental replicates were carried out. Mean of each replicate is shown with colored squares. Individual measurements are depicted with colored dots. Data are presented as mean \pm SE. Statistical significance of the changes indicated (*: p-value < 0.05, **: p-value < 0.01, ***: p-value 0.001, and ns: non-significant). Statistics with 2-way ANOVA and Dunnet multiple comparison test was used. The Ctrl set was considered as reference for the statistical test.

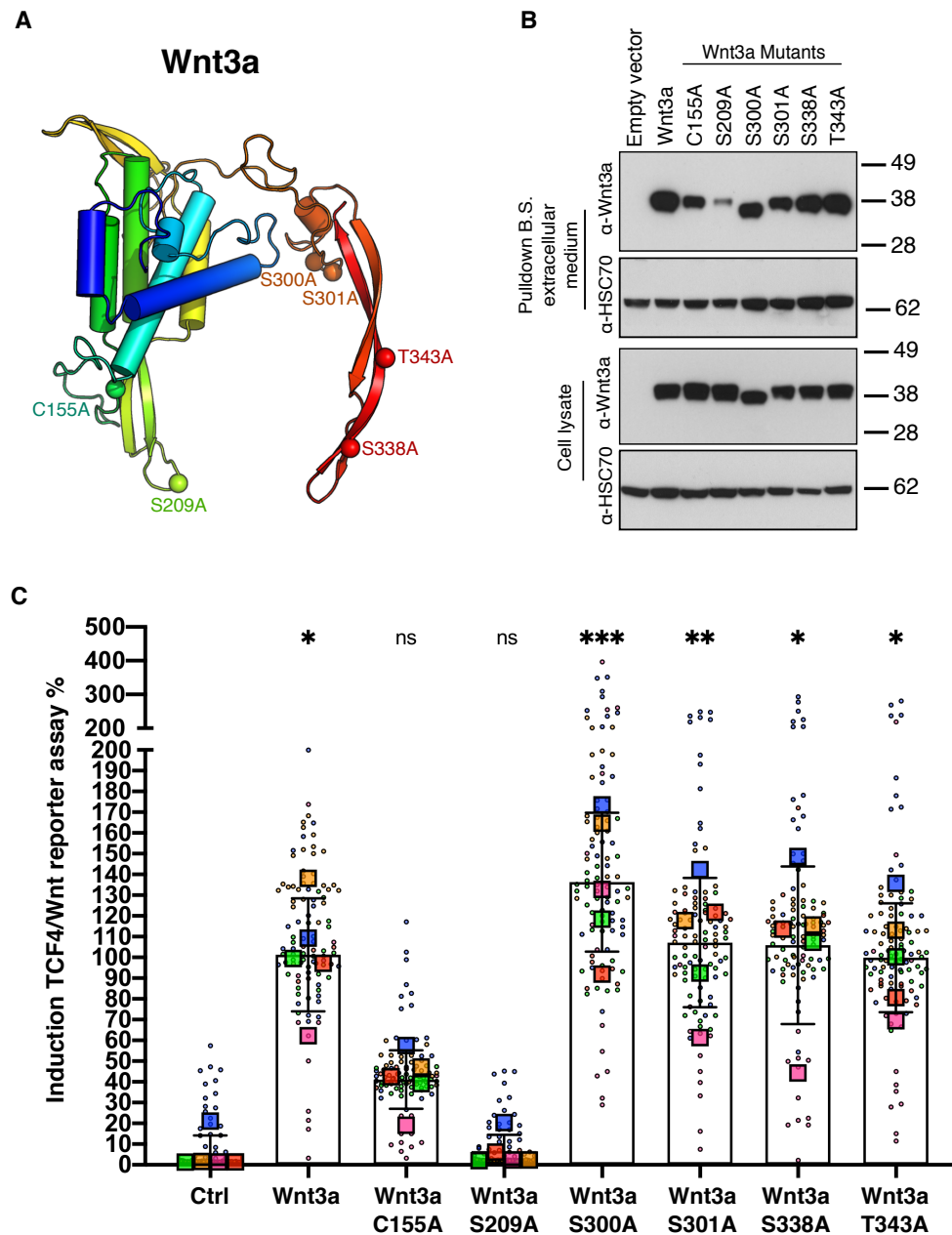


Figure 3.8: Secretion and functional assays of Wnt3a mutant variants. **A** 3D structure of Wnt3a (cartoon) showing the residues that have been selected for alanine mutagenesis screen (sphere). The cysteine 155 forms a disulfide bond with cysteine 138 (UniProtKB - P56704). **B**. Secretion of Wnt3a wild type or alanine-mutants into the extracellular medium. HEK293T cells were seeded in 6-well plates, 2 wells per condition at a seeding density of 3×10^5 cells/well. Twenty-four hours later, HEK293T cells were transfected with either Wnt3a wild type or one of the mutants C155A, S209A, S300A, S301A, S338A, T343A and T340A plasmids. 48 hrs later extracellular medium and lysates of cells were collected. Wnts were precipitated from the extracellular medium with the help of blue

sepharose beads (B.S.). Samples from blue sepharose pull down and cell lysate were run by SDS-PAGE and western blot. HSC70 served as the loading control for lysate and extracellular medium. Western blots are shown as representatives of 3 independent experiments. **C.** Percentage of induction of TCF4/Wnt reporter activity is presented for Wnt3a and the mutants with the indicated residue substituted by alanine. HEK293T cells were seeded into 384-well plates, the final volume per well was 50 μ l at a concentration 5×10^4 cells/ml. After 24 h cells were transfected with 20 ng TCF4/Wnt firefly luciferase reporter, 10 ng actin-Renilla luciferase reporter, 10 ng of pcDNA Wnt3a wild type or the Wnt3a mutants C155A, S209A, S300A, S301A, S338A, T343A and T340A plasmids. The read-out was performed 48 h after plasmid transfection. HEK293T cells transfected with empty vector (pcDNA) was considered as control (Ctrl). Five independent experimental replicates were carried out. Mean of each replicate is shown with colored squares. Individual measurements are depicted with colored dots. Data are presented as mean \pm SE. Statistical significance of the changes is indicated (*: p-value < 0.05, **: p-value < 0.01, ***: p-value 0.001, and ns: non-significant). Statistics with 2-way ANOVA and Dunnet multiple comparison test was used. The Ctrl set was considered as reference for the statistical test.

To investigate if cellular functions are strictly related to the serine 215 in Wnt11, a gelatin degradation assay implemented by L. Wolf (M. Boutros group, DKFZ, Heidelberg), see methods **section 2.21**. Unfortunately, due to technical problems, these experiments did not show a clear trend that could indicate functional differences between different Wnt variants. The results of these experiments are shown in the appendix **Figure 5.6**.

3.8 Dissecting the region in Wnt that regulates Evi-independent Wnt secretion

In parallel to the study of lipidation of Wnts, I have contributed to the project of O. Voloshanenko (M. Boutros group, DKFZ, Heidelberg) that aimed at investigating if the secretion of Wnt11 could proceed independently of the carrier protein Evi. Evi has been demonstrated to facilitate secretion of Wnt3a and Wnt3 [17, 56, 57, 128]. Contrary to that, previous experiments of O. Voloshanenko showed that Wnt11 was still being secreted in Evi knockout cells, suggesting this protein is secreted without the assistance of Evi. Comparing the sequences of Wnt11 and Wnt3, they share 35% of identity. However, the similarity of the first 48 N-terminal amino acids is only 17%. O. Voloshanenko hence formulated the hypothesis that the different secretion behavior between Wnt11 and Wnt3 is related to the distinct N-terminal sequences. To test this hypothesis, O. Voloshanenko designed chimera proteins of Wnt11 and Wnt3 with their first 48 N-terminal residues swapped: one chimera protein contained the first 48 amino acids of Wnt11 and the rest from Wnt3 (construct called Wnt11¹⁻⁴⁸-Wnt3), while the other chimera protein consisted of the 48 N-terminal amino acids of Wnt3 and the rest from Wnt11 (construct called Wnt3¹⁻⁴⁸-Wnt11) (**Figure 3.9A**). The expression of these chimera proteins was assessed in experiments with cells lacking Evi (HEK293T ^{Δ Evi}).

First, focusing on the N-terminal region of Wnt11, the presence in the extracellular media of the chimera Wnt11¹⁻⁴⁸-Wnt3 was investigated and compared with that of Wnt11 and Wnt3 in HEK293T and HEK293T ^{Δ Evi} cells (**Figure 3.9B**). In HEK293T wild type cells, Wnt11¹⁻⁴⁸-Wnt3, Wnt11, and Wnt3 were detected either in the cell lysate or in the extracellular medium (**Figure 3.9B**). In the cell lysate of HEK293T ^{Δ Evi} cells, the three proteins were detected. In the extracellular media, there was no evidence of secretion of Wnt3. However, Wnt11 and the chimera Wnt11¹⁻⁴⁸-Wnt3 were still secreted (**Figure 3.9B**). In contrast to Wnt3, the chimeric Wnt11¹⁻⁴⁸-Wnt3 protein was secreted in the absence of Evi. Therefore, my results suggest that the N-terminal region of Wnt11 confers to Wnt3 protein the property to be secreted into the extracellular medium independently of the carrier protein Evi.

A surprising finding was that Wnt11¹⁻⁴⁸-Wnt3 and Wnt3 expressed in HEK293T cells showed a different running behavior in SDS-PAGE gels (**Figure 3.9B**), with the Wnt11¹⁻⁴⁸-Wnt3 chimera displaying a significantly higher apparent molecular weight than Wnt3. I checked if this band shift was associated with another post-translational modification. One possibility is that the chimera protein featured a different glycosylation pattern. To test this, a kit containing a cocktail of endoglycosydases was used for protein deglycosylation. After treatment with this deglycosylation mix, both proteins Wnt11¹⁻⁴⁸-Wnt3 and Wnt3 displayed the same molecular weight, (**Figure 3.9C**). This result suggests that the N-termini of Wnt11 and Wnt3 have a different glycosylation patterns, causing the observed shift in the size of the bands in SDS-PAGE analysis.

Second, with regard to the N-terminal region of Wnt3, previous work has reported a glycosylation site at asparagine 40 [35]. To test whether this residue is involved in Evi-dependent secretion of Wnt11, O. Voloshanenko designed mutants with asparagine 40 and threonine 42 being replaced by glutamine and proline, respectively, as these amino acids are part of the consensus sequence (Asn-X-Ser/Thr) required for glycosylation [129]. The secretion of these mutants was evaluated in cells lacking Evi (HEK293T^{ΔEvi}, see method in **section 2.16**). In contrast to the mutant Wnt11 T42P, the mutant Wnt11 N40Q was not secreted in the extracellular medium (data from O. Voloshanenko, not shown here). These results suggested that asparagine 40 is relevant for the secretion of Wnt11 in HEK293T^{ΔEvi} cells.

To gain insight on how asparagine 40 is involved in the secretion of Wnt11, we studied the binding of Wnt11 to Evi, by performing co-immunoprecipitation experiments. In this experiment, the chimera protein Wnt3¹⁻⁴⁸-Wnt11 and the mutant Wnt11 N40Q interacted more strongly with Evi than Wnt11 did (**Figure 3.9D**). Replacement of the glycosylation site, i.e. asparagine 40, therefore has an impact on the interaction of Wnt11 with Evi. By weakening its interaction with Evi, glycosylation of asparagine 40 may favor Wnt11 to explore other secretion routes rather than the one regulated by Evi.

Moreover, it was observed that Wnt11 T42P was co-immunoprecipitated in similar amounts as Wnt11 but less than the mutant variant Wnt11 N40Q (**Figure 3.9E**). The fact that the mutant variant Wnt11 T42P does not increase the interaction with Evi as Wnt11 N40Q did, but on the contrary at a similar amount as the wild type protein is still puzzling and requires further analysis.

Using click labeling assays with cC16:1n-7, I tested whether the mutation on the asparagine 40 or the threonine 42 affects lipidation of Wnt11. I observed lipidation of mutants to a comparable extent as for the Wnt11 wild type protein (**Figure 3.9F**). These results suggest that neither asparagine 40 nor threonine 42 affect the lipidation of Wnt11 by the monounsaturated cC16:1n-7 fatty acid.

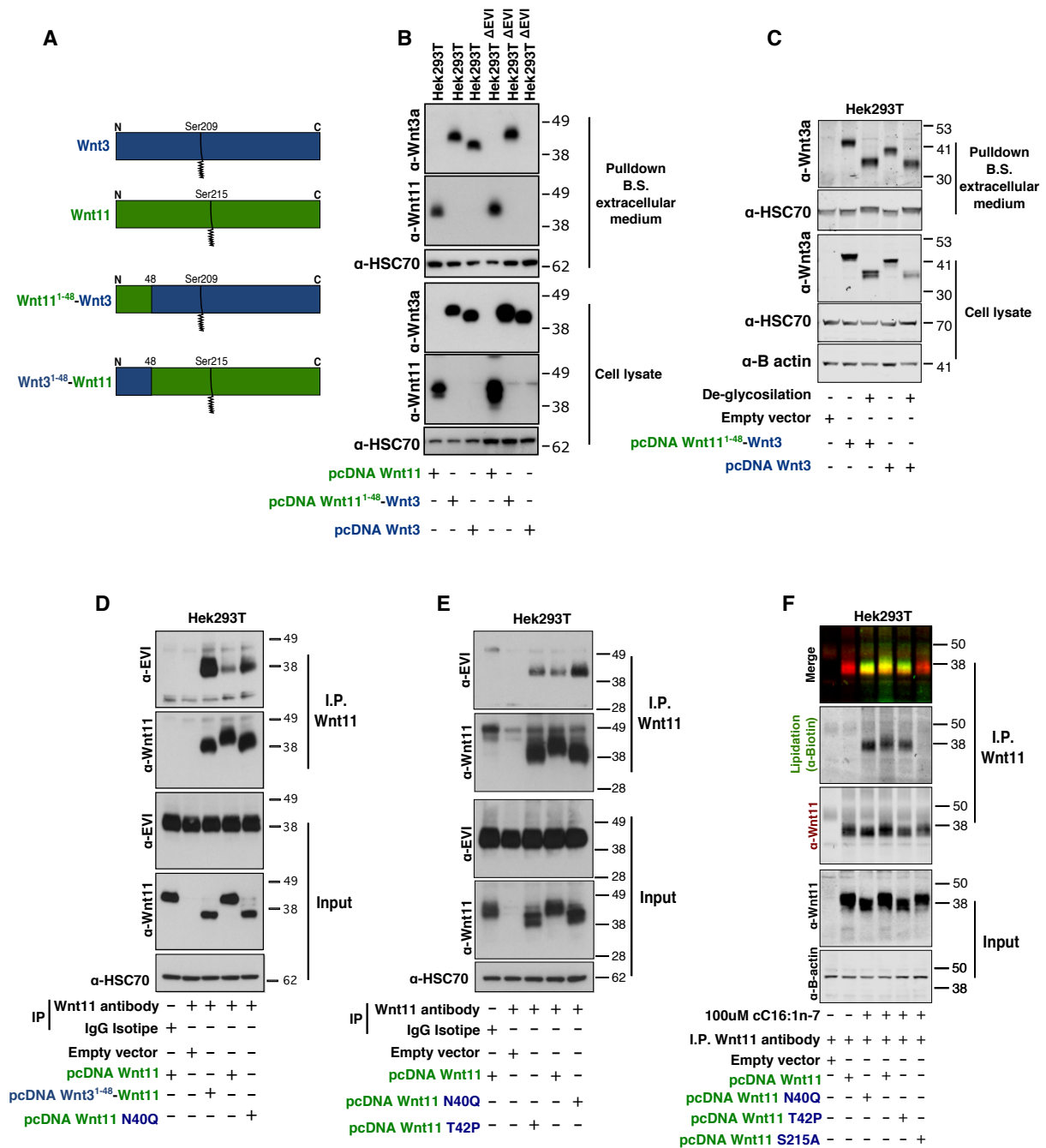


Figure 3.9: Evi-independent Wnt11 secretion is related to N terminus region 1-48.

A. Scheme of Wnt3, Wnt11, and the chimera proteins Wnt11¹⁻⁴⁸-Wnt3 and Wnt3¹⁻⁴⁸-Wnt11. **B-C.** HEK293T cells were seeded in 6-well plates at a seeding density of 3×10^5 cells/well. Twenty-four hours later, HEK293T cells were transfected with constructs that overexpress wild-type Wnt11, wild-type Wnt3 or the Wnt11¹⁻⁴⁸-Wnt3 chimera protein. 48 hours later, extracellular medium and cell lysates were collected. Wnts were precipitated from the extracellular medium with the help of blue sepharose beads (B.S.). Samples from blue sepharose pull down and cell lysate were analyzed directly by SDS-PAGE and western blot (as in **B**, see **section 2.16**) or subjected first to deglycosylation assay and then to SDS-PAGE and western blot (as in **C**, see **section 2.15**). The blots were analyzed by a chemiluminescent system using ECL substrates and a COMPACT 2 X-ray film processor. HSC70 served as loading control for lysate and extracellular medium, and B actin served as loading control for lysate. Western blots are shown as representatives of 3 independent experiments. **B.** The N terminus region 1-48 of Wnt11 allows the secretion of Wnt3 independently of Evi. Here the chimera protein Wnt11¹⁻⁴⁸-Wnt3 is secreted in the extracellular media in Evi knockout cells. **C.** N terminus region 1-48 of Wnt11 confers a different glycosylation pattern to the chimera Wnt11¹⁻⁴⁸-Wnt3. Here the chimera Wnt11¹⁻⁴⁸-Wnt3 shifts its migration pattern compared to Wnt3 in Western blot (see lanes two and four). Deglycosylation assay equals the migration pattern between

Wnt11¹⁻⁴⁸-Wnt3 and Wnt3 (see lanes three and five). **D-E.** Interaction of Evi with either Wnt11 wild type, the chimera Wnt3¹⁻⁴⁸-Wnt11, or the mutants Wnt11 N40Q or Wnt11 T42P was detected by co-immunoprecipitation. HEK293T cells were seeded in 10 cm plates at a density of 1×10^6 cells/plate. 24 h later, cells were transfected with constructs for overexpression of either Wnt11 wild type, the chimera Wnt3¹⁻⁴⁸-Wnt11, or the mutants Wnt11 N40Q or Wnt11 T42P. Immunoprecipitations were performed by pull down of Wnt11 as described in **section 2.12**. The samples were run by western blot, and the membranes were probed for the presence of Evi and Wnt11 using the respective antibodies **from table 2.2**. The blots were analyzed by a chemiluminescent system using ECL substrates and a COMPACT 2 X-ray film processor. HSC70 served as loading control. **D.** N-terminus 1-48 region of Wnt3 or mutation in asparagine 40 confer enhanced interaction with Evi to the Wnt11¹⁻⁴⁸-Wnt3 chimera and the Wnt11 N40Q mutant rather than to Wnt11 wild-type. **E.** Mutation in asparagine 40 but not in threonine 42 confers enhanced interaction of Wnt11 with Evi. **F.** Lipid modification is not affected in the mutant variants Wnt11 N40Q or Wnt11 T42P. The mutant Wnt11 S215A was used as negative control of lipidation. Here, HEK293T cells were seeded in 10 cm plates as indicated in **section 2.14.1**, and treated with 100 μ M of cC16:1n-7 as is described in **section 2.14.1**. Cells were transfected with the indicated overexpression constructs for either Wnt11 wild type or the mutants N40Q, T42P, or S215A. After incubation with the respective treatments, cells were collected for immunoprecipitation and click labeling as outlined in **sections 2.11, 2.12, and 2.14.3**. Samples were eluted from the beads and analyzed by western blot. Antibodies specific for Wnt11 were used for protein detection and its lipid modification was detected using IRDye 800CW streptavidin. The blots were analyzed using Odyssey CLX-1014 LI-COR fluorescence imaging system controlled with ImageStudio Ver 5.0. HSC70 was used as loading control. α : indicates the protein to which the primary antibody is directed. I.P.: Immunoprecipitated protein. Western blot is representative of two independent experiments.

3.9 Evaluation of other candidate acyltransferases possibly involved in Wnt11 secretion

O. Voloshanenko (M. Boutros group, DKFZ, Heidelberg) identified potential acyltransferases that could be involved in the secretion and activity of Wnt11 or even more that may interact directly with this protein (unpublished data). Among them, three acyltransferases, namely, ZDHHC5, ZDHHC6, and CPT1A are promising candidates for further analysis. ZDHHC5 localizes to the plasma membrane, ZDHHC6 to the ER, and CPT1A to the mitochondria. To test their effect on secretion of Wnt11, these proteins were knocked down using in HEK293T cells and the amount of Wnt11 protein secreted in the extracellular medium was monitored by blue sepharose and western blot assays.

At first glance, knockdown of ZDHHC5 in HEK293T cells led to decreased secretion of Wnt11 into the extracellular medium for three of the four siRNAs used (i.e. siRNA#1, siRNA#2 and siRNA#3, but not for siRNA#4, **Figure 3.10A**). However, when a semi-quantitative analysis of the bands was performed by normalizing first the intensity of the bands with respect to their loading control and then calculating the fold change of each treatment with respect to the internal control (Ctrl), only the siRNA#3 showed a reproducible inhibitory effect on Wnt11 secretion (**Figure 3.10B**). Furthermore, the siRNA#4 enhanced the amount of Wnt11 in the extracellular medium and in the cell lysate (**Figure 3.10B**). A similar effect was observed in HEK293T ^{Δ PORCN} cells (**Figure 3.10A**), in this case the blots give the perception that there is a decrease in the amount of Wnt11 in the extracellular medium for cells treated with siRNA#1, siRNA#2, and siRNA#3 but not for siRNA#4. However, with the semi-quantitative analysis was observed that only siRNA#3 showed a reproducible inhibitory effect on Wnt11 secretion, and the siRNA#4 enhanced the amount of Wnt11 in the extracellular medium and in the cell lysate (**Figure 3.10B**). In addition to the above, when comparing the HEK293T and HEK293T ^{Δ PORCN} cells, it gave the appearance that the amount of Wnt11 secreted was lower in HEK293T ^{Δ PORCN} cells than in HEK293T cells (**Figure 3.10A**). To verify the knockdown efficiency of ZDHHC5 using these siRNAs, the amount of mRNA of ZDHHC5 present in the cells was measured by RT-qPCR.

siRNA#1, siRNA#3, and to a lesser extent siRNA#4, but not siRNA#2, displayed a reduction in the mRNA of ZDHHC5 (**Figure 3.10C**). Together these results suggest that ZDHHC5 could be involved in the secretion of Wnt11. However, due to the high variation in the results, and the opposite effect between siRNAs #3 and #4 further experiments are needed to confirm and understand how ZDHHC5 impacts Wnt secretion. Furthermore, because ZDHHC5 was described to mainly localizes to the plasma membrane [130], it may not directly be involved in Wnt11 transport through the early secretory pathway. Instead, it could be involved in the sorting of Wnt11 into a specific secretion route at the plasma membrane; for example, via incorporation of Wnt11 into exosomes.

When ZDHHC6 was knocked down in HEK293T cells with three different siRNAs, a slight reduction of Wnt11 secretion into the medium was observed (**Figure 3.10D**). With the semi-quantitative analysis was also observed a trend towards inhibition (**Figure 3.10E**), however, in all cases the standard error was quite high. In HEK293T^{ΔPORCN} cells, there was no apparent reduction with any of the three siRNAs and a high variability was observed between the experimental replicates (**Figure 3.10D,E**). Using RT-qPCR, a reduction in the mRNA levels of ZDHHC6 with all three siRNAs was confirmed (**Figure 3.10F**). Together these data suggest that ZDHHC6 may play a role in Wnt11 secretion. However, due to the high variation in the results further experiments are needed to confirm and understand how ZDHHC6 impacts Wnt secretion

When CPT1A was knocked down using four different siRNAs, I could not observe a reduction in Wnt11 in the extracellular media of HEK293T cells (**Figure 3.10G,H**). In HEK293T^{ΔPORCN} cells, I observed a slight reduction of secreted Wnt11 with siRNAs#1, #2 and #4 (**Figure 3.10G**). However, with the semi-quantitative analysis none of the siRNAs showed a clear signal of reduction and between the replicates there was a high variation. CPT1A mRNA knockdown was observed with all four siRNAs (**Figure 3.10I**). These results suggest that CPT1A is not involved in Wnt11 secretion.

Taking together, these results suggest that ZDHHC5 and ZDHHC6 are candidates to further explore its function in Wnt secretion and signaling. However, further analysis with other approaches such as using sgRNA, inhibitors and rescue experiments with overexpressed ZDHHC5 and ZDHHC6 would be required to validate the initial results.

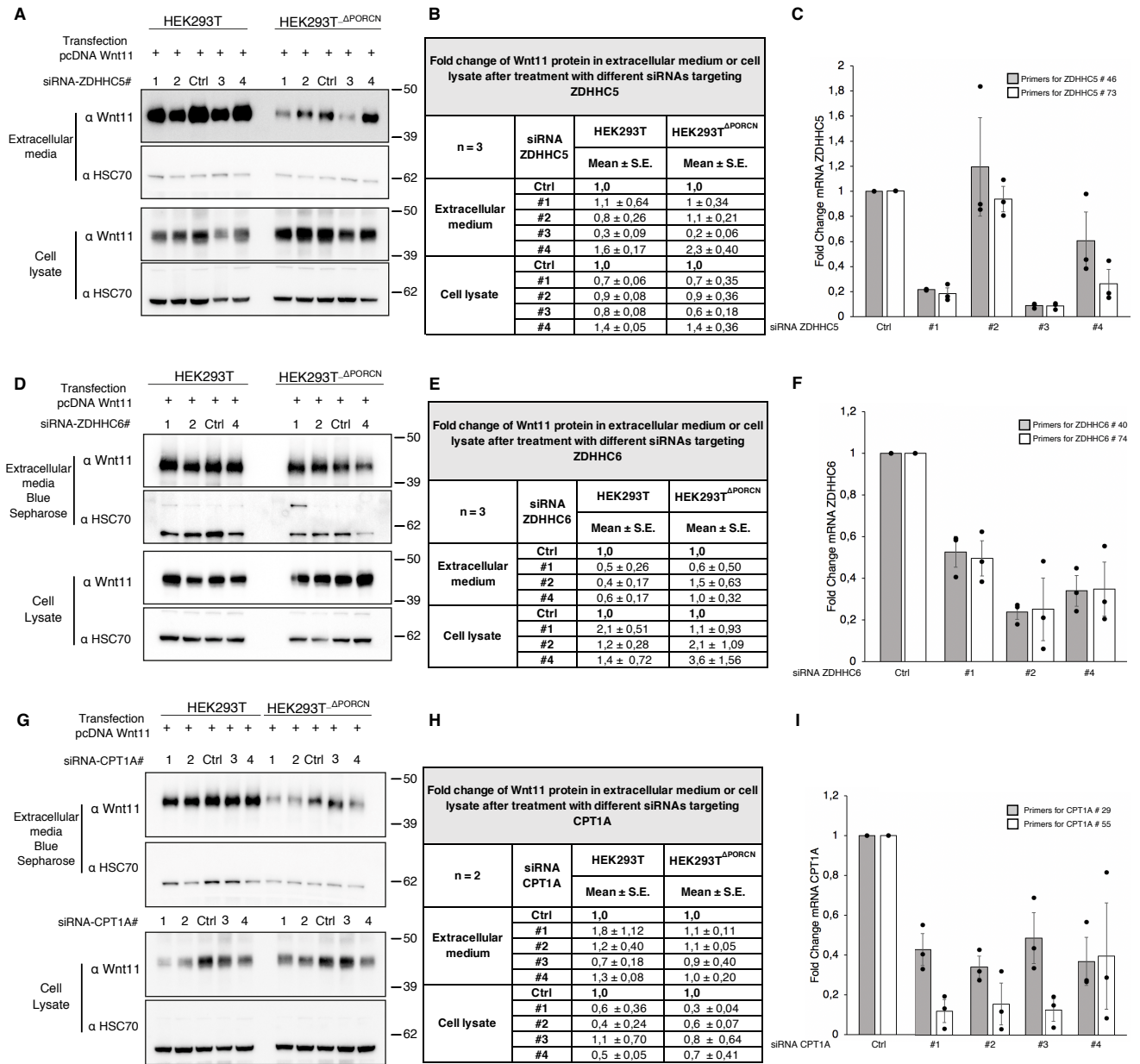


Figure 3.10: Knockdown effect of ZDHC5, ZDHC6, and CPT1A on Wnt11 secretion.

HEK293T cells were seeded in 6 well plates (5×10^5 cells/well) and transfected in parallel with siRNAs (siRNA reverse transfection) to silence the ZDHC5, ZDHC6, and CPT1A genes. For this purpose, Dharmacon siGENOME Human siRNAs were used (Table 2.11), and transfection with the siRNAs was performed as described in section 2.8. The next day the cells were transfected with a construct to overexpress Wnt11 (see section 2.7). 48 hours later, the extracellular media and lysates of cells were collected. Wnt11 was precipitated from extracellular medium with the help of blue sepharose beads. Samples from blue sepharose pull down and cell lysate were run by SDS-PAGE and western blot. The blots were analyzed by a chemiluminescent system using ECL substrates and a COMPACT 2 X-ray film processor. **A, D, G.** Representative images of western blots showing Wnt11 protein levels in cell lysates and blue sepharose pull downs of extracellular media from siRNA-treated cells targeting ZDHC5 (n = 3), ZDHC6 (n = 3), and CPT1A (n = 2). HSC70 served as loading control for lysate and extracellular medium. **α:** indicates the protein to which the primary antibody is directed. **B, E, H.** Semi-quantitative analysis of the bands was performed by normalizing first the intensity of the bands with respect to their loading control (HSC70) and then calculating the fold change of each treatment with respect to the internal control (Ctrl). The intensity of the bands was measured using Fiji software. **C, F, I.** Validation of knockdown through RT-qPCR analysis of the acyltransferases ZDHC5, ZDHC6, and CPT1A transcripts. Validation by RT-qPCR was performed as described in section 2.9.

3.10 Summary of part B: Molecular factors that contribute to Wnt11 secretion and function

In this part, biochemical and functional assays were used to investigate molecular factors that might affect the secretion and function of Wnt11 and Wnt3a. I could show that the amino acid serine 209 in Wnt3a is essential for its secretion to the extracellular media and for activating the canonical Wnt/ β -catenin pathway; this was consistent with previously published works [32, 43, 44, 55]. I also observed that the amino acid serine 215 in Wnt11 is essential for inhibiting the canonical Wnt/ β -catenin pathway. Nevertheless, the mutation in serine 215 only partially affects the secretion of Wnt11, suggesting that this amino acid is relevant but not indispensable for its secretion. We also investigated whether other domains of Wnt11 could be determinants for its secretion. Contributing to the project of O. Voloshanenko (M. Boutros group, DKFZ, Heidelberg), experiments with chimeric Wnt11 and Wnt3 variants were carried out. In those experiments, we found that the first 48 amino acids in the N-terminal region of Wnt11 and specifically the asparagine 40 control the secretion of Wnt11, possibly through its glycosylation and the interaction with Evi.

Besides that, I also investigated the effect of knocking down ZDHHC5, ZDHHC6, and CPT1A on Wnt11 secretion following a knockdown approach. I observed that the knockdown of ZDHHC5 and ZDHHC6 affects the secretion of Wnt11, suggesting that ZDHHC5 and ZDHHC6 may be involved in the secretion of Wnt11.

C. Lipidomic analysis of HEK293T and HCT116 cells

Besides studying acylation and trafficking of Wnt11, I was interested in investigating the correlation between Wnt signaling and lipidome changes. A growing number of reports has shown that Wnt signaling also impacts lipid homeostasis, with aberrations leading for example to steatosis or lipid droplet accumulation in cellular assays [99-101, 131].

To test for a functional link between Wnt signaling and cellular lipid homeostasis I addressed the following questions:

Does overexpression of Wnts in HEK293T cells affect the cellular lipidome?

Does the presence or activity of PORCN or Evi, proteins acting early in Wnt trafficking, impact the cellular lipid composition of cells?

To address these questions, I made use of the cellular systems already investigated in this thesis, including overexpression of Wnt proteins, PORCN or Evi knockout cells, as well as inhibition of PORCN activity using a small molecule inhibitor. Besides the well-established HEK293T cells I included colon cancer derived HCT116 cells as a second model system. Lipidomics analyses were performed together with Iris Leibrecht, Timo Sachsenheimer and Christian Luchtenborg from the CellNetworks Lipidomics Platform Heidelberg.

3.11 Lipid profile in HEK293T cells overexpressing Wnts

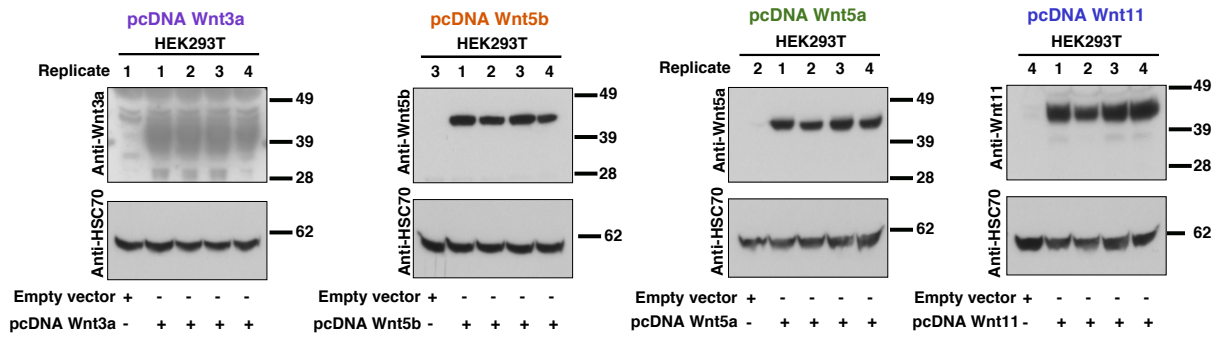
To evaluate if the overexpression of Wnts affects the lipid composition of HEK293T cells, HEK293T cells transfected with plasmids that overexpressed Wnt3a, Wnt5a, Wnt5b or Wnt11 were used. Lipidomics analysis for each one of the conditions was performed. 22 different lipid classes were evaluated, mainly belonging to glycerophospholipids, glycerolipids, sphingolipids, and cholesterol (**Figure 1.5**).

In general, I did not observe statistically significant difference in the lipid classes under Wnt overexpression compared to control cells (**Figure 3.11**). Nevertheless, I observed slight differences in the lipid composition between cells that overexpress either the canonical or the non-canonical Wnt proteins, however, due to a high variability these changes were not statistically significant. Overexpression of Wnt3a induced a slight increase in the amount of PC and PC O- and a decrease in PE, PI, PS, PS O-, PG O-, CE, and Hex2Cer (**Figure 3.11B**). These slight changes were not observed for the non-canonical Wnts (**Figure 3.11B**). In contrast, overexpression of non-canonical Wnts (Wnt5a, Wnt5b, and Wnt11) slightly increased the amount of PA, PG, PE P-, and the ether lipids PI O-, PA O- and PS O- (**Figure 3.11B**). I also observed that some lipid classes were affected independently of which type of Wnts were overexpressed. For example, SM slightly increased in canonical (Wnt3a) and non-canonical Wnts (Wnt11 and Wnt5a but not Wnt5b) (**Figure 3.11B**). The TAG lipid class decreased in all overexpressed Wnts (**Figure 3.11B**). Alternatively, the LPC lipid class increased only in cells overexpressing Wnt5a and Wnt5b, and the amount of PE O- increased only under overexpression of Wnt11 (**Figure 3.11B**). Taken together, none of these alterations was of statistical significance, both when comparing different Wnt proteins and in comparison to control cells in the absence of Wnt overexpression. Here a significant increase of sample replicates would be important to clarify whether overexpression of Wnt proteins in HEK293T cells impacts the cellular lipidome.

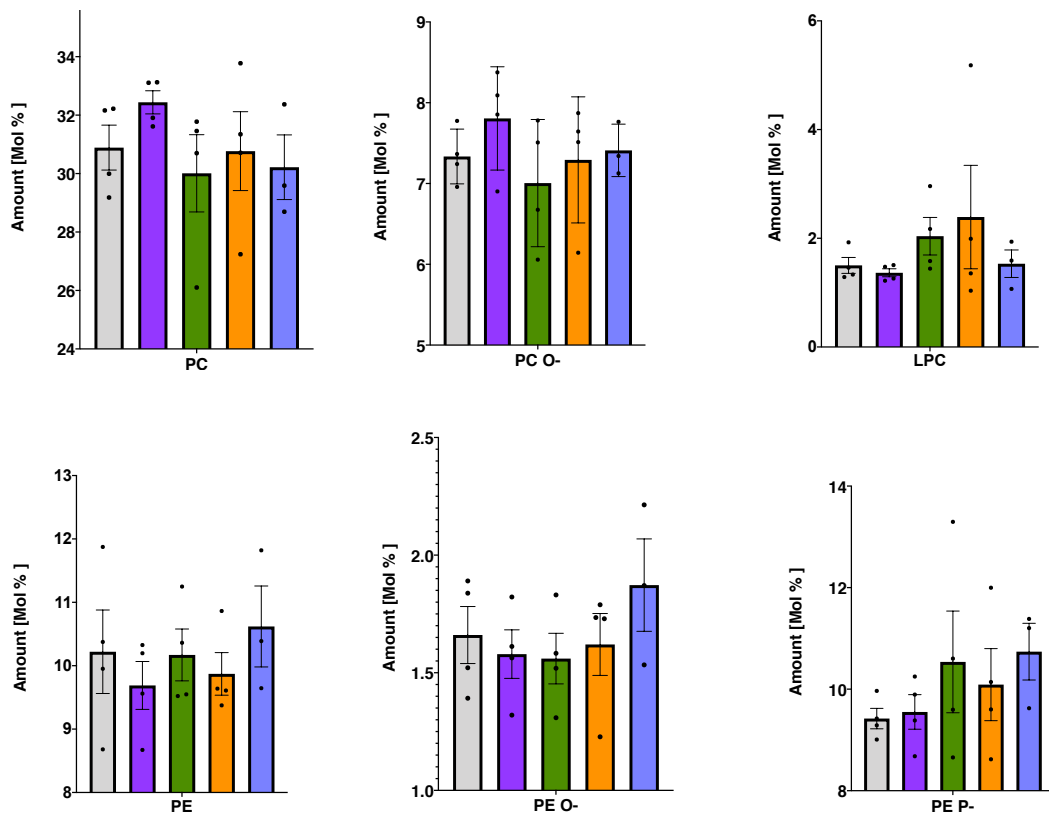
HEK293T + pcDNA
HEK293T + pcDNA Wnt3a

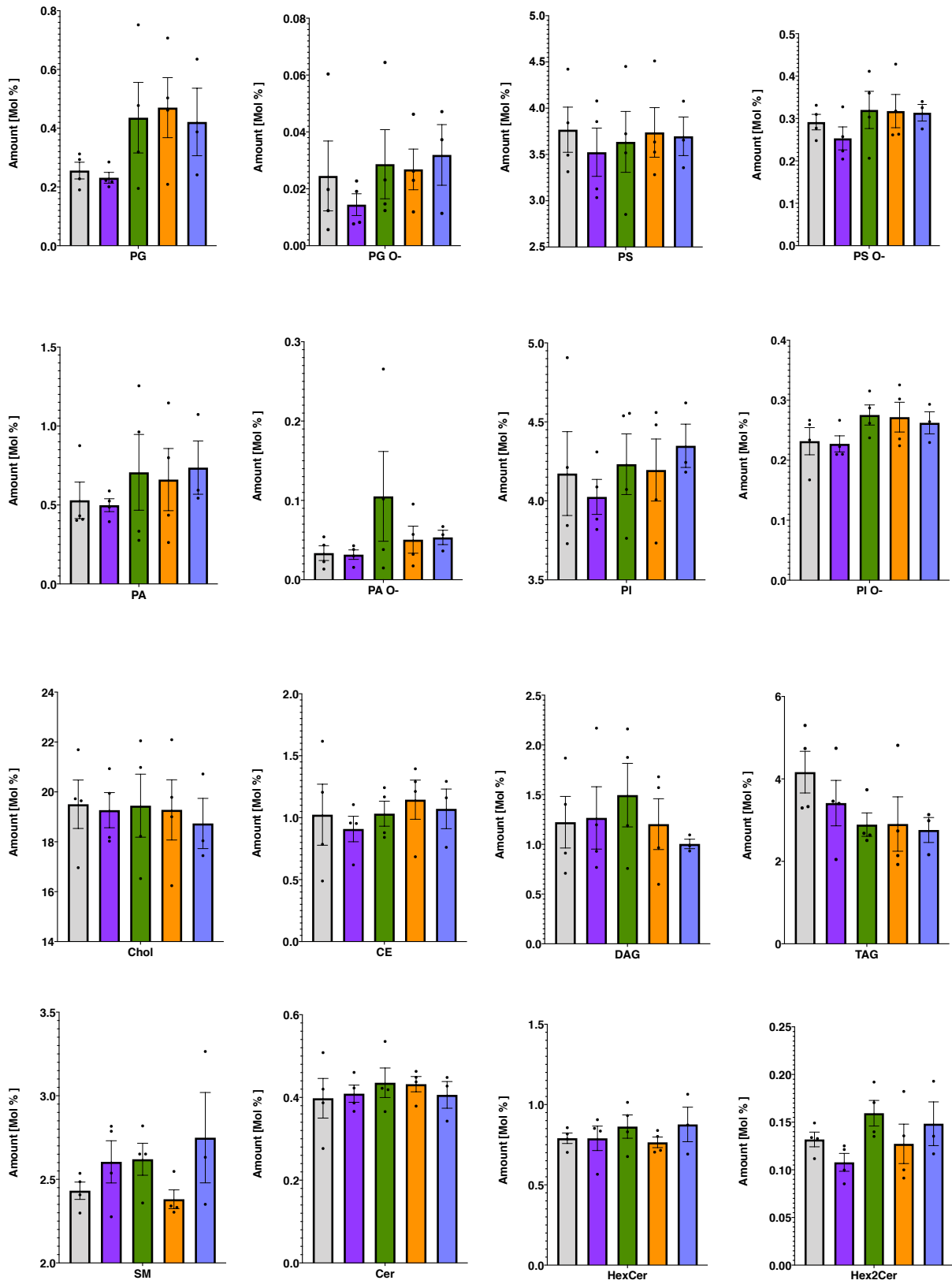
HEK293T + pcDNA Wnt5a
HEK293T + pcDNA Wnt5b
HEK293T + pcDNA Wnt11

A



B





3.12 Lipid profile of HEK293T cells after inhibition of PORCN, knockout of PORCN and knockout of Evi

To test whether inhibition or depletion of PORCN and Evi affects the lipid composition of HEK293T cells, HEK293T cells were treated with LGK974 at 5 μ M and 20 μ M for 48 h (to inhibit PORCN, see **section 2.2**), and the lipid composition of HEK293T ^{Δ Evi} and HEK293T ^{Δ PORCN} cells was measured. Statistically significant reduction in the levels of some lipid classes was observed after treated with LGK974; this is the case of HexCer, Chol, and the ether lipids PI O- (**Figure 3.12**). In contrast, a statistically significant increase in PC, PE and SM was observed after treating cells with LGK974, and also for SM in HEK293T ^{Δ PORCN} cells (**Figure 3.12**). A slightly decreasing trend was observed for the Hex2Cer, TAG, PC O-, PE O-, PG O-, PS O-, PA O- and CE lipid classes (**Figure 3.12**). As for HEK293T ^{Δ Evi} cells, a slight but not statistically significant trend of an increase in PE, PG, PS, PI, HexCer, Hex2Cer, PG O- and PS O- lipid classes were observed, whereas there was a decrease in PC O-, PI O-, Cer and TAG levels. (**Figure 3.12**). This result suggests that the absence of Evi does not affect the lipid composition of HEK293T cells.

A

HEK293T
 HEK293T^{ΔEvi}
 HEK293T^{ΔPORCN}
 HEK293T + 5 μ M LGK974
 HEK293T + 20 μ M LGK974

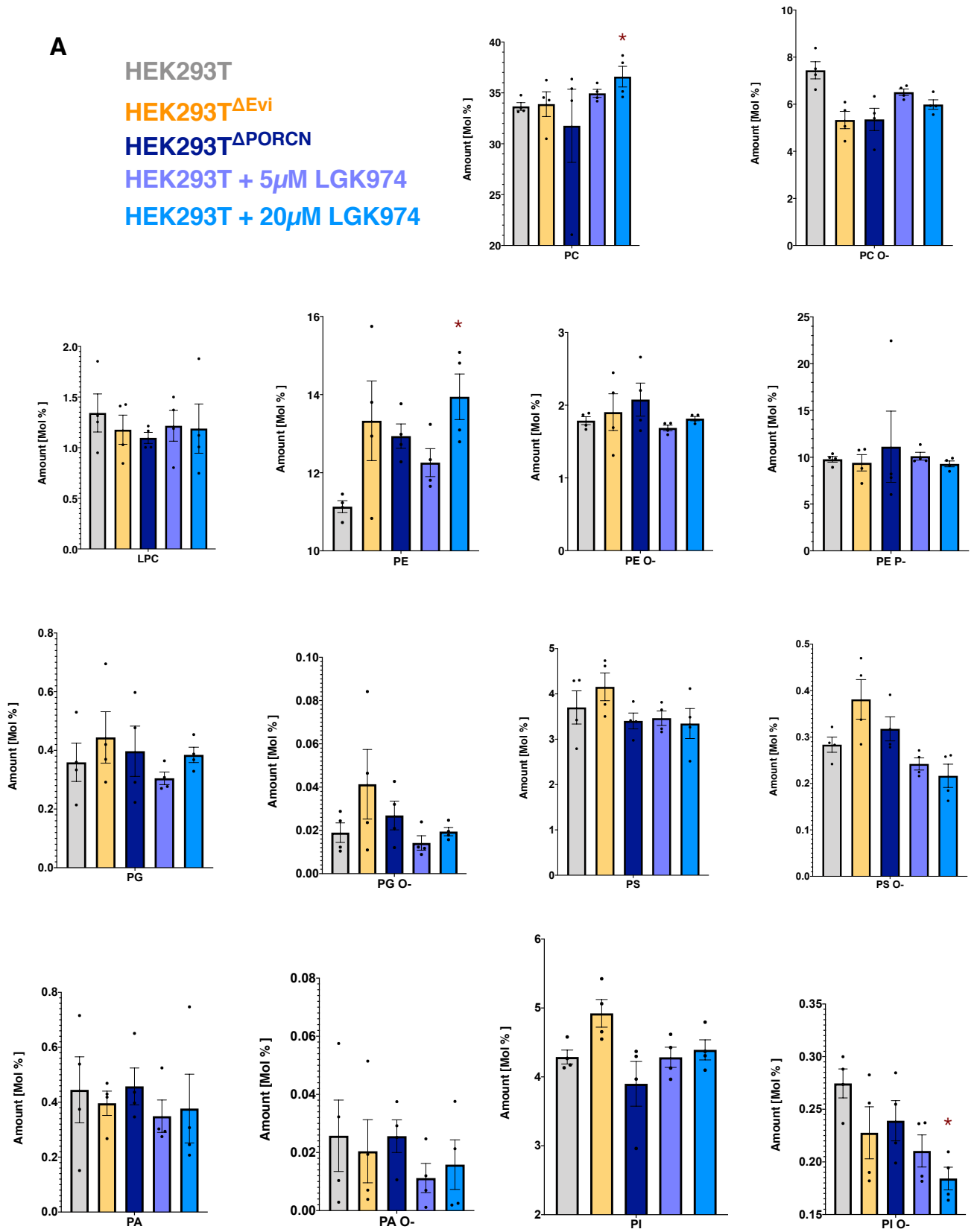


Figure 3.12: Lipid profile of HEK293T cells after inhibition or depletion of PORCN and Evi.

1×10^6 cells were collected from cell cultures of the stable cell lines HEK293T, HEK293T^{ΔPORCN}, HEK293T^{ΔEvi}; or HEK293T cells treated either with LGK974 as described in **section 2.2**. Cells were pelleted by centrifugation. Then the pellet was resuspended in ammonium bicarbonate ((NH₄)HCO₃, 155 mM) methanol 1:1 (v/v) and the samples were subjected to acidic Bligh and Dyer lipid extraction (SBD-extraction) as is described in **[115, 116]** and **section 2.19**. Mass spectrometric measurements were performed in positive ion mode on an AB SCIEX QTRAP 6500+ mass spectrometer equipped with chip-based (HD-D ESI Chip, Advion Biosciences) nano-electrospray infusion and ionization (TriVersa NanoMate, Advion Biosciences) as described in **[115, 116]**. Data evaluation was done using LipidView (Sciex) and ShinyLipids. **A.** Amount in Mol% of each one of the lipid classes from HEK293T cells after inhibition of PORCN by 5μM LGK974 (purple), 20μM LGK974 (light blue), knockout of PORCN (dark blue) and knockout of Evi (yellow). Four independent experimental replicates were carried out. Data are presented as mean ± SE. Statistical significance of the changes indicated (*: p-value < 0.05). Statistics with 2-way ANOVA and Dunnett multiple comparison test were used. The untreated cells were considered as reference for the statistical test. Lipid extraction was done by Iris Leibrecht, Christian Luchtenborg and Timo Sachsenheimer. Lipidome data was analyzed and provided by Christian Luchtenborg and Timo Sachsenheimer (Brügger lab). **B.** Scheme of the biosynthesis pathways of glycerolipids, ether-linked glycerolipids, and sphingolipids. It illustrated the increase (red arrow) or decreases (blue arrow) in the lipid classes when HEK293T cells were depleted of Porcupine by inhibition with LGK974 or by knockout (upper panel), and when Evi was depleted by knockout (lower panel). Please note that the changes illustrated may not reflect only statistically significant changes, but also some lipid classes with a slight trend of change.

To test whether the slight but not significant effect of PORCN on ether PC observed in the first set of lipidome studies could be confirmed, I repeated these analyses now including different sgRNAs targeting PORCN. Nonetheless, to obtain the results quickly, I proceeded to evaluate the PC and PC O- lipid composition of the pool of cells treated with three different sgRNAs without going through the single cell cloning selection. Using LGK974 inhibitor, the PC O- levels diminished compared to the control (**Figure 3.13**). Also, in HEK293T^{ΔPORCN} cells, there was a significant reduction in the PC O- levels (**Figure 3.13**). However, there were no changes for the pools of cells treated with the different sgRNAs compared to the control (**Figure 3.13**). This variation between the results with inhibitor and sgRNAs suggests that the changes in the lipid composition of ether lipids could be indirectly affected by the inhibitor LGK974, and in the case of HEK293T^{ΔPORCN} stable cell line could be a clonal effect instead of a specific effect due to PORCN, which should be verified in further experiments.

Hek293T
 Hek293T + DMSO
 Hek293T^{ΔEvi}
 Hek293T^{ΔPORCN}
 Hek293T + 5μM LGK974
 Hek293T + 20μM LGK974
 Hek293T sgPORCN_192
 Hek293T sgPORCN_11
 Hek293T sgPORCN_35

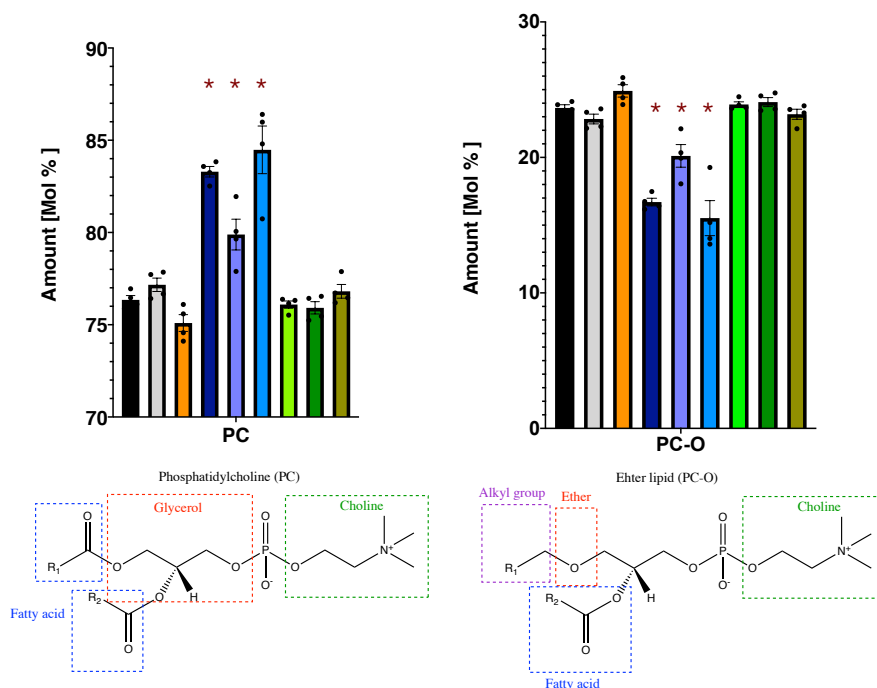


Figure 3.13: Amount of PC and PC-O lipids under different knockout conditions and LGK974 treatments

1×10^6 cells were collected from cell cultures of the stable cell lines HEK293T, HEK293T^{ΔPORCN}, HEK293T^{ΔEvi}, and HEK293T cells treated either with LGK974 as described in **section 2.2** or with sgRNAs to induce depletion of Porcupine as described in **section 2.10**. Cells were pelleted by centrifugation. Then the pellet was resuspended in ammonium bicarbonate ((NH₄)HCO₃, 155 mM) methanol 1:1 (v/v) and the samples were subjected to acidic Bligh and Dyer lipid extraction (SBD-extraction) as is described in **[115, 116]** and **section 2.19**. Mass spectrometric measurements were performed in positive ion mode on an AB SCIEX QTRAP 6500+ mass spectrometer equipped with chip-based (HD-D ESI Chip, Advion Biosciences) nano-electrospray infusion and ionization (TriVersa NanoMate, Advion Biosciences) as described in **[115, 116]**. Data evaluation was done using LipidView (Sciex) and ShinyLipids. HEK293T cells either lacking PORCN (Δ PORCN, dark blue) or under LGK974 treatment (purple and light blue) increase PC content (**left**) and reduce PC O- content (**right**). HEK293T cells treated with different sgRNAs targeting PORCN did not change the levels of PC or PC O- (green colors). Four independent experimental replicates were carried out. Data are presented as mean \pm SE. Statistical significance of the changes indicated (*: p-value < 0.05). Statistics with 2-way ANOVA and Dunnet multiple comparison test were used. The untreated cells were considered as reference for the statistical test. Lipid extraction was done by Iris Leibrecht, Christian Luchtenborg and Timo Sachsenheimer. Lipidome data was analyzed and provided by Christian Luchtenborg and Timo Sachsenheimer (Brügger lab).

Interestingly, ether PC (PC O-) and SM have recently been shown to be important for p24-dependent cargo transport in the early secretory pathway **[73, 102, 103]**, which is used by Wnt proteins**[73, 74]**. These results suggest a functional link between PORCN activity, Wnt transport and cellular lipids which should be explored in further experiments.

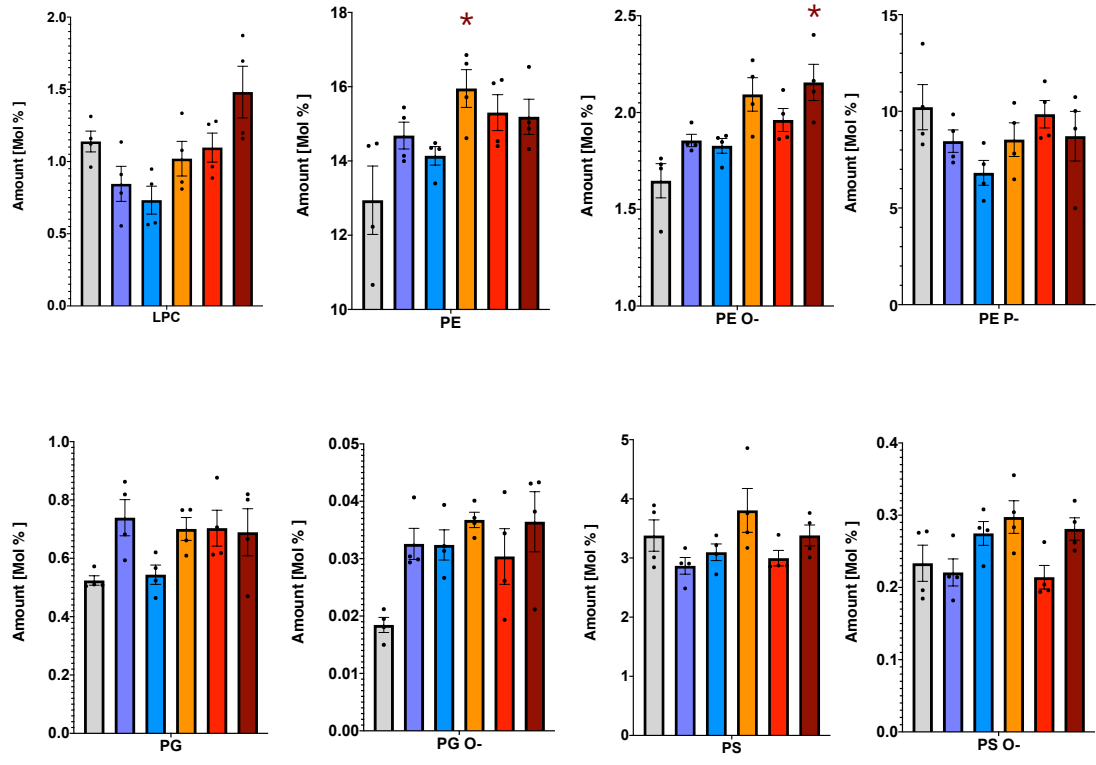
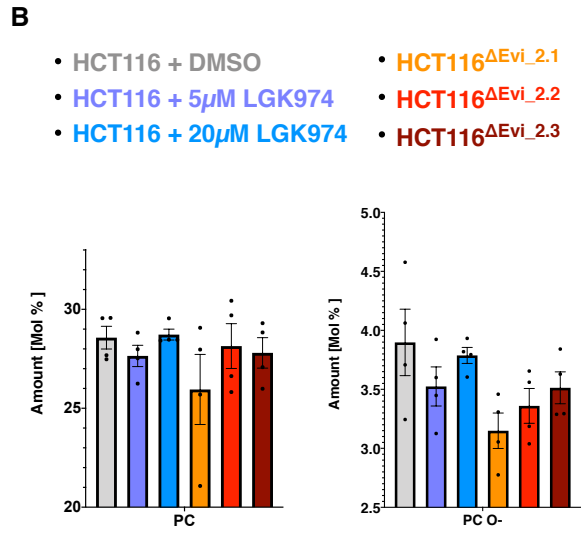
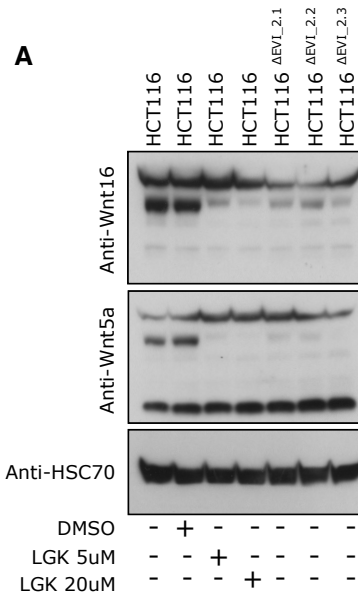
3.13 Lipid profile of HCT116 cells after LGK974 inhibition of PORCN and knockout of Evi

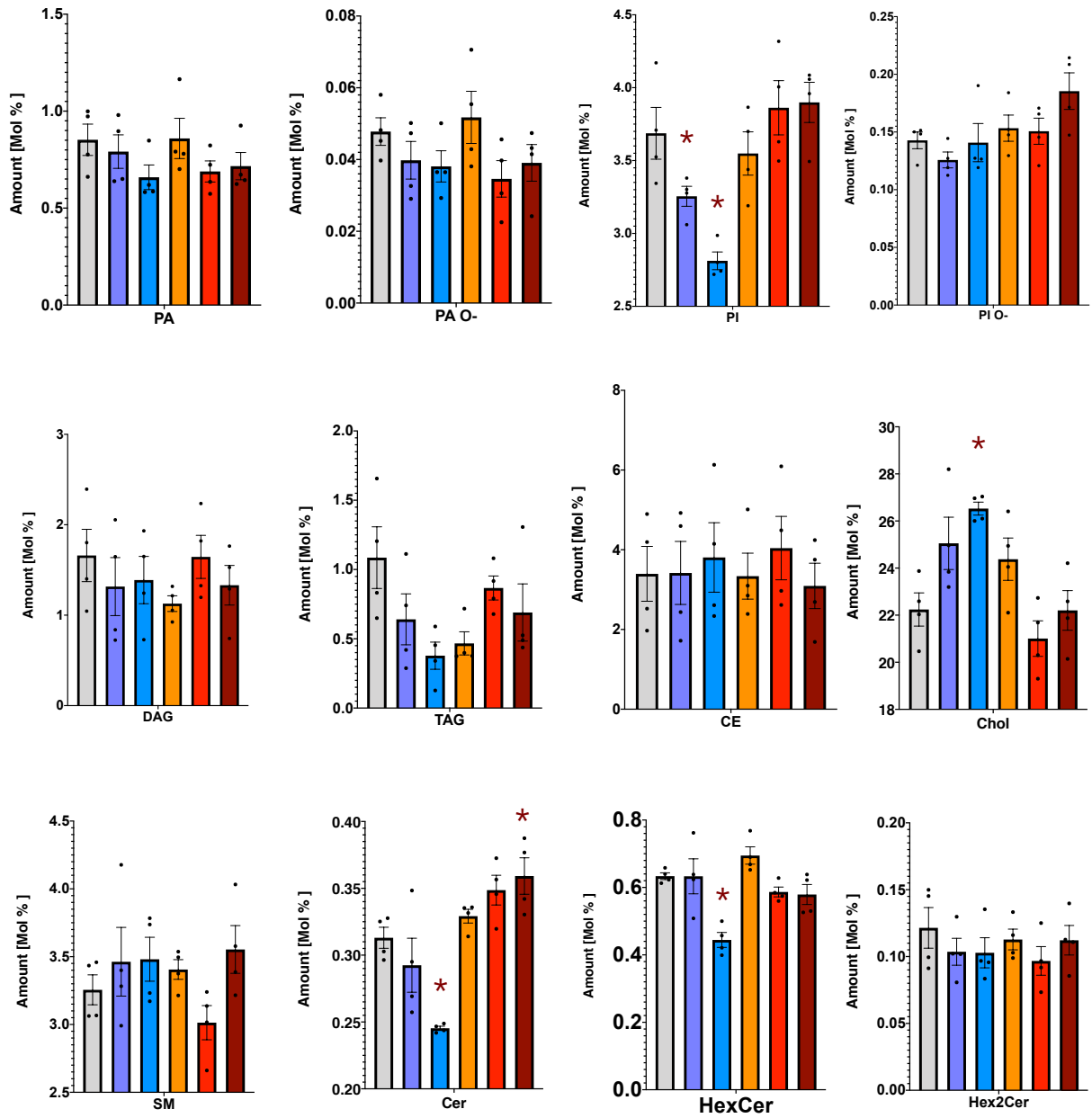
In addition to HEK293T cells, I tested whether inhibition of PORCN activity or absence of Evi had an impact on the cell lipidome of HCT116 cancer cells, which endogenously express Wnts. For this purpose, lipidomic analysis was performed from HCT116 cells treated with 5 μ M and 20 μ M LGK974, to inhibit PORCN, or from three monoclonal cell lines lacking Evi (HCT116 Δ Evi_{-2.1}, HCT116 Δ Evi_{-2.2} and HCT116 Δ Evi_{-2.3}, see **Table 2.5** and **section 2.1**, these cells were provided by O. Voloshanenko (M. Boutros group, DKFZ, Heidelberg).

Wnt5a and Wnt16 are two Wnt proteins that are predominantly expressed in HCT116 cells [132, 133] and seems to be dependent on PORCN and Evi (private communication, M. Boutros lab, DKFZ). Therefore, as a control to verify the effect of PORCN inhibition with LGK974 and lack of Evi in HCT116 cells, the secretion of Wnt5a and Wnt16 was assessed. To check this, the proteins were pulled down with blue sepharose beads from extracellular media coming from the same HCT116 cells used in the lipidomic analysis. Then the enriched proteins were analyzed by Western blot (for details on the method, see **section 2.16**). Reduced secretion of both Wnt5a and Wnt16 was observed in LGK974-treated HCT116 cells and in HCT116 cells lacking Evi (**Figure 3.14A**).

In LGK974-treated cells, a statistically significant decrease in Cer, HexCer and PI lipid classes was observed (**Figure 3.14**). In addition, a slight decrease of LPC, PE P-, PA, PA O-, Hex2Cer, TAG was observed, although it was not statistically significant. This decrease in the levels of the different lipid classes appeared to be dose-dependent. A statistically significant increase in Chol was also observed in cells treated with LGK974 (**Figure 3.14**). When I compared these results with those of HEK293T cells, I observed that HexCer, Hex2Cer, TAG, PA O- tend to decrease in both cell types; however, in HCT116 cells, most ether lipids are not reduced, suggesting that the inhibition of PORCN by LGK974 affects the lipid composition of HCT116 cells differently than in HEK293T cells.

In Evi knockouts, a slight decrease in PC O- and TAG lipid levels was observed, although it was not statistically significant. Overall, there were variations among the three different HCT116 Δ Evi clones (Δ Evi_{-2.1}, Δ Evi_{-2.2} and Δ Evi_{-2.3}). For instance, a decrease in the levels of one lipid class was observed in one of the clones but not in the others, as in PC, PC O-, PI, TAG for HCT116 Δ Evi_{-2.1}, or PG O-, PS, PS O-, SM, Chol for HCT116 Δ Evi_{-2.2} (**Figure 3.14**). In other cases, an increase in lipid class was observed in one of the clones but not in the others, such as PA, PA O- and HexCer for HCT116 Δ Evi_{-2.1} or LPC, PI O- for HCT116 Δ Evi_{-2.3} (**Figure 3.14**). This variation indicates an unclear pattern in the lipid profile of Evi-depleted HCT116 cells, and the observable changes are likely due to an individual clonal effect rather than a common effect of Evi knockout. In conclusion, these results suggest that Evi has no apparent effect on the lipid composition of HCT116 cells.





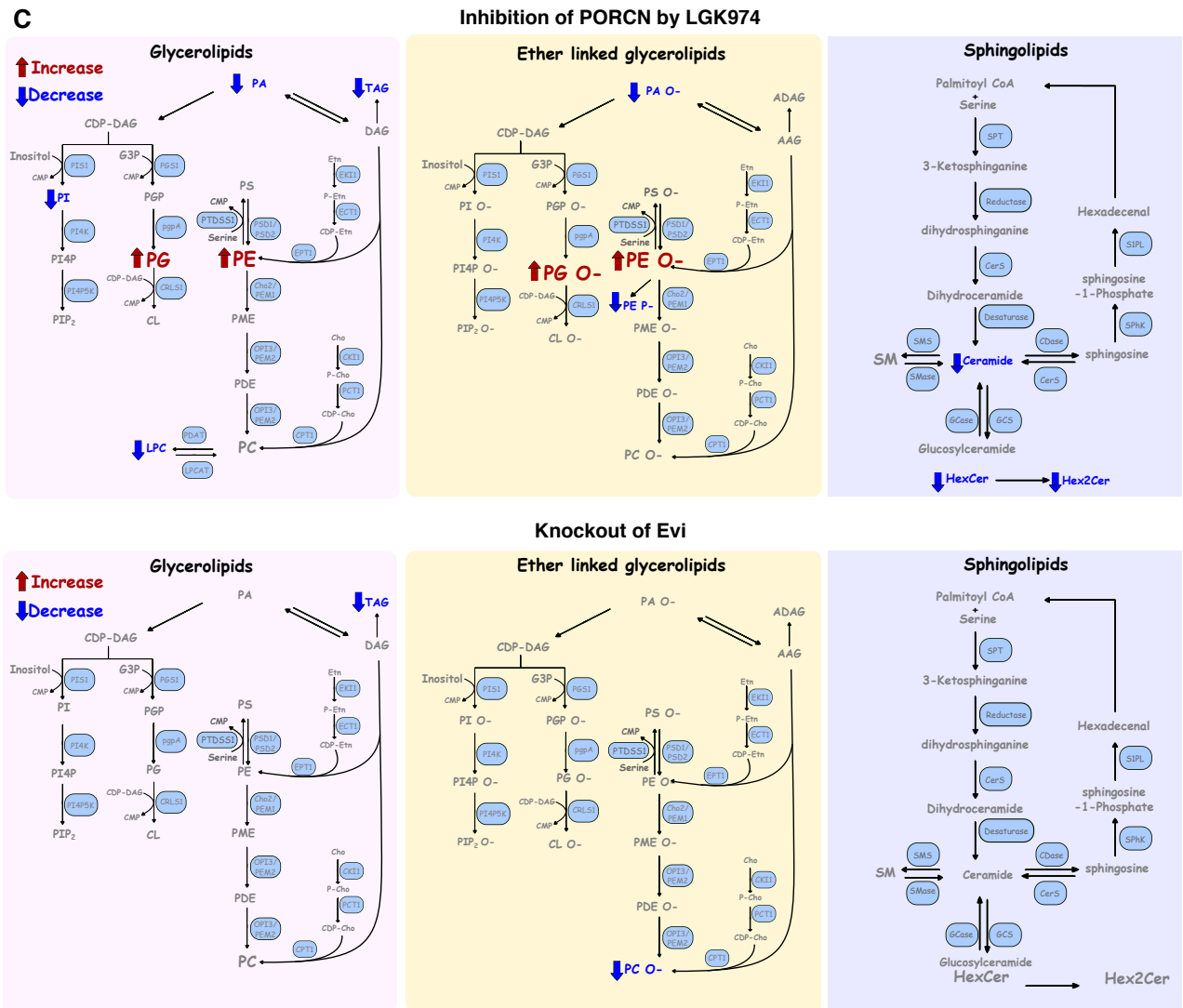


Figure 3.14: Lipid profile of HTC116 cells after inhibition of PORCN by LGK974 and knockout of Evi, recovered by mass spectrometry. Extracellular media and cells were collected from cultures of the stable cell lines HTC116, HTC116^{ΔEvi} cells (clones HCT116^{ΔEvi_2.1}, HCT116^{ΔEvi_2.2}, HCT116^{ΔEvi_2.3}) or HTC116 cells treated with either 5 μM or 20 μM of LGK974 as described in **section 2.2**. The extracellular media was used to pull down secreted Wnt proteins, whereas cells were used for lipidomic analysis. **A** Wnt5a and Wnt16 proteins were pulled down with blue sepharose beads from extracellular media and tested by Western blot as described in **section 2.16**. The amount of Wnt5a and Wnt16 secreted in extracellular media were used as a control to verify the effect of PORCN inhibition with LGK974 and lack of function of Evi in the HTC116^{ΔEvi} cells. **B**. Amount in Mol% of each one of the lipid classes from HTC116^{ΔEvi} cells (clones HCT116^{ΔEvi_2.1}, HCT116^{ΔEvi_2.2}, HCT116^{ΔEvi_2.3}) or HTC116 cells treated with LGK974. Sample processing was performed as follows: 1×10^6 cells from the different conditions were pelleted by centrifugation. Then the pellet was resuspended in ammonium bicarbonate ((NH₄)HCO₃, 155 mM) methanol 1:1 (v/v) and the samples were subjected to acidic Bligh and Dyer lipid extraction (SBD-extraction) as is described in **[115, 116]** and **section 2.19**. Mass spectrometric measurements were performed in positive ion mode on an AB SCIEX QTRAP 6500+ mass spectrometer equipped with chip-based (HD-D ESI Chip, Advion Biosciences) nano-electrospray infusion and ionization (TriVersa NanoMate, Advion Biosciences) as described in **[115, 116]**. Data evaluation was done using LipidView (Sciex) and ShinyLipids. Four independent experimental replicates were carried out. Data are presented as mean ± SE. Statistical significance of the changes indicated (*: p-value < 0.05). Statistics with 2-way ANOVA and Dunnet multiple comparison test was used. Cells treated with DMSO were considered as reference for the statistical test. Lipid extraction was done by Iris Leibrecht, Christian Luchtenborg and Timo Sachsenheimer. Lipidome data was analyzed and provided by Christian Luchtenborg and Timo Sachsenheimer (Brügger lab). **C**. Scheme of the biosynthesis pathways of glycerolipids, ether-linked glycerolipids, and sphingolipids. It illustrated the increase (red arrow) or decreases (blue arrow) in the lipid classes when HCT116

cells were depleted of Porcupine by inhibition with LGK974 (upper panel), and when Evi was depleted by knockout (lower panel). Please note that the changes illustrated may not reflect only the statistically significant changes, but also some lipid classes with a slight trend of change.

3.14 Summary of the part C: Lipidomic analysis in HEK293T and HCT116 cells

In this part, the effect on the lipid composition of HEK293T and HCT116 cells was investigated when components of the Wnt signaling or Wnt secretion were either overexpressed or depleted. Through lipidomics analysis, changes were analyzed in 22 lipid classes. In general, I did not observe a statistically significant difference in lipid composition of membranes under Wnt overexpression compared to control cells. However, I observed small changes in the lipid composition that could be associated with canonical or non-canonical Wnt proteins: For example, overexpression of non-canonical Wnts (Wnt5a, Wnt5b, and Wnt11) slightly increased the amount of PA, PG, PE P-, and the ether lipids PI O-, PA O- and PS O-. However, these changes were not observed for the canonical Wnt3a. Other changes seem to only depend on the overexpression of specific Wnts, no matter if it was a canonical or a non-canonical Wnt. Here a significant increase of sample replicates would be important to clarify whether overexpression of Wnt proteins in HEK293T cells impacts the cellular lipidome.

In HEK293T cells, when Porcupine activity was depleted through inhibition with LGK974 or in a HEK293T Porcupine knockout cell line, a slight increase in PC, PE, and SM and a reduction in the ether lipids was observed. Nevertheless, I did not observe the same effect in treatments with sgRNAs targeting Porcupine. This result suggests that the changes in the amount of ether lipids could be indirectly affected by the inhibitor LGK974, or the Porcupine knockout stable cell line. Further experiments should be done to clarify this aspect. When Porcupine activity was inhibited using LGK974 in HCT116 cells, I did not observe statistically significant changes in ether lipids, only slight changes in PG O- and PE O-. Statistically significant changes in the lipid classes Cer, HexCer, PI and Chol were observed for HCT116 cells treated with LGK974. This suggests that the inhibition of Porcupine by LGK974 affects the lipid composition of HCT116 cells differently than in HEK293T cells.

When the effect of the absence of Evi was investigated regarding lipid composition of HEK293T^{ΔEvi} cells, none statistically significant changes was observed in the lipid composition. This result suggests that the absence of Evi does not affect the lipid composition of HEK293T cells. In HCT116 cells, the lipid composition was evaluated in different clones of Evi knockout cells. Variation was observed in the lipid composition between the clones of Evi knockout cells, which indicates there is unclear pattern in the lipid profile of HCT116 cells in the absence of Evi. These observable changes are probably due to individual clonal effects instead of a common effect of the knockout of Evi. In conclusion, these results suggest that Evi does not have an apparent effect on the lipid composition of HCT116 cells.

4 Discussion

Wnt proteins are essential components of the signaling machinery of cells. All functional aspects of Wnts, including trafficking, secretion, and signaling are tightly regulated by post-translational modifications [31, 36, 72, 134]. In particular, lipidation has emerged as a critical regulatory mechanism to control the signaling ability of Wnts [31, 36, 72, 134]. Currently, the palmitoylation of a serine around amino acids 205-215 by the ER-resident O-acyltransferase Porcupine (PORCN) is the best described mechanism of lipidation of Wnts [36, 43, 134, 135]. Nevertheless, there still exists a debate on the exact location where Wnt proteins are lipidated, and ultimately, the implications of such specific lipidation positions. This thesis addressed this issue. A combination of chemical biology tools and mass spectrometric approaches were employed, both on wild type proteins and variants with defined point mutations, to characterize the bound acyl moieties and new possible sites of lipidation of Wnts. Previous experiments of O. Voloshanenko (unpublished data, M. Boutros group, DKFZ, Heidelberg) indicated that Wnt11 is secreted independently of Evi, PORCN, and the predicted lipidated serine. Even more, Wnt11 was found soluble in a hydrophobic environment when the predicted lipidated serine was mutated to alanine. All these observations suggest a new mechanism by which lipidation regulates Wnt11 function. Wnt11 was thus chosen as a study model to investigate new sites of acylation and the roles of lipidation in Wnt11 secretion. Furthermore, employing secretion, biochemical, and functional assays, it was investigated whether other amino acids, besides the previously-established ones, in Wnt11 or acyltransferases candidates besides PORCN are involved in Wnt11 secretion.

The interplay between Wnt proteins and lipids goes beyond the post-translational regulation of Wnts by lipid moieties. Changes in lipid composition at different biologically-relevant stages have been linked to the action of Wnt proteins [99-101]. The present thesis also analyzed this interplay. The impact of Wnt signaling and Wnt secretion on the lipidome of HEK293T and HCT116 cells was investigated by measuring the lipid composition of cells that overexpressed Wnt proteins and cells depleted of the Wnt partners PORCN and Evi.

4.1 Alternative acylation site and the role of saturation on Wnt11 lipidation

To understand whether lipidation of Wnt11 was mediated by serine 215 or cysteine 80, as it has been pointed out before [42, 43], I used click labeling assays with palmitic acid alkyne cC16:0 in HEK293T cells transfected with plasmids coding for wild type Wnt11 or S215A, C80A, and C80A/S215A mutants (Figure 3.1A). Unexpectedly, lipidation of Wnt11 was detected, not only for the wild-type protein but also for both mutants S215A, C80A, and the double mutant C80A/S215A. In addition to the Wnt11 mutants, the role of Porcupine on the lipidation of Wnt11 was investigated. HEK293T knockout cells lacking Porcupine also displayed a Wnt11 lipid modification (Figure 3.1). These results are in line with previous observations of O. Voloshanenko (unpublished data, M. Boutros group, DKFZ, Heidelberg), suggesting alternative lipidation sites and lipidation by an alternative acyltransferase, besides the one described in the literature [35, 42, 43]. However, the trend I observed displayed only a low reproducibility, despite the relative-large number of replicas (Figure 3.1D-E). I attribute this to the low and most likely unspecific labeling efficiency of the cC16:0 fatty acid. Also, the cellular response to the overexpression of the Wnt mutants or the removal of Porcupine may have yielded lipidation on an alternative site that may have not often been lipid-modified and thus not easily

detectable. Nonetheless, even if this lipidation process is infrequent, the results hint towards another lipidation site besides the residues C80 and S215 and another acyltransferase apart from PORCN involved in the lipidation. Nevertheless, further mass spectrometry experiments on purified Wnt11 protein (either wild type or mutant variants) from either wild type cells or PORCN depleted cells would be necessary to confirm this observation.

To identify alternative lipidation sites, mass spectrometry analysis from recombinant Wnt11 and Wnt3a proteins was carried out. The analysis by mass spectrometry of the intact Wnt11 protein suggested only one acylation per molecule (data not shown). Nevertheless, several lipidation sites were identified. Some of them were selective to the acyl chain of either 16:0 or 16:1n-7, while few others were labeled with both fatty acids. We did not expect these results because there is no report suggesting multiple lipidation sites on Wnt proteins. One possibility is that the commercial purified proteins were not of sufficient quality and therefore may have generated false-positive peaks during the mass spectrometry analysis. To validate the obtained list of lipidation sites, point mutations for some of those residues were performed. It was then investigated if point mutations on Wnts impact lipidation with cC16:1n-7, Wnt secretion, and signaling activity. These experiments confirmed that serine 215 in Wnt11 and serine 209 in Wnt3a play a critical role in the lipidation with cC16:1n-7 and also influence Wnt signaling activity (**see, sections 3.2, 3.6, and 3.7**). These data indicate that some of the potential lipidation sites identified by mass spectrometry could be false positives. As an outlook to clarify which of those potential residues are indeed real lipidation sites, we suggest to overexpress and optimize the purification of Wnt11 and other Wnt proteins from HEK293T, HEK293T^{ΔPORCN}, HEK293T^{ΔEvi} cells.

The detection of lipid modifications drastically improved when using the cC16:1n-7 fatty acid. Lipid labeling efficiency using cC16:1n-7 was higher than that of cC16:0. This improvement allowed to confirm that, among the differently-studied point mutations, serine 215 is the only lipidated site labeled with cC16:1n-7 in Wnt11 (**Figure 3.2-3.3**). Furthermore, the impaired lipidation of Wnt11 due to the absence of Porcupine could be recapitulated (**Figure 3.2**). Therefore, the results using palmitoleic acid alkyne cC16:1n-7, confirm the central role of S215 and the importance of Porcupine for the lipidation of Wnt11, which is consistent with the literature [33, 35, 43, 44, 46, 55, 67]. Importantly, these data highlight the importance of the saturation of the acyl chain on the lipidation of Wnt11.

Regarding the incorporation of the clickable fatty acids cC16:0 and cC16:1n-7 into different lipid classes, it was observed by TLC that both fatty acids were metabolized into lipid classes such as PC, PE, and TAG, but cC16:0 in a higher amount than cC16:1n-7 (**Figure 3.5**). Accordingly, this data suggest that cells may uptake cC16:0 and metabolize it into lipid classes more efficiently than cC16:1n-7. This correlates with the fact that the proportion of saturated lipids is higher than that of monounsaturated lipids in HEK293 cells [131, 136]. As a consequence, the pool of activated fatty acid as a substrate for PORCN is likely to be lower for cC16:0 than for cC16:1. Further studies would be necessary to understand the uptake and incorporation of clickable fatty acids in HEK293 cells and their implications in cellular metabolism.

With the aim of studying in more detail in which lipid species the clickable fatty acids cC16:0 and cC16:1n-7 is metabolized, lipidomic analysis by mass spectrometry was performed (**Figure**

3.6). The data shows that cC16:0 is incorporated into PC species of 16 hydro-carbon chains in higher amounts than the cC16:1n-7 fatty acid did. For longer fatty acids of 18 carbons, on the contrary, both cC16:0 and cC16:1n-7 are incorporated in similar amounts into PC species. I also observed that similar incorporation of cC16:0 and cC16:1n-7 into PE species of 16 carbons and, by elongation, into species of 18 hydro-carbon chains, with either saturated 18:0, unsaturated 18:2, or 18:3 fatty acids. The cells thus accumulated PE lipid species with a fatty acid length of 18 carbons rather than 16 carbons, contrary to what was observed for the PC class. Similar to our results, Greaves and co-workers observed that the C16:0-azide was elongated to C18:0-azide, which was subsequently desaturated to C18:1-azide [136]. Altogether, our results indicate that cC16:0 has a higher efficiency than cC16:1n-7 to be incorporated into PC species of 16 carbons. PE species showed a prevalence of longer hydrocarbon chains of 18 carbons, but their incorporation was independent of the saturation of the cC16 chain (either cC16:0 or cC16:1n-7). The importance of the lipid classes (either PC or PE) and the acyl-chain length (16 or 18) on the lipidation and function of Wnt proteins remains to be elucidated in future studies.

In conclusion, our results highlight that the saturation state of the clickable fatty acids has a strong effect on the lipidation of Wnt11. With the saturated cC16:0, Wnt11 may be lipidated in another site besides serine 215 and PORCN activity seems not to be required. However, this model needs further validation as the low efficiency of lipidation with this lipid resulted in a low reproducibility of the experiments. Contrary to cC16:0, with the monounsaturated cC16:1n-7 fatty acid, the lipidation of Wnt11 drastically improved, and this accordingly enhanced the reproducibility of the experiments. It was then possible to demonstrate that cC16:1n-7 binds at the canonical serine 215 of Wnt11 and that PORCN mediates this lipidation process, consistent with the previously-proposed model of lipidation for Wnts [33, 35, 43, 44, 46, 55, 67]. Finally, these results show that the saturation state of the clickable fatty acids has a strong effect on the incorporation of these fatty acids into the lipid classes PC and PE.

4.2 Molecular factors that contribute to Wnt11 secretion and function

Wnt11 secretion and function in polarized cells have been linked to the acylation of serine 215 [35]. However, recent experiments of O. Voloshanenko (M. Boutros group, DKFZ, Heidelberg) revealed that mutation in serine 215, or depletion of PORCN and Evi proteins by knockout, does not abolish the secretion of Wnt11. We asked whether other uncharacterized amino acids of the Wnt proteins, or other acyltransferases involved in their lipidation, could affect the secretion and other functions of Wnt11 and Wnt3a. To this end, first, the impact site-directed mutagenesis has in the secretion and function of these two proteins was investigated (**section 3.3**). Second, in a contribution to the project of O. Voloshanenko, it was investigated whether inside the amino acid sequence of Wnt11 there is a specific region or amino acid in Wnt11 that affects Evi-independent secretion, the post-translational modification of Wnt11, or the interaction with Evi. Third, we investigated if there are other acyltransferases that could be involved in the secretion of Wnt11, apart from PORCN.

Concerning Wnt signaling function, the results confirm that serine 209 is an essential residue of Wnt3a for the activation of the canonical Wnt/ β -catenin pathway, mediated by this protein (**Figure 3.8**). This is consistent with the studies of Wnt3a from Rios-Esteves et al. [46], Doubravska et al. [32], and Galli et al. [40]. Regarding Wnt11, our results reveal that serine 215, more specifically its lipidation state, is relevant for the inhibitory function that Wnt11 has on the canonical Wnt/ β -catenin pathway (**Figure 3.7**). This is an interesting observation that was

not reported in the literature before and emphasizes the importance of lipidation for the correct function of Wnt11.

Focusing on Wnt secretion, mutation of serine 209 drastically reduced the secretion of Wnt3a (**Figure 3.8**). This is consistent with the most accepted model, which established that this residue is indispensable for the exit of Wnt3a from the ER and its subsequent secretion to extracellular media [17, 32, 43, 57, 72, 84]. For the case of Wnt11, nevertheless, a reduction but not a total suppression of the secretion of Wnt11 was observed when serine 215 was mutated to alanine, in HEK293T cells (**Figure 3.7**). This suggests that a portion of Wnt11 proteins may be secreted independently of serine 215 and possibly independently of the lipidation state on this residue. However, our results differ from the observation by Yamamoto et al. where mutation of serine 215 abolishes Wnt11 secretion in L-cells [35]. This difference could be linked to a distinct mechanism between HEK293T and L cells, and thus intrinsic to each cell type. It remains to be clarified what role the residually-secreted Wnt11 protein, lacking a lipid attached to S215A, plays for HEK293T cells.

We also investigated whether there is a specific region within Wnt11 that affects Evi-independent secretion. It was found that the first 48 amino acids in the N-terminal region of Wnt11 regulate the secretion of Wnt11, reducing its interaction with Evi (**Figure 3.9 A-D**). Furthermore, asparagine 40 was identified as a critical factor that reduces the binding to Evi and facilitates Wnt11 secretion by an alternative route besides the one regulated by Evi (**Figure 3.9 D-E**). Similar to our results, Yamamoto et al. described that Evi is not required for the secretion of Wnt11 to the apical side of polarized MDCK cells, and even more, mutation of asparagine 40 to glutamine impaired the secretion of Wnt11 in L-cells [35]. However, the components and the exact mechanism of how Wnt11 can be secreted independently of Evi remain unknown. Besides that, the mutant variant Wnt11 T42P, which also disrupts glycosylation on asparagine 40, does not increase the interaction with Evi at similar levels as it was observed for Wnt11 N40Q (**Figure 3.9 E**). This indicates that glycosylation may not be involved in the interaction with Evi, and perhaps another post-translational modification of asparagine 40 regulates the binding to Evi. This is still puzzling and requires further analysis. I also tested whether the mutation on asparagine 40 or threonine 42 could affect the lipidation of Wnt11 and observed that neither mutations in asparagine 40 nor threonine 42 affect the lipidation of Wnt11 with cC16:1n-7 (**Figure 3.9F**).

In addition, we analyzed, several acyltransferases that could possibly be involved in Wnt11 secretion. The acyltransferase ZDHHC5 is suggested to also participate in Wnt11 secretion (**Figure 3.10**). Because ZDHHC5 localizes to the plasma membrane, it may not directly be involved in the early secretory pathway. We hence speculate that ZDHHC5 might be engaged in Wnt11 sorting into a specific secretion route at the plasma membrane, for example, by incorporating Wnt11 into exosomes. ZDHHC5 has been associated with multiple cellular processes such as endocytosis, cell adhesion, cardiac function, and pathogen-host interaction [137]. Therefore, ZDHHC5 could indirectly affect Wnt secretion by altering e.g. the retromer complex and subsequently affecting the recycling of Evi from endosomes to the trans-Golgi network [138, 139]. Also, ZDHHC5 may have implications on Wnt signaling by interfering with the localization of LRP6 into detergent-resistant membrane fractions through the palmitoylation of cytoskeleton-associated protein 4 (CKAP4) [140]. ZDHHC5 palmitoylates Protocadherin-7 (PCDH7) during cell division, targeting it to the cell cortex and cleavage furrow

during cytokinesis. Depleting ZDHHC5 or PCDH7 leads to cytokinesis defects, which could affect the partitioning of Notch and Wnt signaling during asymmetric cell division indirectly [141, 142]. These are some examples for roles of ZDHHC5 in the regulation of Wnt signaling or secretion. Further experiments are required to define the exact mechanism that links ZDHHC5 with the secretion of Wnt11.

So far, there is no direct relationship between ZDHHC6 acyltransferase and Wnt11 protein secretion. However, the E3 ubiquitin ligase GP78 (also known as AMFR) is known to be a substrate of ZDHHC6 [143]. GP78 is part of the ER-associated degradation complex (ERAD), which has been implicated in the degradation or stability of components of Wnt secretion such as the carrier protein Evi in the ER [144, 145]. I do not exclude the possibility that GP78 regulates components involved in Wnt11 secretion. However, this is a question for further investigation. In addition to this, it has previously been shown that GP78 is not the main E3 ubiquitin ligase involved in Evi degradation, but rather the E3 ubiquitin ligase CGRRF1 [144, 145]. Interestingly, both GP78 and the ubiquitin ligase CGRRF1 share by homology 6 cysteines within a RING finger motif that are essential for their ubiquitin ligase function. In the case of GP78, these cysteines within this RING finger motif are palmitoylated by ZDHHC6 [143] (sequence alignment in Uniprot). So far, it is not known whether CGRRF1 is lipid-modified, however, given that CGRRF1 shares by homology with GP78 some of those cysteines in its RING finger motif, it is possible that CGRRF1 may also be a substrate of ZDHHC6. Experiments to detect lipidation in CGRRF1 would be necessary to test this hypothesis and to validate whether ZDHHC6 would be implicated in Wnt11 secretion indirectly by regulating CGRRF1 or GP78 activity.

In conclusion, our results highlight that serine 209 is indispensable for activating the canonical Wnt/ β -catenin pathway and secretion of Wnt3a. The equivalent serine in Wnt11, namely, serine 215, and more specifically its lipidation state, are suggested to be crucial for the inhibitory role Wnt11 has on the canonical Wnt/ β -catenin pathway. Concerning Wnt secretion, our results suggest that a portion of Wnt11 proteins can be secreted independently of serine 215 and possibly independently of the lipidation on this residue. Moreover, our mutagenesis experiments suggest that asparagine 40 reduces the binding to Evi and is involved in Wnt11 secretion by an alternative route that may not require Evi. Finally, the acyltransferases ZDHHC5 and ZDHHC6 were identified as potential candidates linked to Wnt11 secretion besides PORCN.

4.3 Lipidomics analysis in HEK293T and HCT116 cells

In this final section, by lipidomics analysis, the effect on the lipid composition of HEK293T and HCT116 cells was investigated when components of the Wnt signaling or Wnt secretion pathways were overexpressed or depleted. Changes of 22 lipid classes were evaluated. Only small changes were observed in the lipid composition associated with the canonical or non-canonical Wnt proteins (Figure 3.11). For example, overexpression of non-canonical Wnts (Wnt5a, Wnt5b, Wnt11) slightly increased the amount of glycerophospholipids PA, PG, PE P-, and the ether lipids PI O-, PA O- and PS O-. These changes were not observed for the canonical Wnt3a, which rather displayed a slight increase in PC and PC O- and a decrease of PI, PS, PE, PG O- and PS O-, when being over-expressed (Figure 3.11). Note, however, that the difference in lipid classes of cells overexpressing Wnts compared to control cells was not statistically significant (section 3.14). Therefore, a larger number of replicates is required to test whether some of the trends observed in our results become statistically significant. In addition, to our

knowledge, there is no evidence to support these lipid changes between canonical and noncanonical Wnt proteins. Further studies, such as transcriptomic and functional analysis, are therefore required to identify the enzymes involved in these changes and their connection with Wnt signaling or Wnt activity.

In HEK293T cells, Porcupine activity was abolished through the inhibition with the small molecule inhibitor LGK974 or knockout of Porcupine. A slight increase in PC, PE, and SM was observed, as well as a reduction of all ether lipids. These results suggest that the acylation of Wnt proteins or an unknown substrate of Porcupine might impact the lipid homeostasis by a yet unknown mechanism. In order to clarify this aspect, other experiments should be performed to identify possible substrate candidates for PORCN. Besides that, the changes in the lipid composition of sphingolipids and ether lipids could affect the vesicular transport in the early secretory pathway [102, 103]. This could occur by interaction of these lipids with p24, a protein involved in COP-I/II mediated vesicular transport in the early secretory pathway [102, 103], which could directly affect Wnt secretion [73, 74]. To validate the effect of PORCN regarding changes in ether lipids, we used different sgRNAs targeting PORCN and focused on the lipid classes PC and PC O-. Nevertheless, with the sgRNAs, we did not observe the same changes in the lipid composition. Thus, ether lipids could be indirectly affected by the inhibitor LGK974 or due to a clonal effect in the Porcupine knockout stable cell line.

In HEK293T cells, the absence of Evi induces a slight but not statistically significant increase in PE, PG, PS, PI, PG O-, PS O-, HexCer and Hex2Cer levels, compensated by a decrease in PC O-, PI O-, Cer and TAG levels. With the exception of the lipid classes PC, PE, PC O- and PI O-, it appears that Evi and PORCN have a different effect on lipid composition. However, because these results were not statistically significant, it is only possible to state that the absence of Evi does not affect the lipid composition of HEK293T cells. A larger number of replicates is required to test whether some of the trends observed in our results become statistically significant.

One interesting change observed in HEK293T cells was in the ether lipid class PI O-. The PI O- was slightly reduced in the absence of PORCN or Evi; while, this lipid class was slightly increased under overexpression of the non-canonical Wnts. These changes are interesting, because the ether lipid PI O- could form glycosylphosphatidylinositol anchors (GPI- anchors) [146, 147]. The proteins Oto in mice and the glypicans Dlp in *Drosophila* or Gpc3, Gpc4 in humans are covalently attached to GPI-anchors. These proteins are involved in Wnt secretion [148-156]. Therefore, I hypothesize that the changes in the lipid class PI O- in HEK293T cells could be a response of the cells to regulate the secretion of Wnt proteins in the absence of PORCN, Evi, or under overexpression of Wnts. More data is required to confirm this hypothesis and to elucidate the mechanisms involved.

When Porcupine activity was impaired with LGK974 in HCT116 cells, I did not observe changes in the ether lipids. Instead, I observed changes in PI, Cer and HexCer lipid classes. This suggests that the inhibition of Porcupine by LGK974 affects the lipid composition of HCT116 cells in a different way than in HEK293T cells. In HCT116 cells, the lipid composition was analyzed in different knockout clones of Evi. Variations in the lipid composition between the knockout clones of Evi were observed, indicating there is no pattern in the lipid profile of HCT116 cells in the absence of Evi. The observable changes are probably due to individual clonal effects

instead of a common effect of the knockout of Evi. Together, these results suggest that Evi does not have an apparent impact on the lipid composition of HCT116 cells.

In conclusion, the lipidomics data highlight that the depletion or inhibition of PORCN increases sphingomyelin and reduces the ether lipids PI O- and PC O- in HEK293T cells, which could affect the vesicular transport in the early secretory pathway by binding these lipids to the P24 complex [102, 103]. Besides that, a potential lipid class for possible further investigation is PI O-, which could be linked to the secretion of Wnt proteins through the regulation of GPI-anchors. Lastly and apart from that, Evi depletion does not seem to have an apparent significant effect on the lipidome of HCT116 cells, however, a larger number of replicates would be required to test whether some of the trends observed in our results become statistically significant.

In summary, this thesis was aimed at investigating the molecular interplay between lipids and Wnt proteins. By a combination of biochemical approaches and mass spectrometry measurements, alternative lipidation mechanisms of Wnt proteins were studied, emphasizing the importance of the desaturation of fatty acids involved in Wnt lipidation. The relevance of Wnt lipidation for the secretion and signaling activity of Wnts has also been assessed, demonstrating that lipidation is essential for the functioning of Wnt11 but is not strictly necessary for its secretion. In addition, the impact of Wnts and proteins involved in Wnt lipidation and trafficking on the overall cellular lipidome of HEK293T and HCT116 cells has been tested. This study is expected to contribute to our understanding of how post-translational lipid modifications influence Wnt cellular secretion, signaling and, conversely, how some components of the Wnt signal pathway affect the lipid composition of cells.

5 Appendix

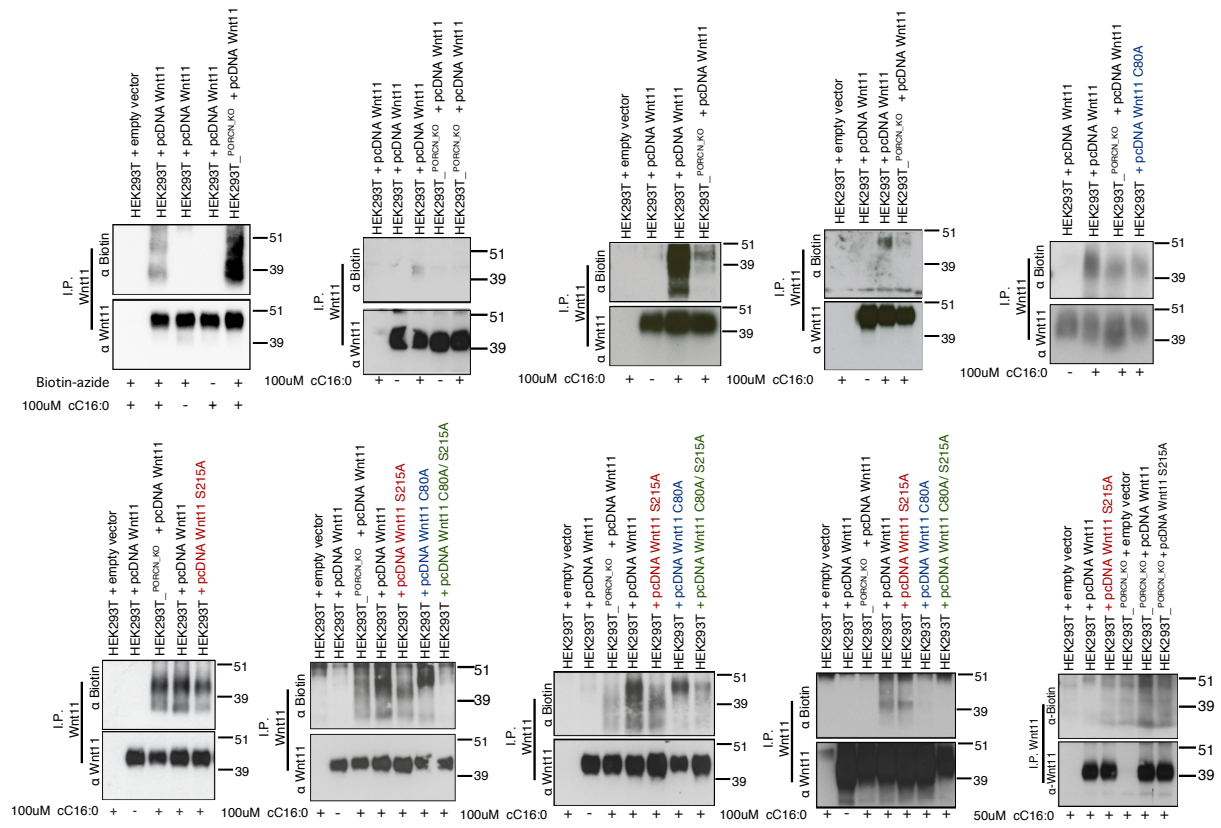


Figure 5.1: Replicates of lipid modification of Wnt11 and Wnt11 mutants with cC16:0 by western blot. α : indicates the protein to which the primary antibody is directed. I.P.: Immunoprecipitated protein.

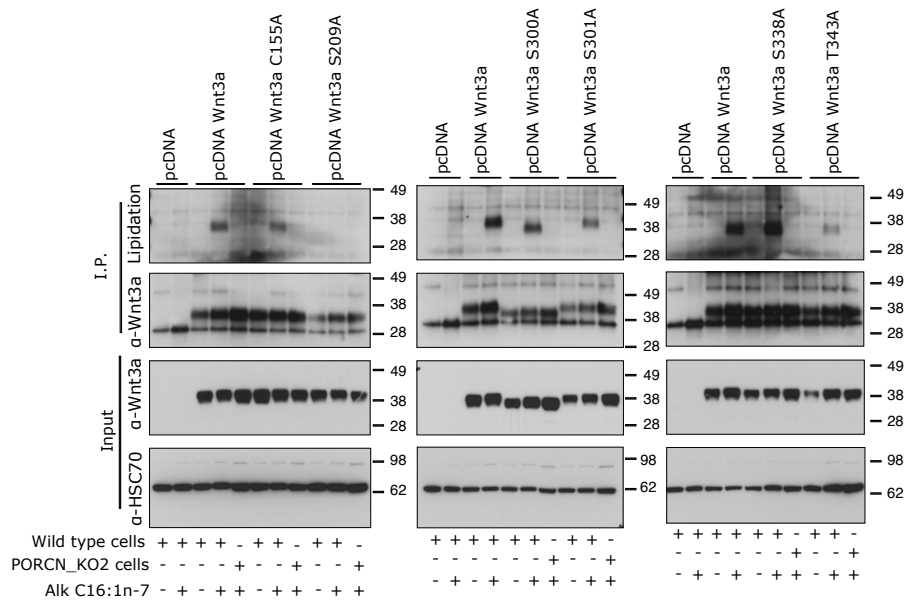


Figure 5.2: Serine 209 impaire lipidation of Wnt3a with cC16:1n.7. Detection of lipid modification in HEK293T cells with overexpression of either Wnt3a wild type or the mutant variants, Wnt3a C155A, Wnt3a S209A, Wnt3a S300A, Wnt3a S301A, Wnt3a S338A, Wnt3a T343A and Wnt3a C80A/S215A. α : indicates the protein to which the primary antibody is directed. I.P.: Immunoprecipitated protein.

5.1.1 Non detectable conversion of free cC16:0 into cC16:1n-7 in Hek293T cells

I wonder if was possible to detect the conversion of the palmitic acid alkyne cC16:0 to palmitoleic acid alkyne cC16:1n-7. To test this, it was used an approach previously establish by Dr. Katharina Beckenbauer and co-workers in Britta Brugger's lab, which uses alkyne-azide cycloaddition click chemistry and precursor ion scanning mass spectrometry [116, 119, 124]. This approach takes as an advantage the labeling of alkyne fatty acids with biotin azide. The adduct formed between alkyne fatty acids with biotin azide can be fragmented during the collision-induced dissociation in MS/MS analysis, generating a specific fragment of 270 m/z [116, 119, 124] (Figure 5.3A). Using the mass of 270 m/z as precursor ion, it is possible to scan the intact masses of fatty acids that can generate that type of fragment. The intact mass scanning was made in a range from 800 to 900 m/z. In the mass spectra, peaks at 868 m/z or 866 m/z would correspond to the intact mass of the adducts cC16:0 + biotin-azide or cC16:1n-7 + biotin-azide, respectively (Figure 2.1). With this in mind it was compared the spectrum of HEK293T cells treated with or without 100 μ M of cC16:0 and check for peaks at 868 m/z or 866 m/z. Unfortunately, in the results (Figure 5.3 red frame) there was not detection of peak at 868 m/z or 866 m/z that correspond to the masses of the free fatty acids cC16:0 or cC16:1n-7. From this experiment, I only can affirm that under this labeling condition (Figure 2.2B) was not possible to detect neither palmitic acid alkyne cC16:0 nor the conversion of cC16:0 to cC16:1n-7.

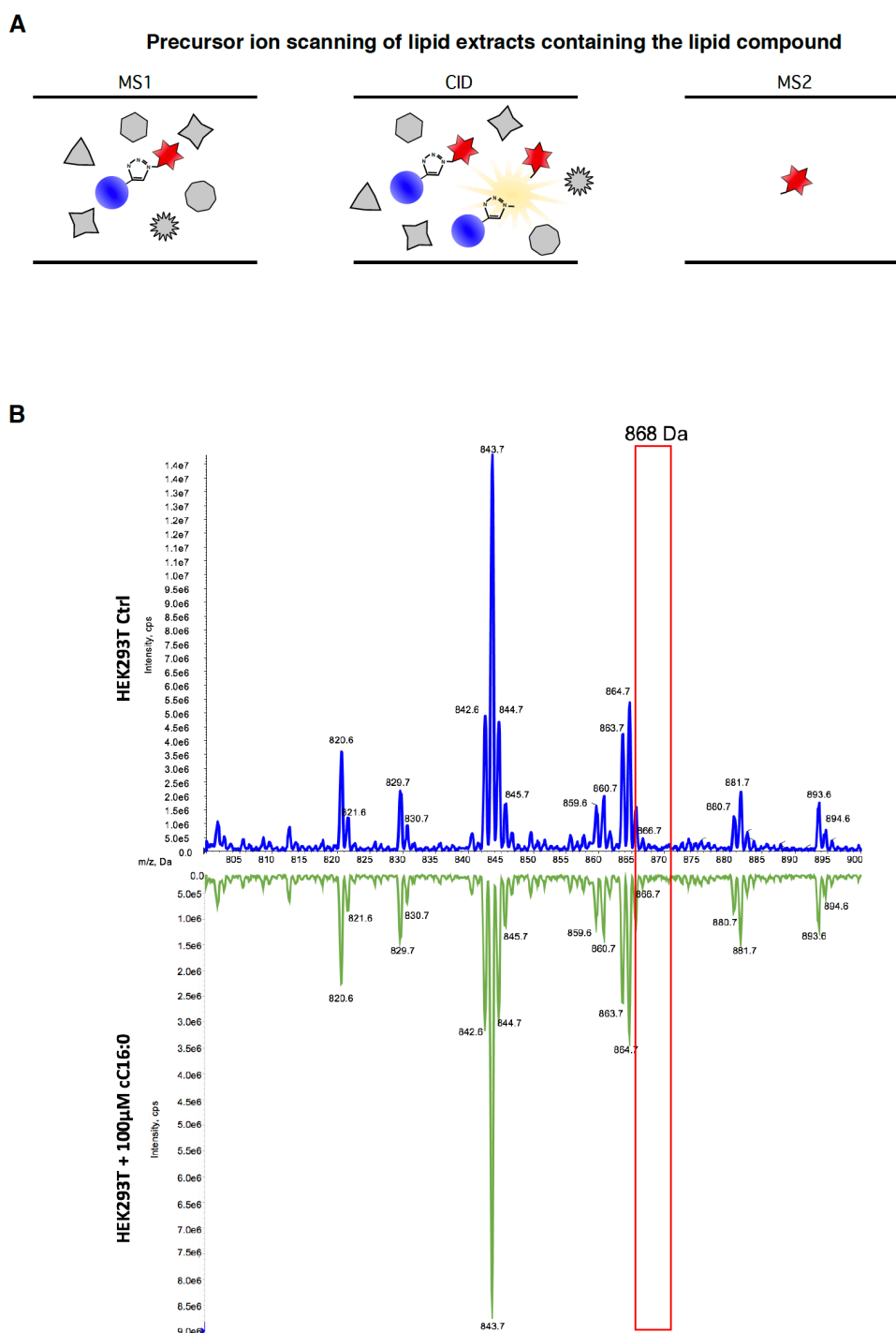


Figure 5.3: Scanning of free cC16:0 or cC16:1n-7 fatty acids. **A.** Strategy for alkyne fatty acids analysis based on click chemistry and precursor ion scanning mass spectrometry. In the first mass analyzer molecules are scanned according to their intact mass m/z (MS1, left panel). Then molecules are fragmented in the collision cell, in a process known as collision-induced dissociation (CID, middle panel). In the second mass analyzer (MS2, right panel), only fragment ions with a specific mass can pass to the detector, in our case the fragment filtered in the MS2 has a mass of 270 m/z . **B.** Scanning of free cC16:0 or cC16:1n-7 from lipid extracts of HEK293T cells incubated for 36h with cC16:0: Mass spectra from HEK293T cells without (blue) and after incubation with 100 μ M cC16:0 (green) was obtained by mass spectrometry. Both samples were submitted to click labeling with biotin azide and detected by MS/MS precursor 270 ion scanning in positive ion mode. The intact mass/charge for the adducts cC16:0 + biotin-azide and or cC16:1n-7 + biotin-azide (868 m/z and 866 m/z , respectively) was expected to be detected in the region indicated in red.

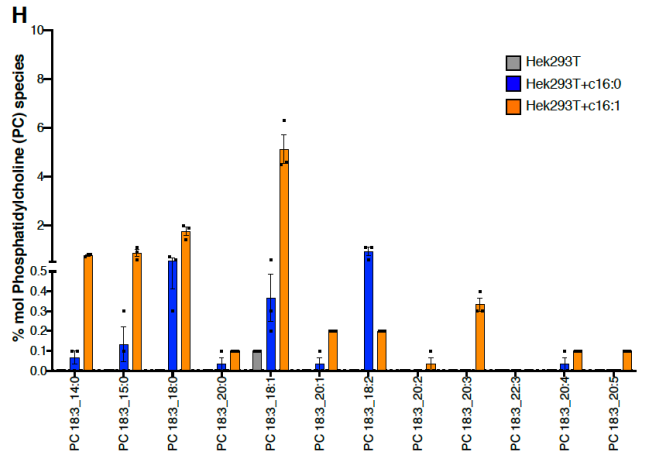
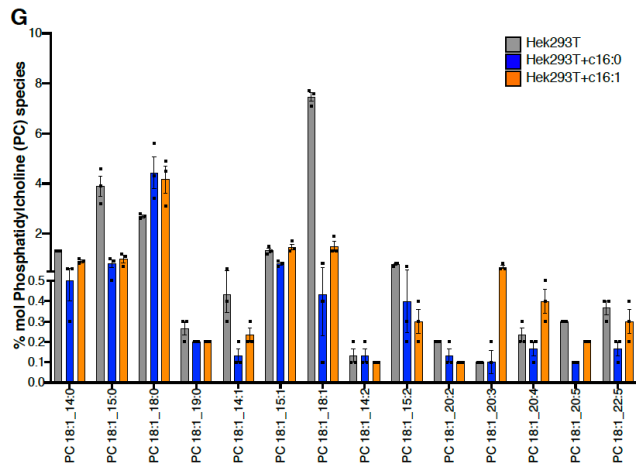
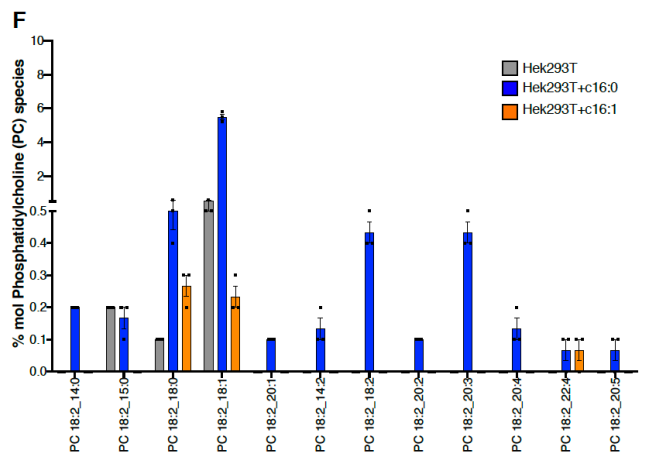
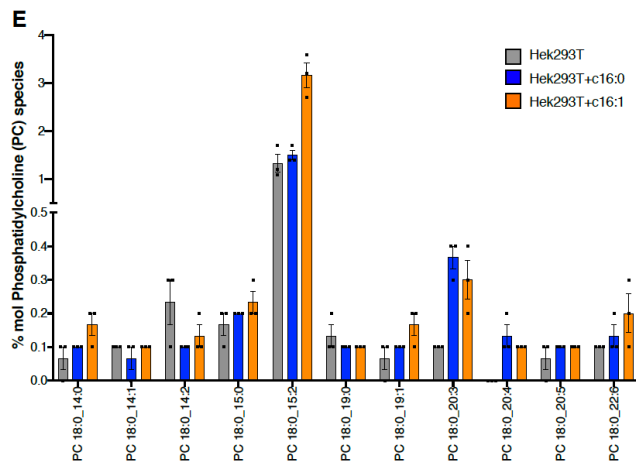
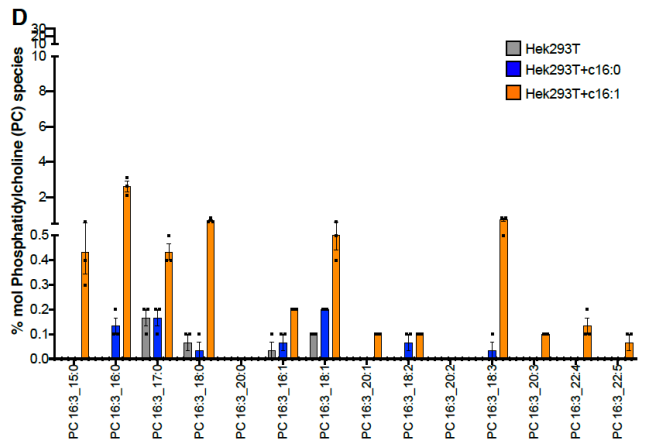
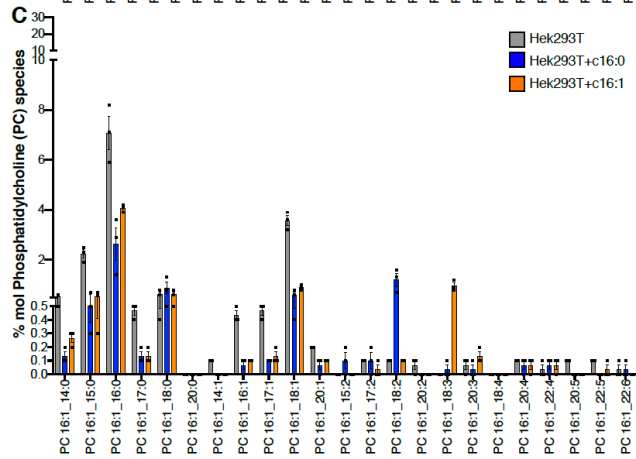
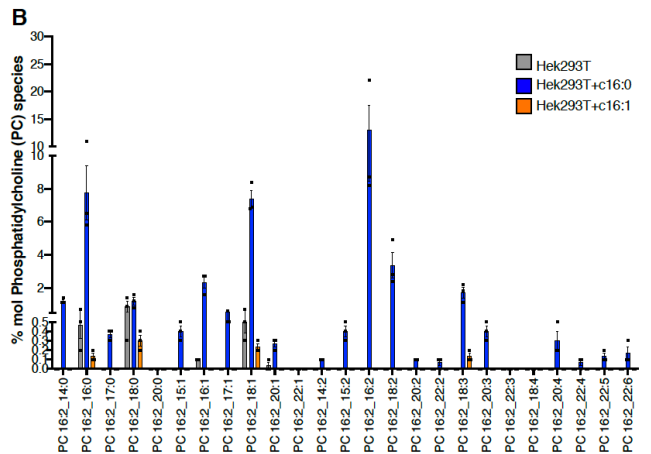
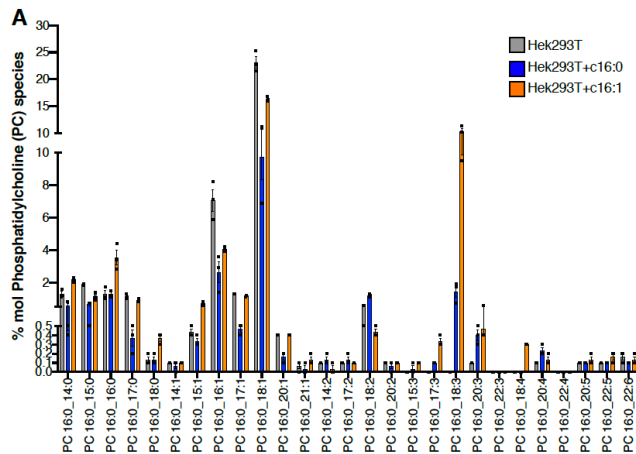


Figure 5.4 Incorporation of cC16:0 and cC16:1n-7 into phosphatidylcholine species: HEK293T cells were treated with either 100 μ M of cC16:0 (blue bars) or 100 μ M of cC16:1n-7 (orange bars). Untreated HEK293T cells (gray bars) were used as control. **A.** % mol of phosphatidylcholine (PC) species with fatty acids of 16 carbons, saturated (PC 16:0). **B.** % mol of phosphatidylcholine (PC) species with fatty acids of 16 carbons, with two unsaturations (PC 16:2). **C.** % mol of phosphatidylcholine (PC) species with fatty acids of 16 carbons, with one unsaturation (PC 16:1). **D.** % mol of phosphatidylcholine (PC) species with fatty acids of 16 carbons, with three unsaturations (PC 16:3). **E.** % mol of phosphatidylcholine species with fatty acids of 18 carbons, saturated (PC 18:0). **F.** % mol of phosphatidylcholine species with fatty acids of 18 carbons, with two unsaturations (PC 18:2). **G.** % mol of phosphatidylcholine species with fatty acids of 18 carbons, with one unsaturation (PC 18:1). **H.** % mol of phosphatidylcholine species with fatty acids of 18 carbons, with three unsaturations (PC 18:3). Three independent experimental replicates were carried out. Standard error of all data points is highlighted with the black bar. Lipid extraction was done by Iris Leibrecht, Christian Lüchtenborg and Timo Sachsenheimer. Lipidome data was analyzed and provided by Christian Lüchtenborg and Timo Sachsenheimer (Brügger lab).

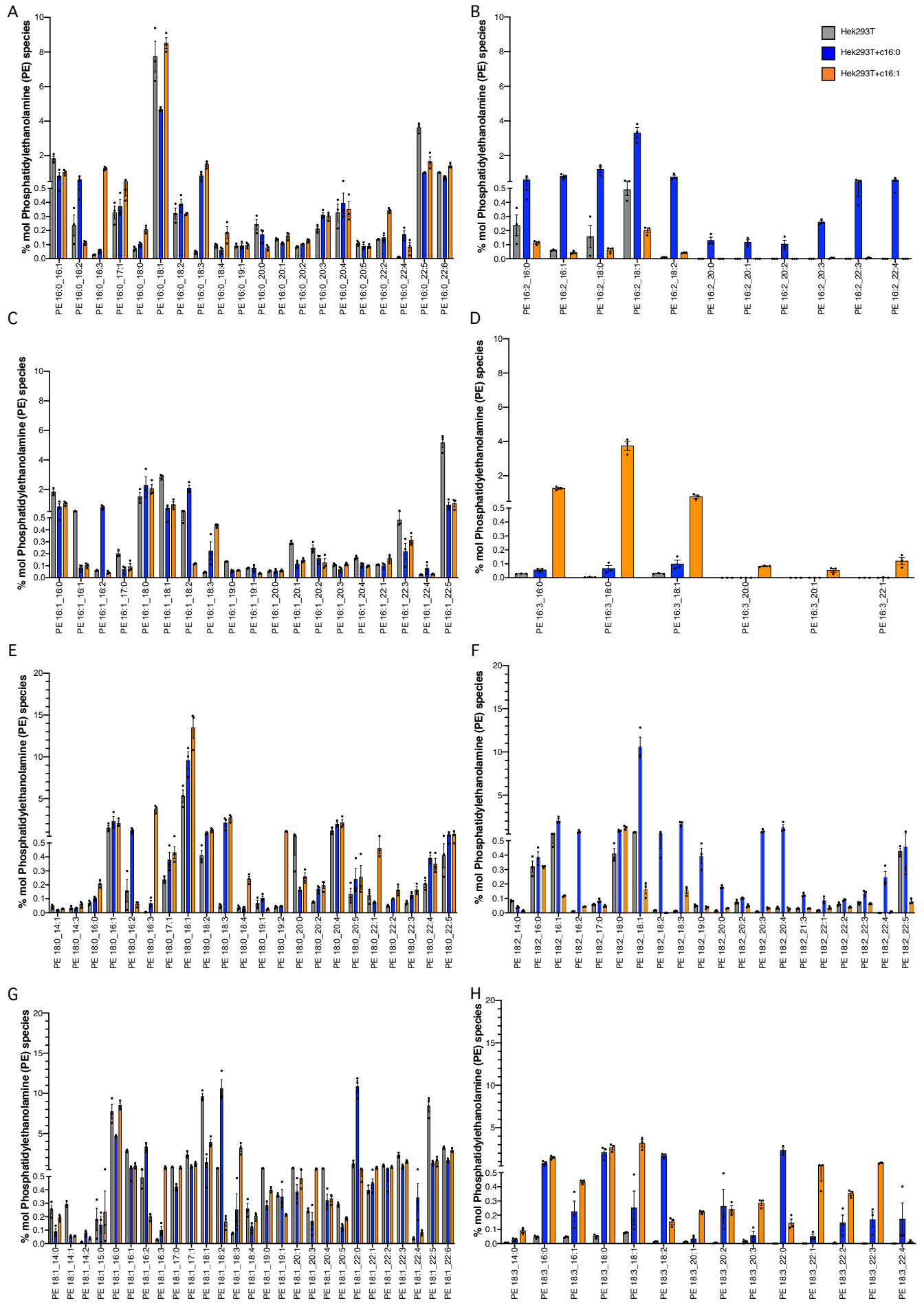


Figure 5.5 Incorporation of cC16:0 and cC16:1n-7 into phosphatidylethanolamine species: HEK293T cells were treated with either 100 μ M of cC16:0 (blue bars) or 100 μ M of cC16:1n-7 (orange bars). Untreated HEK293T cells (gray bars) were used as control. **A.** % mol of phosphatidylethanolamine (PE) species with fatty acids of 16 carbons, saturated (PE 16:0). **B.** % mol of phosphatidylethanolamine (PE) species with fatty acids of 16 carbons, with two unsaturations (PE 16:2). **C.** % mol of phosphatidylethanolamine (PE) species with fatty acids of 16 carbons, with one unsaturation (PE 16:1). **D.** % mol of phosphatidylethanolamine (PE) species with fatty acids of 16 carbons, with three unsaturations (PE 16:3). **E.** % mol of phosphatidylethanolamine (PE) species with fatty acids of 18 carbons, saturated (PE 18:0). **F.** % mol of phosphatidylethanolamine (PE) species with fatty acids of 18 carbons, with two unsaturations (PE 18:2). **G.** % mol of phosphatidylethanolamine (PE) species with fatty acids of 18 carbons, with one unsaturation (PE 18:1). **H.** % mol of phosphatidylethanolamine (PE) species with fatty acids of 18 carbons, with three unsaturations (PE 18:3). Three independent experimental replicates were carried out. Standard error of all data points is highlighted with the black bar. Lipid extraction was done by Iris Leibrecht, Christian Luchtenborg and Timo Sachsenheimer. Lipidome data was analyzed and provided by Christian Luchtenborg and Timo Sachsenheimer (Brügger lab).

5.1.2 Gelatin degradation assay

To investigate another possible cellular function affected by mutation at serine 215 in Wnt11, it was used a gelatin degradation assay implemented by L. Wolf (M. Boutros group, DKFZ, Heidelberg). The assay mimics in vitro the process of remodeling the extracellular matrix during the invasion and metastasis of melanoma cells. L. Wolf previously used this assay to test the function of some Wnt ligands in RPMI7951 melanoma cells [25]. Interestingly, she found that knockdown of Wnt11 leads to an increase in gelatin degradation; meanwhile, the overexpression reduces the gelatin degradation [25]. In the case of Wnt5a, another non-canonical Wnt, it was the opposite; the knockdown of Wnt5a leads to a decrease in gelatin degradation; meanwhile, the overexpression leads to similar levels the control [25].

Considering these results, it was evaluated the behavior of RPMI7951 cells overexpressing Wnt11 wild type (as positive control), the mutant variant Wnt11 S215A and Wnt5a (Figure 5.6). Unfortunately, to our surprise, we got different results on the gelatin degradation in the positive control when it was used two different batches of the same pcDNA Wnt11 plasmid. With one of the batches (pcDNA Wnt11 #1) similar levels of gelatin degradation in comparison to negative control (pcDNA, Figure 5.6B) were observed. Meanwhile in the other case (pcDNA Wnt11 #2) I observed a reduction in gelatin degradation, resembling to the results of L. Wolf. There is no difference in terms of sequence between the plasmids and until now, I can not explain the cause in the difference of behavior. Therefore, I can not give a clear conclusion about this experiment. Nevertheless, regarding Wnt11 S215A and Wnt5a, I observed similar levels of gelatin degradation in comparison to negative control (Figure 5.6C).

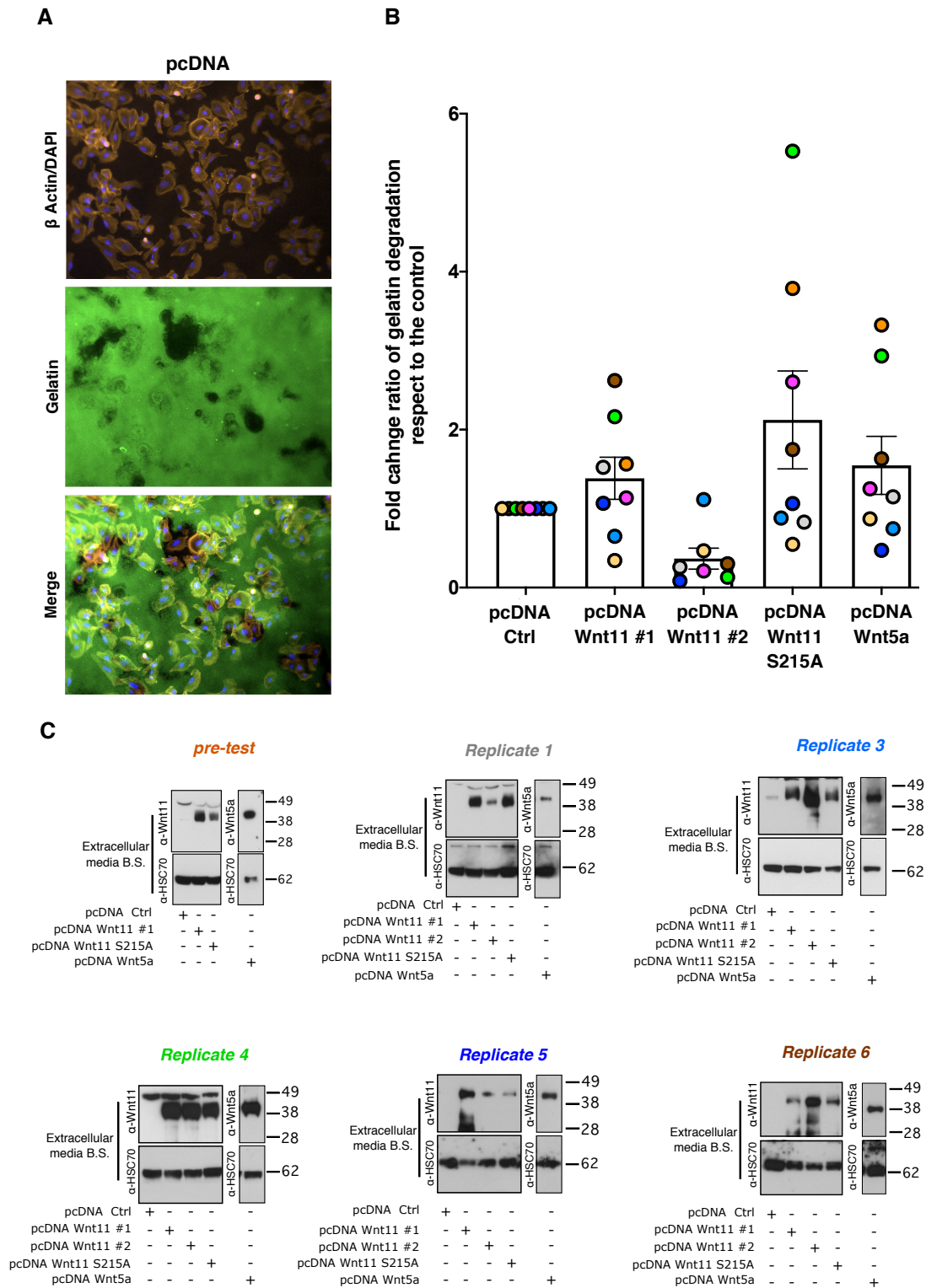


Figure 5.6: Ser 215 Ala mutation in Wnt11 to reduces gelatin degradation of RPMI795 melanoma cells. **A.** Fluorescent images of melanoma cells (top), gelatin (middle) and merge (bottom). Example of the picture of melanoma cells and the fluorescent gelatin. **B** Gelatin degradation for the different studied constructs is presented in fold units relative to the control “Ctrl”. **C** Western blots show the presence of Wnt11, Wnt11 S215A, and Wnt5a in the extracellular media after being pulled down with blue sepharose beads. This experiment was performed with the collaboration of Lucie Wolf (M. Boutros group, DKFZ, Heidelberg).

Bibliography

1. Miller, J. R. (2002) The Wnts, *Genome Biol.* **3**, REVIEWS3001.
2. R&D_systems (2004) Mnireview: The Wnt Family of Secreted Proteins in Web Page: <https://www.rndsystems.com/resources/articles/wnt-family-secreted-proteins>.
3. Nusse, R. & Clevers, H. (2017) Wnt/beta-Catenin Signaling, Disease, and Emerging Therapeutic Modalities, *Cell.* **169**, 985-999.
4. Wiese, K. E., Nusse, R. & van Amerongen, R. (2018) Wnt signalling: conquering complexity, *Development.* **145**.
5. Johnson, M. L. & Rajamannan, N. (2006) Diseases of Wnt signaling, *Rev Endocr Metab Disord.* **7**, 41-9.
6. Zhan, T., Rindtorff, N. & Boutros, M. (2017) Wnt signaling in cancer in *Oncogene* pp. 1461-1473, Nature Publishing Group,
7. Salahshor, S. & Woodgett, J. R. (2005) The links between axin and carcinogenesis, *J Clin Pathol.* **58**, 225-36.
8. Lammi, L., Arte, S., Somer, M., Jarvinen, H., Lahermo, P., Thesleff, I., Pirinen, S. & Nieminen, P. (2004) Mutations in AXIN2 cause familial tooth agenesis and predispose to colorectal cancer, *Am J Hum Genet.* **74**, 1043-50.
9. Gould, T. D. & Manji, H. K. (2002) The Wnt signaling pathway in bipolar disorder, *Neuroscientist.* **8**, 497-511.
10. De Ferrari, G. V. & Inestrosa, N. C. (2000) Wnt signaling function in Alzheimer's disease, *Brain Res Brain Res Rev.* **33**, 1-12.
11. Hurlstone, A. F., Haramis, A. P., Wienholds, E., Begthel, H., Korving, J., Van Eeden, F., Cuppen, E., Zivkovic, D., Plasterk, R. H. & Clevers, H. (2003) The Wnt/beta-catenin pathway regulates cardiac valve formation, *Nature.* **425**, 633-7.
12. Loh, K. M., van Amerongen, R. & Nusse, R. (2016) Generating Cellular Diversity and Spatial Form: Wnt Signaling and the Evolution of Multicellular Animals, *Dev Cell.* **38**, 643-55.
13. MacDonald, B. T., Hien, A., Zhang, X., Iranloye, O., Virshup, D. M., Waterman, M. L. & He, X. (2014) Disulfide bond requirements for active Wnt ligands, *J Biol Chem.* **289**, 18122-36.
14. Janda, C. Y., Waghray, D., Levin, A. M., Thomas, C. & Garcia, K. C. (2012) Structural basis of Wnt recognition by frizzled in *Science*
15. Chu, M. L. H., Ahn, V. E., Choi, H. J., Daniels, D. L., Nusse, R. & Weis, W. I. (2013) Structural studies of wnts and identification of an LRP6 binding site in *Structure* pp. 1235-1242, Elsevier Ltd,
16. Hirai, H., Matoba, K., Mihara, E., Arimori, T. & Takagi, J. (2019) Crystal structure of a mammalian Wnt–frizzled complex in *Nature Structural and Molecular Biology* pp. 372-379, Springer US,
17. Nygaard, R., Yu, J., Kim, J., Ross, D. R., Parisi, G., Clarke, O. B., Virshup, D. M. & Mancia, F. (2021) Structural Basis of WLS/Evi-Mediated Wnt Transport and Secretion, *Cell.* **184**, 194-206 e14.
18. Mihara, E., Hirai, H., Yamamoto, H., Tamura-Kawakami, K., Matano, M., Kikuchi, A., Sato, T. & Takagi, J. (2016) Active and water-soluble form of lipidated wnt protein is maintained by a serum glycoprotein afamin/ α -albumin in *eLife* pp. 1-19
19. Chen, Y., Chen, Z., Tang, Y. & Xiao, Q. (2021) The involvement of noncanonical Wnt signaling in cancers, *Biomed Pharmacother.* **133**, 110946.
20. Stamos, J. L. & Weis, W. I. (2013) The beta-catenin destruction complex, *Cold Spring Harb Perspect Biol.* **5**, a007898.

21. Eubelen, M., Bostaille, N., Cabochette, P., Gauquier, A., Tebabi, P., Dumitru, A. C., Koehler, M., Gut, P., Alsteens, D., Stainier, D. Y. R., Garcia-Pino, A. & Vanhollebeke, B. (2018) A molecular mechanism for Wnt ligand-specific signaling in *Science*
22. Gomez-Orte, E., Saenz-Narciso, B., Moreno, S. & Cabello, J. (2013) Multiple functions of the noncanonical Wnt pathway, *Trends Genet.* **29**, 545-53.
23. Zallen, J. A. (2007) Planar polarity and tissue morphogenesis, *Cell.* **129**, 1051-63.
24. Simons, M. & Mlodzik, M. (2008) Planar cell polarity signaling: from fly development to human disease, *Annu Rev Genet.* **42**, 517-40.
25. Wolf, L. (2021) *Ph.D. Thesis: Ubiquitin-dependent regulation of the WNT cargo protein EVI/WLS*, Heidelberg University.
26. De, A. (2011) Wnt/Ca²⁺ signaling pathway: a brief overview, *Acta Biochim Biophys Sin (Shanghai).* **43**, 745-56.
27. Sheldahl, L. C., Park, M., Malbon, C. C. & Moon, R. T. (1999) Protein kinase C is differentially stimulated by Wnt and Frizzled homologs in a G-protein-dependent manner, *Curr Biol.* **9**, 695-8.
28. Kuhl, M., Sheldahl, L. C., Malbon, C. C. & Moon, R. T. (2000) Ca(2+)/calmodulin-dependent protein kinase II is stimulated by Wnt and Frizzled homologs and promotes ventral cell fates in *Xenopus*, *J Biol Chem.* **275**, 12701-11.
29. Jiang, H., Zhang, X., Chen, X., Aramsangtienchai, P., Tong, Z. & Lin, H. (2018) Protein Lipidation: Occurrence, Mechanisms, Biological Functions, and Enabling Technologies, *Chem Rev.* **118**, 919-988.
30. Corradi, V., Sejdiu, B. I., Mesa-Gallosio, H., Abdizadeh, H., Noskov, S. Y., Marrink, S. J. & Tieleman, D. P. (2019) Emerging Diversity in Lipid-Protein Interactions, *Chem Rev.* **119**, 5775-5848.
31. Kurayoshi, M., Yamamoto, H., Izumi, S. & Kikuchi, A. (2007) Post-translational palmitoylation and glycosylation of Wnt-5a are necessary for its signalling in *Biochemical Journal* pp. 515-523
32. Doubravska, L., Krausova, M., Gradl, D., Vojtechova, M., Tumova, L., Lukas, J., Valenta, T., Pospichalova, V., Fafilek, B., Plachy, J., Sebesta, O. & Korinek, V. (2011) Fatty acid modification of Wnt1 and Wnt3a at serine is prerequisite for lipidation at cysteine and is essential for Wnt signalling, *Cell Signal.* **23**, 837-48.
33. Herr, P. & Basler, K. (2012) Porcupine-mediated lipidation is required for Wnt recognition by Wls in *Developmental Biology* pp. 392-402, Elsevier Inc.,
34. Tang, X., Wu, Y., Belenkaya, T. Y., Huang, Q., Ray, L., Qu, J. & Lin, X. (2012) Roles of N-glycosylation and lipidation in Wg secretion and signaling in *Developmental Biology* pp. 32-41, Elsevier Inc.,
35. Yamamoto, H., Awada, C., Hanaki, H., Sakane, H., Tsujimoto, I., Takahashi, Y., Takao, T. & Kikuchi, A. (2013) The apical and basolateral secretion of Wnt11 and Wnt3a in polarized epithelial cells is regulated by different mechanisms in *Journal of Cell Science* pp. 2931-2943, The Company of Biologists,
36. Nile, A. H. & Hannoush, R. N. (2016) Fatty acylation of Wnt proteins in *Nature Chemical Biology* pp. 60-69, Nature Publishing Group,
37. Ke, J., Xu, H. & Williams, B. (2013) Lipid modification in Wnt structure and function in *Current Opinion in Lipidology* pp. 129-133
38. Chen, Q., Takada, R. & Takada, S. (2012) Loss of Porcupine impairs convergent extension during gastrulation in zebrafish in *Journal of Cell Science*

39. Miranda, M., Galli, L. M., Enriquez, M., Szabo, L. A., Gao, X., Hannoush, R. N. & Burrus, L. W. (2014) Identification of the WNT1 residues required for palmitoylation by Porcupine, *FEBS Lett.* **588**, 4815-24.
40. Galli, L. M. & Burrus, L. W. (2011) Differential palmitoylation of Wnt1 on C93 and S224 residues has overlapping and distinct consequences, *PLoS One.* **6**, e26636.
41. Galli, L. M., Zebarjadi, N., Li, L., Lingappa, V. R. & Burrus, L. W. (2016) Divergent effects of Porcupine and Wntless on WNT1 trafficking, secretion, and signaling, *Exp Cell Res.* **347**, 171-183.
42. Willert, K., Brown, J. D., Danenberg, E., Duncan, A. W., Weissman, I. L., Reya, T., Yates, J. R. & Nusse, R. (2003) Wnt proteins are lipid-modified and can act as stem cell growth factors in *Nature* pp. 448-452
43. Takada, R., Satomi, Y., Kurata, T., Ueno, N., Norioka, S., Kondoh, H., Takao, T. & Takada, S. (2006) Monounsaturated Fatty Acid Modification of Wnt Protein: Its Role in Wnt Secretion in *Developmental Cell*
44. Galli, L. M., Barnes, T. L., Secrest, S. S., Kadowaki, T. & Burrus, L. W. (2007) Porcupine-mediated lipid-modification regulates the activity and distribution of Wnt proteins in the chick neural tube, *Development.* **134**, 3339-48.
45. Rios-Esteves, J. & Resh, M. D. (2013) Stearoyl CoA desaturase is required to produce active, lipid-modified Wnt proteins, *Cell Rep.* **4**, 1072-81.
46. Rios-Esteves, J., Haugen, B. & Resh, M. D. (2014) Identification of key residues and regions important for porcupine-mediated Wnt acylation in *Journal of Biological Chemistry* pp. 17009-17019
47. Gao, X., Arenas-Ramirez, N., Scales, S. J. & Hannoush, R. N. (2011) Membrane targeting of palmitoylated Wnt and Hedgehog revealed by chemical probes, *FEBS Lett.* **585**, 2501-6.
48. Miranda, M., Galli, L. M., Enriquez, M., Szabo, L. A., Gao, X., Hannoush, R. N. & Burrus, L. W. (2014) Identification of the WNT1 residues required for palmitoylation by Porcupine in *FEBS Letters* pp. 4815-4824, Federation of European Biochemical Societies,
49. Gao, X. & Hannoush, R. N. (2014) Single-cell in situ imaging of palmitoylation in fatty-acylated proteins in *Nature Protocols* pp. 2607-2623, Nature Publishing Group,
50. Gao, X. & Hannoush, R. N. (2014) Single-cell imaging of Wnt palmitoylation by the acyltransferase porcupine in *Nature Chemical Biology*
51. Gao, X. & Hannoush, R. N. (2016) Visualizing Wnt Palmitoylation in Single Cells BT - Wnt Signaling: Methods and Protocols in (Barrett, Q. & Lum, L., eds) pp. 1-9, Springer New York, New York, NY.
52. Dhasmana, D., Veerapathiran, S., Azbazar, Y., Nelanuthala, A. V. S., Teh, C., Ozhan, G. & Wohland, T. (2021) Wnt3 Is Lipidated at Conserved Cysteine and Serine Residues in Zebrafish Neural Tissue in *Frontiers in Cell and Developmental Biology* pp. 1-22
53. Azbazar, Y., Ozalp, O., Sezgin, E., Veerapathiran, S., Duncan, A. L., Sansom, M. S. P., Eggeling, C., Wohland, T., Karaca, E. & Ozhan, G. (2019) More Favorable Palmitic Acid Over Palmitoleic Acid Modification of Wnt3 Ensures Its Localization and Activity in Plasma Membrane Domains in *Frontiers in Cell and Developmental Biology* pp. 1-15
54. Gao, X. & Hannoush, R. N. (2016) Visualizing Wnt Palmitoylation in Single Cells in *Methods in Molecular Biology* pp. 1-9, Humana Press, New York, NY,
55. Tuladhar, R., Yarravarapu, N., Ma, Y., Zhang, C., Herbert, J., Kim, J., Chen, C. & Lum, L. (2019) Stereoselective fatty acylation is essential for the release of lipidated WNT proteins from the acyltransferase Porcupine (PORCN), *Journal of Biological Chemistry.* **294**, 6273-6282.

56. Bartscherer, K., Pelte, N., Ingelfinger, D. & Boutros, M. (2006) Secretion of Wnt ligands requires Evi, a conserved transmembrane protein, *Cell*. **125**, 523-33.
57. Banziger, C., Soldini, D., Schutt, C., Zipperlen, P., Hausmann, G. & Basler, K. (2006) Wntless, a conserved membrane protein dedicated to the secretion of Wnt proteins from signaling cells, *Cell*. **125**, 509-22.
58. Kurayoshi, M., Yamamoto, H., Izumi, S. & Kikuchi, A. (2007) Post-translational palmitoylation and glycosylation of Wnt-5a are necessary for its signalling, *Biochem J*. **402**, 515-23.
59. Tuladhar, R., Yarravarapu, N. & Lum, L. (2016) Monitoring wnt protein acylation using an in vitro cyclo- addition reaction in *Methods in Molecular Biology* pp. 11-16, Humana Press Inc.,
60. Hausmann, G. & Basler, K. (2006) Wnt Lipid Modifications: Not as Saturated as We Thought in *Developmental Cell* pp. 751-752
61. Nile, A. H., Mukund, S., Stanger, K., Wang, W. & Hannoush, R. N. (2017) Unsaturated fatty acyl recognition by Frizzled receptors mediates dimerization upon Wnt ligand binding in *Proceedings of the National Academy of Sciences of the United States of America* pp. 4147-4152
62. Chamberlain, L. H. & Shipston, M. J. (2015) The physiology of protein S-acylation, *Physiol Rev*. **95**, 341-76.
63. Salaun, C., Locatelli, C., Zmuda, F., Cabrera Gonzalez, J. & Chamberlain, L. H. (2020) Accessory proteins of the zDHHC family of S-acylation enzymes, *J Cell Sci*. **133**.
64. Kadowaki, T., Wilder, E., Klingensmith, J., Zachary, K. & Perrimon, N. (1996) The segment polarity gene porcupine encodes a putative multitransmembrane protein involved in Wingless processing, *Genes Dev*. **10**, 3116-28.
65. van den Heuvel, M., Harryman-Samos, C., Klingensmith, J., Perrimon, N. & Nusse, R. (1993) Mutations in the segment polarity genes wingless and porcupine impair secretion of the wingless protein, *EMBO J*. **12**, 5293-302.
66. Masumoto, N., Lanyon-Hogg, T., Rodgers, Ursula R., Konitsiotis, Antonios D., Magee, Anthony I. & Tate, Edward W. (2015) Membrane bound O-acyltransferases and their inhibitors in *Biochemical Society Transactions*
67. Lee, C. J., Rana, M. S., Bae, C., Li, Y. & Banerjee, A. (2019) In vitro reconstitution of Wnt acylation reveals structural determinants of substrate recognition by the acyltransferase human Porcupine, *J Biol Chem*. **294**, 231-245.
68. Zhai, L., Chaturvedi, D. & Cumberledge, S. (2004) Drosophila wnt-1 undergoes a hydrophobic modification and is targeted to lipid rafts, a process that requires porcupine, *J Biol Chem*. **279**, 33220-7.
69. Yu, J., Liao, P. J., Xu, W., Jones, J. R., Everman, D. B., Flanagan-Steet, H., Keller, T. H. & Virshup, D. M. (2021) Structural model of human PORCN illuminates disease-associated variants and drug-binding sites, *J Cell Sci*. **134**.
70. Wang, L., Qian, H., Nian, Y., Han, Y., Ren, Z., Zhang, H., Hu, L., Prasad, B. V. V., Laganowsky, A., Yan, N. & Zhou, M. (2020) Structure and mechanism of human diacylglycerol O-acyltransferase 1, *Nature*. **581**, 329-332.
71. Jia Yu, P. J. L., Weijun Xu, Julie R. Jones, David B. Everman, Heather Flanagan-Steet, Thomas H. Keller, David M. Virshup (2021) Structural model of PORCN illuminates disease-associated variants and drug binding sites, *bioRxiv Preprint*.
72. Coombs, G. S., Yu, J., Canning, C. A., Veltri, C. A., Covey, T. M., Cheong, J. K., Utomo, V., Banerjee, N., Zhang, Z. H., Jadulco, R. C., Concepcion, G. P., Bugni, T. S., Harper, M. K., Mihalek,

- I., Jones, C. M., Ireland, C. M. & Virshup, D. M. (2010) WLS-dependent secretion of WNT3A requires Ser209 acylation and vacuolar acidification, *J Cell Sci.* **123**, 3357-67.
73. Buechling, T., Chaudhary, V., Spirohn, K., Weiss, M. & Boutros, M. (2011) P24 proteins are required for secretion of Wnt ligands in *EMBO Reports* pp. 1265-1272, Nature Publishing Group,
74. Port, F., Hausmann, G. & Basler, K. (2011) A genome-wide RNA interference screen uncovers two p24 proteins as regulators of Wingless secretion, *EMBO Rep.* **12**, 1144-52.
75. Sun, J., Yu, S., Zhang, X., Capac, C., Aligbe, O., Daudelin, T., Bonder, E. M. & Gao, N. (2017) A Wntless-SEC12 complex on the ER membrane regulates early Wnt secretory vesicle assembly and mature ligand export, *J Cell Sci.* **130**, 2159-2171.
76. Das, S., Yu, S., Sakamori, R., Vedula, P., Feng, Q., Flores, J., Hoffman, A., Fu, J., Stypulkowski, E., Rodriguez, A., Dobrowolski, R., Harada, A., Hsu, W., Bonder, E. M., Verzi, M. P. & Gao, N. (2015) Rab8a vesicles regulate Wnt ligand delivery and Paneth cell maturation at the intestinal stem cell niche, *Development.* **142**, 2147-62.
77. Gross, J. C., Chaudhary, V., Bartscherer, K. & Boutros, M. (2012) Active Wnt proteins are secreted on exosomes in *Nature Cell Biology* pp. 1036-1045, Nature Publishing Group,
78. Mehta, S., Hingole, S. & Chaudhary, V. (2021) The Emerging Mechanisms of Wnt Secretion and Signaling in Development, *Front Cell Dev Biol.* **9**, 714746.
79. Routledge, D. & Scholpp, S. (2019) Mechanisms of intercellular Wnt transport, *Development.* **146**.
80. Maureen H. Richards, M. S. S., Jennilee Wallace, Lena Al-Harhi (2014) Porcupine Is Not Required for the Production of the Majority of Wnts from Primary Human Astrocytes and CD8+ T Cells, *PLOS ONE. Volume 9*
81. Speer, K. F., Sommer, A., Tاجر, B., Mullins, M. C., Klein, P. S. & Lemmon, M. A. (2019) Non-acylated Wnts Can Promote Signaling, *Cell Rep.* **26**, 875-883 e5.
82. Rao, D. M., Shackelford, M. T., Bordeaux, E. K., Sottnik, J. L., Ferguson, R. L., Yamamoto, T. M., Wellberg, E. A., Bitler, B. G. & Sikora, M. J. (2019) Wnt family member 4 (WNT4) and WNT3A activate cell-autonomous Wnt signaling independent of porcupine O-acyltransferase or Wnt secretion, *J Biol Chem.* **294**, 19950-19966.
83. Ching, W., Hang, H. C. & Nusse, R. (2008) Lipid-independent secretion of a Drosophila Wnt protein, *J Biol Chem.* **283**, 17092-8.
84. Moti, N., Yu, J., Boncompain, G., Perez, F. & Virshup, D. M. (2019) Wnt traffic from endoplasmic reticulum to filopodia, *PLoS One.* **14**, e0212711.
85. Carron, C., Pascal, A., Djiane, A., Boucaut, J. C., Shi, D. L. & Umbhauer, M. (2003) Frizzled receptor dimerization is sufficient to activate the Wnt/beta-catenin pathway, *J Cell Sci.* **116**, 2541-50.
86. van Vliet, P. P., Lin, L., Boogerd, C. J., Martin, J. F., Andelfinger, G., Grossfeld, P. D. & Evans, S. M. (2017) Tissue specific requirements for WNT11 in developing outflow tract and dorsal mesenchymal protrusion, *Dev Biol.* **429**, 249-259.
87. Nagy, II, Railo, A., Rapila, R., Hast, T., Sormunen, R., Tavi, P., Rasanen, J. & Vainio, S. J. (2010) Wnt-11 signalling controls ventricular myocardium development by patterning N-cadherin and beta-catenin expression, *Cardiovasc Res.* **85**, 100-9.
88. Zhou, W., Lin, L., Majumdar, A., Li, X., Zhang, X., Liu, W., Etheridge, L., Shi, Y., Martin, J., Van de Ven, W., Kaartinen, V., Wynshaw-Boris, A., McMahon, A. P., Rosenfeld, M. G. & Evans, S. M. (2007) Modulation of morphogenesis by noncanonical Wnt signaling requires ATF/CREB family-mediated transcriptional activation of TGFbeta2, *Nat Genet.* **39**, 1225-34.

89. Guo, Y., Dorn, T., Kuhl, S. J., Linnemann, A., Rothe, M., Pfister, A. S., Vainio, S., Laugwitz, K. L., Moretti, A. & Kuhl, M. (2019) The Wnt inhibitor Dkk1 is required for maintaining the normal cardiac differentiation program in *Xenopus laevis*, *Dev Biol.* **449**, 1-13.
90. McEnerney, L., Duncan, K., Bang, B. R., Elmasry, S., Li, M., Miki, T., Ramakrishnan, S. K., Shah, Y. M. & Saito, T. (2017) Dual modulation of human hepatic zonation via canonical and non-canonical Wnt pathways, *Exp Mol Med.* **49**, e413.
91. Gros, J., Serralbo, O. & Marcelle, C. (2009) WNT11 acts as a directional cue to organize the elongation of early muscle fibres, *Nature.* **457**, 589-93.
92. Nagy, I., Xu, Q., Naillat, F., Ali, N., Miinalainen, I., Samoylenko, A. & Vainio, S. J. (2016) Impairment of Wnt11 function leads to kidney tubular abnormalities and secondary glomerular cystogenesis, *BMC Dev Biol.* **16**, 30.
93. O'Brien, L. L., Combes, A. N., Short, K. M., Lindstrom, N. O., Whitney, P. H., Cullen-McEwen, L. A., Ju, A., Abdelhalim, A., Michos, O., Bertram, J. F., Smyth, I. M., Little, M. H. & McMahon, A. P. (2018) Wnt11 directs nephron progenitor polarity and motile behavior ultimately determining nephron endowment, *Elife.* **7**.
94. Heisenberg, C. P., Tada, M., Rauch, G. J., Saude, L., Concha, M. L., Geisler, R., Stemple, D. L., Smith, J. C. & Wilson, S. W. (2000) Silberblick/Wnt11 mediates convergent extension movements during zebrafish gastrulation, *Nature.* **405**, 76-81.
95. Eisenberg, C. A. & Eisenberg, L. M. (1999) WNT11 promotes cardiac tissue formation of early mesoderm, *Dev Dyn.* **216**, 45-58.
96. Pandur, P., Lasche, M., Eisenberg, L. M. & Kuhl, M. (2002) Wnt-11 activation of a non-canonical Wnt signalling pathway is required for cardiogenesis, *Nature.* **418**, 636-41.
97. Liu, X., Wu, S., Xia, Y., Li, X. E., Xia, Y., Zhou, Z. D. & Sun, J. (2011) Wingless homolog Wnt11 suppresses bacterial invasion and inflammation in intestinal epithelial cells, *Am J Physiol Gastrointest Liver Physiol.* **301**, G992-G1003.
98. Kirikoshi, H., Sekihara, H. & Katoh, M. (2001) Molecular cloning and characterization of human WNT11, *Int J Mol Med.* **8**, 651-6.
99. Yao, Y., Sun, S., Wang, J., Fei, F., Dong, Z., Ke, A. W., He, R., Wang, L., Zhang, L., Ji, M. B., Li, Q., Yu, M., Shi, G. M., Fan, J., Gong, Z. & Wang, X. (2018) Canonical Wnt Signaling Remodels Lipid Metabolism in Zebrafish Hepatocytes following Ras Oncogenic Insult, *Cancer Res.* **78**, 5548-5560.
100. Castanon, I., Hannich, J. T., Abrami, L., Huber, F., Dubois, M., Muller, M., van der Goot, F. G. & Gonzalez-Gaitan, M. (2020) Wnt-controlled sphingolipids modulate Anthrax Toxin Receptor palmitoylation to regulate oriented mitosis in zebrafish, *Nat Commun.* **11**, 3317.
101. Zhang, T., Hsu, F. N., Xie, X. J., Li, X., Liu, M., Gao, X., Pei, X., Liao, Y., Du, W. & Ji, J. Y. (2017) Reversal of hyperactive Wnt signaling-dependent adipocyte defects by peptide boronic acids, *Proc Natl Acad Sci U S A.* **114**, E7469-E7478.
102. Jiménez-Rojo, N., Leonetti, M. D., Zoni, V., Colom, A., Feng, S., Iyengar, N. R., Matile, S., Roux, A., Vanni, S., Weissman, J. S. & Riezman, H. (2020) Conserved Functions of Ether Lipids and Sphingolipids in the Early Secretory Pathway in *Current Biology* pp. 3775-3787.e7
103. Contreras, F. X., Ernst, A. M., Haberkant, P., Björkholm, P., Lindahl, E., Gönen, B., Tischer, C., Elofsson, A., Von Heijne, G., Thiele, C., Pepperkok, R., Wieland, F. & Brügger, B. (2012) Molecular recognition of a single sphingolipid species by a protein's transmembrane domain in *Nature* pp. 525-529
104. Gibellini, F. & Smith, T. K. (2010) The Kennedy pathway--De novo synthesis of phosphatidylethanolamine and phosphatidylcholine, *IUBMB Life.* **62**, 414-28.

105. Heacock, A. M. & Agranoff, B. W. (1997) CDP-diacylglycerol synthase from mammalian tissues, *Biochim Biophys Acta*. **1348**, 166-72.
106. Ran, F. A., Hsu, P. D., Wright, J., Agarwala, V., Scott, D. A. & Zhang, F. (2013) Genome engineering using the CRISPR-Cas9 system in *Nature Protocols* pp. 2281-2308
107. Heigwer, F., Kerr, G. & Boutros, M. (2014) E-CRISP: fast CRISPR target site identification, *Nat Methods*. **11**, 122-3.
108. Voloshanenko, O., Gmach, P., Winter, J., Kranz, D. & Boutros, M. (2017) Mapping of Wnt-Frizzled interactions by multiplex CRISPR targeting of receptor gene families, *FASEB J*. **31**, 4832-4844.
109. Technologies, L. (2012) XCell SureLock® Mini-Cell in
110. Thiele, C., Papan, C., Hoelper, D., Kusserow, K., Gaebler, A., Schoene, M., Piotrowitz, K., Lohmann, D., Spandl, J., Stevanovic, A., Shevchenko, A. & Kuerschner, L. (2012) Tracing fatty acid metabolism by click chemistry in *ACS Chemical Biology* pp. 2004-2011
111. Hannoush, R. N. & Sun, J. (2010) The chemical toolbox for monitoring protein fatty acylation and prenylation in *Nature Chemical Biology* pp. 498-506, Nature Publishing Group,
112. BioLabs, N. E. Reaction Protocols for Protein Deglycosylation Mix II (P6044) in <https://international.neb.com/protocols/2016/07/29/reaction-protocols-for-protein-deglycosylation-mix-ii-p6044>.
113. Glaeser, K., Boutros, M. & Gross, J. C. (2016) Biochemical Methods to Analyze Wnt Protein Secretion. in *Methods in molecular biology (Clifton, NJ)*
114. Zhang, J., Xin, L., Shan, B., Chen, W., Xie, M., Yuen, D., Zhang, W., Zhang, Z., Lajoie, G. A. & Ma, B. (2012) PEAKS DB: de novo sequencing assisted database search for sensitive and accurate peptide identification, *Mol Cell Proteomics*. **11**, M111 010587.
115. Bligh, E. G. & Dyer, W. J. (1959) A rapid method of total lipid extraction and purification, *Can J Biochem Physiol*. **37**, 911-7.
116. Özbalci, C., Sachsenheimer, T. & Brügger, B. (2013) Quantitative analysis of cellular lipids by nano-electrospray ionization mass spectrometry in *Methods in Molecular Biology* pp. 3-20
117. Herzog, R., Schwudke, D., Schuhmann, K., Sampaio, J. L., Bornstein, S. R., Schroeder, M. & Shevchenko, A. (2011) A novel informatics concept for high-throughput shotgun lipidomics based on the molecular fragmentation query language, *Genome Biol*. **12**, R8.
118. Herzog, R., Schuhmann, K., Schwudke, D., Sampaio, J. L., Bornstein, S. R., Schroeder, M. & Shevchenko, A. (2012) LipidXplorer: a software for consensual cross-platform lipidomics, *PLoS One*. **7**, e29851.
119. Brügger, B. (2014) Lipidomics: Analysis of the lipid composition of cells and Subcellular organelles by Electrospray ionization mass spectrometry in *Annual Review of Biochemistry* pp. 79-98
120. Demir, K., Kirsch, N., Beretta, C. A., Erdmann, G., Ingelfinger, D., Moro, E., Argenton, F., Carl, M., Niehrs, C. & Boutros, M. (2013) RAB8B is required for activity and caveolar endocytosis of LRP6, *Cell Rep*. **4**, 1224-34.
121. Wesslowski, J., Kozielwicz, P., Wang, X., Cui, H., Schihada, H., Kranz, D., Pradhira Karuna, M., Levkin, P., Gross, J. C., Boutros, M., Schulte, G. & Davidson, G. (2020) eGFP-tagged Wnt-3a enables functional analysis of Wnt trafficking and signaling and kinetic assessment of Wnt binding to full-length Frizzled in *Journal of Biological Chemistry* pp. 8759-8774
122. Chick, J. M., Kolippakkam, D., Nusinow, D. P., Zhai, B., Rad, R., Huttlin, E. L. & Gygi, S. P. (2015) A mass-tolerant database search identifies a large proportion of unassigned spectra in shotgun proteomics as modified peptides, *Nat Biotechnol*. **33**, 743-9.

123. Beausoleil, S. A., Villen, J., Gerber, S. A., Rush, J. & Gygi, S. P. (2006) A probability-based approach for high-throughput protein phosphorylation analysis and site localization, *Nat Biotechnol.* **24**, 1285-92.
124. Beckenbauer, K. (2016) *Ph.D Thesis: Identification and characterization of novel cholesteroylated proteins using a click chemistry based approach.*, Heidelberg University.
125. Bisson, J. A., Mills, B., Paul Helt, J. C., Zwaka, T. P. & Cohen, E. D. (2015) Wnt5a and Wnt11 inhibit the canonical Wnt pathway and promote cardiac progenitor development via the Caspase-dependent degradation of AKT, *Dev Biol.* **398**, 80-96.
126. Weidinger, G. & Moon, R. T. (2003) When Wnts antagonize Wnts, *J Cell Biol.* **162**, 753-5.
127. Maye, P., Zheng, J., Li, L. & Wu, D. (2004) Multiple mechanisms for Wnt11-mediated repression of the canonical Wnt signaling pathway, *J Biol Chem.* **279**, 24659-65.
128. Jin, J., Morse, M., Frey, C., Petko, J. & Levenson, R. (2010) Expression of GPR177 (Wntless/Evi/Sprinter), a highly conserved Wnt-transport protein, in rat tissues, zebrafish embryos, and cultured human cells, *Dev Dyn.* **239**, 2426-34.
129. Nr, E. T. H., Sciences, D. O. F., Dipl, C. N., Aebi, M. & Helenius, A. (2010) N-linked protein glycosylation in the endoplasmic reticulum : focus on the RFT1 flippase in *Cold Spring Harbor Perspectives in Biology* pp. 1-16
130. Kokkola, T., Kruse, C., Roy-Pogodzik, E. M., Pekkinen, J., Bauch, C., Honck, H. H., Hennemann, H. & Kreienkamp, H. J. (2011) Somatostatin receptor 5 is palmitoylated by the interacting ZDHHC5 palmitoyltransferase, *FEBS Lett.* **585**, 2665-70.
131. Zhang, Y., Baycin-Hizal, D., Kumar, A., Priola, J., Bahri, M., Heffner, K. M., Wang, M., Han, X., Bowen, M. A. & Betenbaugh, M. J. (2017) High-Throughput Lipidomic and Transcriptomic Analysis To Compare SP2/O, CHO, and HEK-293 Mammalian Cell Lines, *Anal Chem.* **89**, 1477-1485.
132. Huang, T. C., Lee, P. T., Wu, M. H., Huang, C. C., Ko, C. Y., Lee, Y. C., Lin, D. Y., Cheng, Y. W. & Lee, K. H. (2017) Distinct roles and differential expression levels of Wnt5a mRNA isoforms in colorectal cancer cells, *PLoS One.* **12**, e0181034.
133. Voloshanenko, O., Schwartz, U., Kranz, D., Rauscher, B., Linnebacher, M., Augustin, I. & Boutros, M. (2018) beta-catenin-independent regulation of Wnt target genes by RoR2 and ATF2/ATF4 in colon cancer cells, *Sci Rep.* **8**, 3178.
134. Kikuchi, A., Kishida, S. & Yamamoto, H. (2006) Regulation of Wnt signaling by protein-protein interaction and post-translational modifications in *Experimental & Molecular Medicine 2006 38:1* pp. 1-10, Nature Publishing Group,
135. Yamamoto, H., Awada, C., Hanaki, H., Sakane, H., Tsujimoto, I., Takahashi, Y., Takao, T. & Kikuchi, A. (2013) The apical and basolateral secretion of Wnt11 and Wnt3a in polarized epithelial cells is regulated by different mechanisms, *J Cell Sci.* **126**, 2931-43.
136. Greaves, J., Munro, K. R., Davidson, S. C., Riviere, M., Wojno, J., Smith, T. K., Tomkinson, N. C. & Chamberlain, L. H. (2017) Molecular basis of fatty acid selectivity in the zDHHC family of S-acyltransferases revealed by click chemistry, *Proc Natl Acad Sci U S A.* **114**, E1365-E1374.
137. Woodley, K. T. & Collins, M. O. (2021) Regulation and function of the palmitoyl-acyltransferase ZDHHC5, *FEBS J.*
138. Belenkaya, T. Y., Wu, Y., Tang, X., Zhou, B., Cheng, L., Sharma, Y. V., Yan, D., Selva, E. M. & Lin, X. (2008) The retromer complex influences Wnt secretion by recycling wntless from endosomes to the trans-Golgi network, *Dev Cell.* **14**, 120-31.
139. Breusegem, S. Y. & Seaman, M. N. J. (2014) Genome-wide RNAi screen reveals a role for multipass membrane proteins in endosome-to-golgi retrieval, *Cell Rep.* **9**, 1931-1945.

140. Sada, R., Kimura, H., Fukata, Y., Fukata, M., Yamamoto, H. & Kikuchi, A. (2019) Dynamic palmitoylation controls the microdomain localization of the DKK1 receptors CKAP4 and LRP6 in *Science Signaling* pp. 1-15
141. Özkan Küçük, N. E., Yiğit, B. N., Değirmenci, B. S., Qureshi, M. H., Kamacıoğlu, A., Bavili, N., Kiraz, A. & Özlü, N. (2021) ZDHHC5 directs Protocadherin 7 to the mitotic cell surface and cleavage furrow by a palmitoylation-dependent mechanism for a successful cell division, *bioRxiv*, 2020.05.24.111831.
142. Stypulkowski, E., Asangani, I. A. & Witze, E. S. (2018) The depalmitoylase APT1 directs the asymmetric partitioning of Notch and Wnt signaling during cell division, *Sci Signal*. **11**.
143. Fairbank, M., Huang, K., El-Husseini, A. & Nabi, I. R. (2012) RING finger palmitoylation of the endoplasmic reticulum Gp78 E3 ubiquitin ligase, *FEBS Lett*. **586**, 2488-93.
144. Glaeser, K., Urban, M., Fenech, E., Voloshanenko, O., Kranz, D., Lari, F., Christianson, J. C. & Boutros, M. (2018) ERAD-dependent control of the Wnt secretory factor Evi, *EMBO J*. **37**.
145. Wolf, L. M., Lambert, A. M., Haenlin, J. & Boutros, M. (2021) EVI/WLS function is regulated by ubiquitylation and is linked to ER-associated degradation by ERLIN2, *Journal of Cell Science*. **134**.
146. Kanzawa, N., Maeda, Y., Ogiso, H., Murakami, Y., Taguchi, R. & Kinoshita, T. (2009) Peroxisome dependency of alkyl-containing GPI-anchor biosynthesis in the endoplasmic reticulum, *Proc Natl Acad Sci U S A*. **106**, 17711-6.
147. Jimenez-Rojo, N. & Riezman, H. (2019) On the road to unraveling the molecular functions of ether lipids, *FEBS Lett*. **593**, 2378-2389.
148. Traister, A., Shi, W. & Filmus, J. (2008) Mammalian Notum induces the release of glypicans and other GPI-anchored proteins from the cell surface, *Biochem J*. **410**, 503-11.
149. Franch-Marro, X., Marchand, O., Piddini, E., Ricardo, S., Alexandre, C. & Vincent, J. P. (2005) Glypicans shunt the Wntless signal between local signalling and further transport, *Development*. **132**, 659-66.
150. McGough, I. J., Vecchia, L., Bishop, B., Malinauskas, T., Beckett, K., Joshi, D., O'Reilly, N., Siebold, C., Jones, E. Y. & Vincent, J. P. (2020) Glypicans shield the Wnt lipid moiety to enable signalling at a distance, *Nature*. **585**, 85-90.
151. Zoltewicz, J. S., Ashique, A. M., Choe, Y., Lee, G., Taylor, S., Phamluong, K., Solloway, M. & Peterson, A. S. (2009) Wnt signaling is regulated by endoplasmic reticulum retention, *PLoS One*. **4**, e6191.
152. Song, H. H., Shi, W., Xiang, Y. Y. & Filmus, J. (2005) The loss of glypican-3 induces alterations in Wnt signaling, *J Biol Chem*. **280**, 2116-25.
153. Capurro, M., Martin, T., Shi, W. & Filmus, J. (2014) Glypican-3 binds to Frizzled and plays a direct role in the stimulation of canonical Wnt signaling, *J Cell Sci*. **127**, 1565-75.
154. Waghmare, I. & Page-McCaw, A. (2021) Glypicans and cytonemes unite to distribute Wnt ligands, *J Cell Biol*. **220**.
155. Hu, B., Rodriguez, J. J., Kakkerla Balaraju, A., Gao, Y., Nguyen, N. T., Steen, H., Suhaib, S., Chen, S. & Lin, F. (2021) Glypican 4 mediates Wnt transport between germ layers via signaling filopodia, *J Cell Biol*. **220**.
156. Balaraju, A. K., Hu, B., Rodriguez, J. J., Murry, M. & Lin, F. (2021) Glypican 4 regulates planar cell polarity of endoderm cells by controlling the localization of Cadherin 2, *Development*. **148**.

Acknowledgements

First of all, I would like to thank Professor Britta Brügger, Professor Michael Boutros and Dr. Oksana Voloshanenko for giving me the opportunity to pursue my PhD under their guidance. Their supervision and constant support have been crucial to achieve the goals set out in this work.

I am very grateful to Bianca Pokrandt for synthesizing the monounsaturated palmitoleic acid cC16: 1n-7; to Iris Leibrecht, Timo Sachsenheimer and Christian Luchtenborg for helping me with the lipidomic analysis of the samples; to Daniela Schweinfurth for her help with the thin layer chromatography experiment; to Lucie Wolf for her help with the gelatin degradation assays; to Prof. Carsten Hopf and Diego for the mass spectrometry analysis of the recombinant proteins. I would also like to thank Francesca Caroti, Frauke Kikul, Rainer Beck, Camilo Aponte, Oksana Voloshanenko and Britta for their constant help in the process of correcting the manuscript and discussions on the results. I would also like to thank all the people in Britta's and Michael's group who participated in some direct or indirect way in this project.

On the institutional side, I would like to thank the Biochemistry Center of the University of Heidelberg (BZH), and the Deutsches Krebsforschungszentrum (DKFZ) for providing their facilities, equipment and personnel for the process of setting up the experiments. And to the HBIGS program and its team for allowing me to be part of their Ph.D. program and for advising me throughout the process.

Outside of the lab group, I want to thank all my friends; who in some way have been a small part of who I am and have shared many good moments with me. Finally, I want to express my infinite gratitude to my girlfriend Francesca, my parents Blanca and Agustin, my brother Camilo, my sister-in-law Nadine, my nephew Emilio, my niece Yuna and my other family members. They are my inspiration for all the things that happen in my life and the reason to keep going forward with my dreams.

